Effect of Dissolved Carbon Dioxide on Very-High-Gravity Fermentation

A Thesis submitted to the College of Graduate Studies and Research

in partial fulfillment of the requirements for the degree of

Master of Science

In the Department of Chemical and Biological Engineering,

University of Saskatchewan,

Saskatoon, Saskatchewan

By

Shyam Srinivasan

PERMISSION TO USE

I agree that this thesis, presented in partial fulfillment of the requirements for a Master of Science degree from the University of Saskatchewan, be made freely available for inspection by the Libraries of the University of Saskatchewan. I further agree that permission to copy this thesis, in whole or in part, for scholarly purposes only be granted by the professor who supervised the work presented in this thesis. In his absence, such permission shall be granted by the Head of the Department of Chemical and Biological Engineering or the Dean of the College of Graduate Studies and Research. Copying, publishing or use of this thesis or part thereof for financial gain shall not be permitted without my written consent. Due recognition shall be given to me and the University of Saskatchewan for any scholarly use of materials in this thesis in whole or part thereof.

All requests for permission pertaining to use of materials in this thesis in whole or part thereof for the purpose of copying should be addressed to

Head of the Department of Chemical & Biological Engineering

University of Saskatchewan, Saskatoon, SK, S7N 5A9

Canada

ABSTRACT

The stoichiometric relationship between carbon dioxide (CO_2) generated and glucose consumed during fermentation can be utilized to predict glucose consumption as well as yeast growth by measuring the CO_2 concentration. Dissolved CO_2 was chosen as opposed to off-gas CO_2 due to the high solubility of CO_2 in the fermentation broth as well as its ability to reflect on yeast growth more accurately than off-gas CO_2. Typical very-high-gravity (VHG) ethanol fermentation is plagued by incomplete glucose utilization and longer durations. Aiming to improve substrate utilization and enhance VHG fermentation performance, characteristics of dissolved CO_2 concentration in fermentation broths using *Saccharomyces cerevisiae* were studied under batch conditions. Based on this study a novel control methodology based on dissolved CO2 was developed and its effectiveness on enhancing VHG fermentation was evaluated by measuring the fermentation duration, glucose conversion efficiency and ethanol productivity.

Four different initial concentrations 150, 200.05±0.21, 250.32±0.12, and 300.24±0.28 g glucose/L were used for batch ethanol fermentation without control. Zero substrate was indicated for 150 and 200.05±0.21 g glucose/L by a characteristic abrupt drop in dissolved CO_2 concentration. On the other hand sluggish fermentation and incomplete substrate utilization were witnessed for 250.32±0.12, and 300.24±0.28 g glucose/L. A material balance equation was developed to compensate for the inability of the dissolved CO_2 profiles to accurately predict the different growth phases of yeast.

Dissolved CO_2 was controlled at three distinct levels of 500, 750 and 1000 mg/L using aeration rates of 820 and 1300 mL/min for initial concentrations of 259.72±7.96 and 303.92±10.66 g glucose/L. Enhancement of VHG fermentation was achieved in the form of complete glucose utilization and higher ethanol productivities and shorter fermentation duration in comparison to batches without control. Complete glucose utilization was facilitated under ~250 and ~300 g glucose/L in 27.02±0.91 and 36.8±3.56 h respectively. Irrespective of the control set points and aeration rates, ethanol productivities of 3.98±0.28 g/L-h and 3.44±0.32 g/L-h were obtained for 259.72±7.96 and 303.92±10.66 g glucose/L respectively. The glucose conversion efficiencies for both 259.85±9.02 and 299.36±6.66 g glucose/L when dissolved CO_2 was controlled were on par with that of batches without control.

Keywords: dissolved carbon dioxide, very-high-gravity fermentation, control, *Saccharomyces cerevisiae*, ethanol productivity

ACKNOWLEDGEMENTS

My gratitude goes to my supervisor, Dr. Yen-Han Lin for his guidance and support throughout the course of my project. I appreciate his constant appraisals of my work and his invaluable troubleshooting skills whenever I was in a pinch. I sincerely thank my committee members Dr. Jian Peng and Dr. Oon-Doo Baik who have provided me without invaluable comments and suggestions for all my reports and presentations.

I also thank the staff at the Department of Chemical and Biological Engineering, especially, Mr. Dragan Cekic, and Mr. Rlee Prokopishyn for their technical expertise. I also thank Mr. Richard Blondin and Ms. Heli Eunike for their patience and help with the HPLC and other equipments despite my impatience.

I would not have been able to complete my work if not for the help provided by fellow lab partner Sijing Feng. Our mutual discussions have given me invaluable knowledge on a lot of subjects including but not limited to the current work. Thank you for enriching my life and maintaining a lively atmosphere in the lab throughout the course of my work.

Finally I thank my parents and sister who have supported me from afar for the past two years.

TABLE OF CONTENTS

LIST OF TABLES

LIST OF FIGURES

NOMENCLATURE

$CER(t)$	Carbon dioxide evolution or production rate (mole/L-h)
$[CO_2]$	Total carbon dioxide concentration in the system (mole/L)
$[CO_2]^*$	Equilibrium carbon dioxide concentration (mole/L)
$[CO_3^{2-}]$	Concentration of carbonate ions (mole/L
$[DCO_2]$	Total dissolved carbon dioxide concentration (mole/L)
$[HCO_3^-]$	Concentration of bicarbonate ions (mole/L)
H^{CO_2}	Henry's Law constant for CO_2 (L-atm/mole)
$[H^+]$	Concentration of hydrogen ions (mole/L)
K_1, K_2	Equilibrium constant (mole/L)
$K_L^{CO_2}a$	Volumetric mass transfer coefficient for CO_2 (1/h)
k_b	Reaction rate constant for forward reaction (1/h)
k_{-b}	Reaction rate constant for reverse reaction (L/mole-h)
p_{CO_2}	Partial pressure of off-gas CO_2 (atm)
X	Biomass in terms of viable cells (g viable cell dry weight)
Y_{CO_2}	Biomass yield coefficient w.r.t. CO_2 (g CO_2/g viable cell dry weight)

μ	Specific growth rate of *S. cerevisiae* (1/h)
$\hat{\mu}$	Maximum specific growth rate of *S. cerevisiae* (1/h)

CHAPTER 1
LITERATURE REVIEW

1.1 Introduction

Ethyl alcohol or ethanol, as it is commonly known, is a major alcohol in today's energy intensive economy. Ethanol is used as biodiesel and is increasingly being used as a substitute for petroleum based fuels in blended forms. The current decline in fossil fuel production and increase in their cost has made alternative fuels like bio-ethanol and bio-diesel more attractive. The main source of ethanol for both food and energy industries are cereals and grains like corn and maize that are fermented to produce ethanol. Currently, work on using cellulose to produce ethanol through biochemical and physiochemical processes has gained more importance as an alternative to food grains and cereals. The very essence of bio-ethanol production is the conversion of monosaccharaides or sugars present in these sources to ethanol through oxidation. While glucose is the most common monosaccharaide, sugars derived from cellulose also contain pentose and xylose depending on the source of cellulose.

Saccharomyces cerevisiae, otherwise known as baker's yeast in general, is the most common species of yeast used in fermentation of glucose to ethanol. Ethanol obtained through traditional fermentation processes, used for the production of edible alcohol, tend to be of very low concentrations (10-12% v/v), thereby increasing downstream processing costs. The requirement for high ethanol concentration to reduce downstream processing costs has been satisfied by very-high-gravity (VHG) ethanol fermentation where typical feed sugar concentrations used for ethanol production are over 250g/L. Apart from producing higher

ethanol concentrations and being an energy efficient process, VHG fermentation processes also increase the annual ethanol productivity (Devantier et al., 2005; Feng et al., 2012; Ho and Shanahan, 1986; Ingledew and Lin, 2011; Piddocke et al., 2009; Saerens et al., 2008; Wang et al., 2007;). All these advantages accrue together to lower per batch operating costs given that majority of current VHG fermentation processes are batch processes.

1.1.1 Very-High-Gravity Ethanol Fermentation

Very-high-gravity fermentation was extensively studied by Thomas et al., (1994) and Devantier et al., (2005). In VHG ethanol fermentation the high glucose concentrations induce additional osmotic stress on the yeast cells during the initial growth phase (lag phase), while the very high final ethanol concentration inhibit yeast survival towards the end of the process leading to loss of cell viability (Feng et al., 2012; Lin et al., 2010; Liu et al., 2011a, 2011b; Piddocke et al., 2009). High inhibitory ethanol concentrations are observed only under VHG conditions due to high feed glucose concentrations used in the process (Feng et al., 2012; Ingledew and Lin, 2011; Lin et al., 2010; Liu et al., 2011a, 2011b). Ethanol concentrations over 40 g/L exert inhibition on yeast metabolism. Inhibition turns to toxicity when ethanol concentrations in the fermentation broth exceed ~90 g/l (Feng et al, 2012; Lin et al., 2010). Inhibitory stresses combined with loss of cell viability result in shifting of metabolic flux away from ethanol production. These effects have been further elaborated in the following sections.

Ethanol being a primary metabolite is produced during the growth phases of yeast, viz., lag and exponential phases rather than the stationary phase where secondary metabolites are typically produced. Thus, microbial growth is a requirement for ethanol production. Ethanol production is not efficient in a completely anaerobic or aerobic environment. This necessitates the availability of O_2 for microbial growth and efficient ethanol production. This was

demonstrated by Lin et al. (2010) and Liu et al. (2011a, 2011b). They concluded that sparging air through the fermentation broth during the course of fermentation improved yeast viability and consequently ethanol production. Therefore it has been stressed that despite the advantages of ethanol fermentation under VHG environments, inhibitions due to the lack of oxygen, high initial glucose concentrations and high final ethanol concentrations need to be taken into consideration while designing efficient fermentation processes in general for the production of bio-ethanol (Hill, 2006; Ho and Shanahan, 1986; Jones and Greenfield, 1982; Kuhbeck et al., 2007; Kuriyama et al., 1993;).

1.1.2 Glycolysis in *Saccharomyces cerevisiae*

The production of ethanol from glucose in *S. cerevisiae* follows the Glycolytic pathway. Glycolysis culminates in two distinct metabolisms; aerobic and anaerobic. Figure 1.1 represents a simplified representation of glycolysis in unicellular organisms. The acetaldehyde-ethanol shuttle is a part of anaerobic metabolism and is preceded by the catalysis of Pyruvate to Acetaldehyde and carbon dioxide (CO_2). Hence, ethanol production is accompanied by the simultaneous production of CO_2, a by-product of glycolysis. The CO_2 produced is known to exert a certain degree of inhibitory pressure on growth and survival of microorganisms (Jones and Greenfield, 1982; Lacoursiere et al., 1986; McIntyre and McNeil, 1997; McIntyre and McNeil, 1998; Mostafa and Gu, 2003; Pattison et al., 2000; Saucedo-Castaneda and Trejo-Hernandez, 1994).

Acetaldehyde is reduced to ethanol with concomitant oxidation of NADH to NAD^+. In the presence of oxygen, the aerobic route leads to the production of Acetyl-CoA (Ac-CoA) from Pyruvate culminating in the Tricarboxylic Acid (TCA) cycle and production of ATP. Metabolites like Acetic, Succinic and Pyruvic Acid are produced when metabolic flux is present in this

direction. The aerobic route also results in prioritizing production of biomass (from ATP) over production of ethanol (Daoud and Searle, 1990; Zeng and Deckwer, 1994).

It has been established from the biochemical perspective of yeast growth that stress associated with either yeast growth or ethanol production is usually exhibited in the form of production of certain metabolites not produced otherwise. The production of such metabolites is accompanied by the production of ATP to meet the increased energy demands of the cell under stress. Glycerol and trehalose are two such compounds. It is proven fact that these compounds are produced through a branch in glycolysis, with intermediates produced during glycolysis acting as precursors for their production. These compounds remain within the cell membrane and protect the cells against stress while ATP is oxidized for cell maintenance. Once stress is relieved, production stops and these metabolites are excreted through the cell membrane. In the present context, glycerol is usually produced as a response to oxidative stress while trehalose is produced in response to the high osmotic pressure experienced by cells in VHG environments (Belo et al., 2003; Brown et al., 1981; Devantier et al., 2005; Wang et al., 2001).

Glycerol is produced as a means to produce NAD^+. Accordingly a higher concentration of glycerol points to the requirement of NAD^+ and consequent oxidation of NADH (Belo et al., 2003; Devantier et al., 2005). NAD^+ oxidizes glucose to pyruvate as it gets reduced to NADH. The reduction of acetaldehyde to ethanol is also accompanied by NADH oxidation to NAD^+. Therefore during glycolysis, NADH and NAD^+ are continuously recycled (Figure 1.1). Stress induced by the high ethanol concentrations reduces the production of ethanol and the associated NAD^+ as a result. .

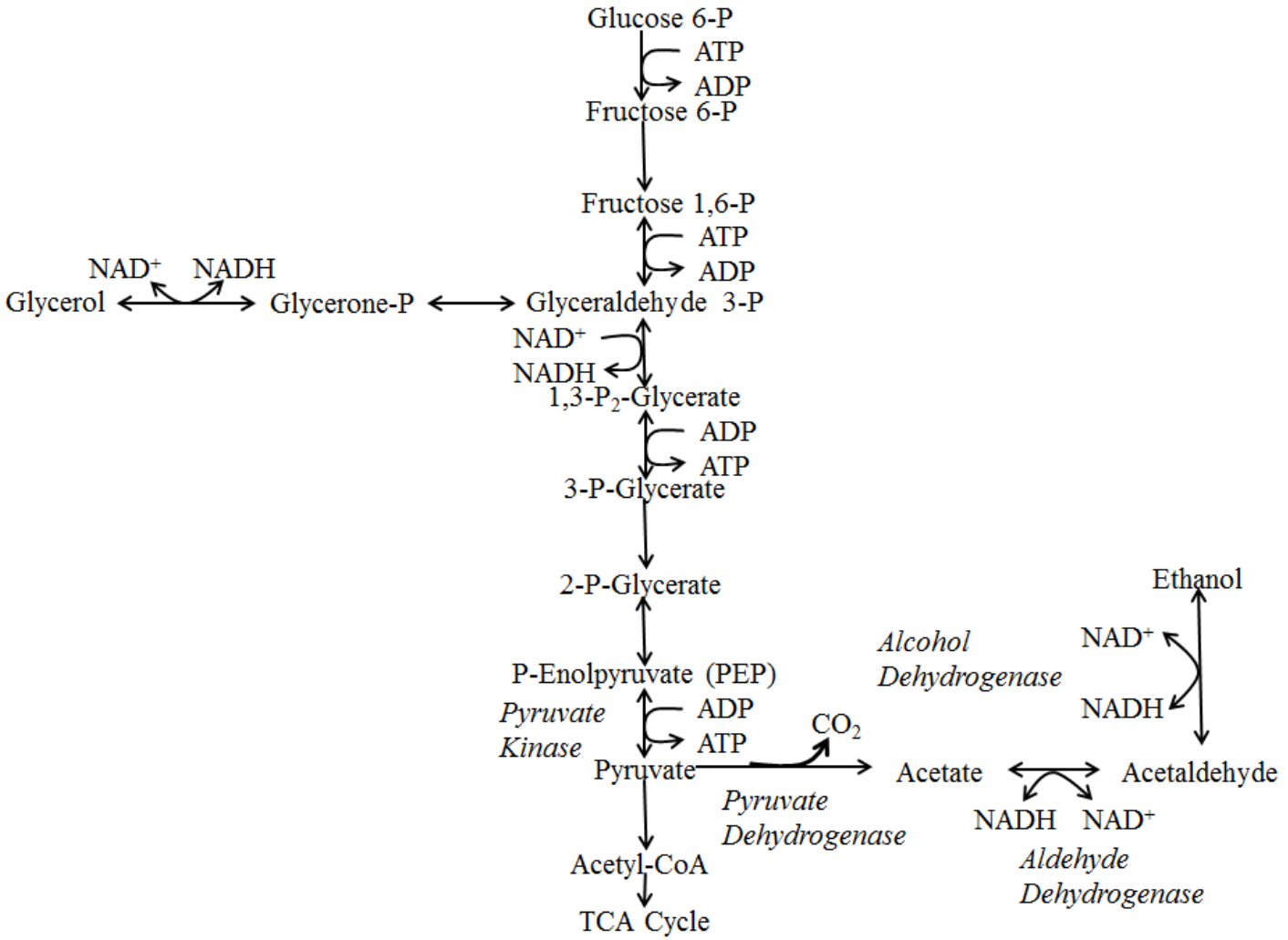

Figure 1.1. Glycolysis in unicellular microorganisms for the utilization of glucose. Adopted from Biochemical pathways, 3rd edition, Part-1, Michal Gerhard (ed.), Roche Molecular Biochemicals.

In order to compensate for the loss of production of NAD^+, theoretically, metabolic flux shifts from production of pyruvate to production of other metabolites that are accompanied by the oxidation of NADH to NAD^+. Generation of Glycerol from Glyceraldehyde-6-phosphate is one such mechanism.

Glycerol is also known to play the role of a redox sink. Consequently, a higher concentration of glycerol in the broth also points to the oxidative stress in the fermentation broth. In VHG broths the very high sugar concentrations apart from resulting in higher osmotic pressures on yeast also increase the viscosity of the medium. This reduces the O_2 solubility and as a result O_2 concentration in the broth (Devantier et al., 2005; Gros et al., 1999; Ho and Shanahan, 1986; Schumpe and Deckwer, 1979; Schumpe et al., 1982; Verbelen et al., 2009). On the other hand, trehalose is produced to compensate for the higher osmotic stress witnessed during the initial stages under VHG conditions. Osmosis affects the intercellular transport characteristics of the cell membrane. Trehalose is known to act as an osmo-protectant and maintain intercellular nutrient transport through the cell membrane under high osmotic pressures. These metabolites although improve yeast survival under stress, are sources of drain of carbon source from the intended product.

The inhibitory effects of the metabolic products of glycolysis have been extensively studied by various authors (Brown et al., 1981; Feng et al., 2012; Ingledew and Lin, 2011; Liu et al., 2011a; Maiorella et al., 1983; Pampulha and Loureiro-Dias, 1989; Piddocke et al., 2009). Inhibitory pressures tend to shift the pathway away from ethanol production. Maiorella et al. (1983) pointed to the inhibitory effect of non-volatile by-products like organic acids and aldehydes that are concentrated in the fermenter as a consequence of ethanol removal. They found that ethanol concentrations over 80g/L resulted in 80% reduction of cell mass and termed

it as the inhibitory concentration. The findings of later authors regarding inhibitions induced by high feed glucose concentrations (Feng et al., 2012; Ingledew and Lin, 2011; Liu et al., 2011a) agreed with that of Maiorella et al. (1983). Maiorella et al. (1983) also hypothesized from their investigations that ethanol productivity (g ethanol/g cell) could be increased as a result of certain type of inhibitions. Inhibitions that usually affect the membrane transport characteristics of the cells were the focused upon for this study. Thus, the various forms of inhibition experienced during the course of fermentation tend to reduce the efficiency of conversion of glucose to ethanol in turn affecting fermentation performance.

1.1.3 Carbon dioxide in Fermentation

CO_2 is a major by-product of ethanol production that has largely been ignored in current literature when it comes to fermentation performance. The evolution of CO_2 from *S. cerevisiae* can be stoichiometrically related to glucose consumption and ethanol production by Equation (1.1).

$$C_6H_{12}O_6 \rightarrow 2C_2H_5OH + 2CO_2 \tag{1.1}$$

Stoichiometry dictates that for every mole of glucose utilized by yeast, 2 moles each of ethanol and CO_2 are produced during glycolysis (Daoud and Searle, 1990). Apart from CO_2 produced by the decarboxylation of Pyruvate to Acetaldehyde, decarboxylation steps in the TCA cycle also result in CO_2 production. However, for the production of certain metabolites in the carboxylation steps of the TCA cycle like succinic acid, CO_2 also acts as a substrate (Ho and Shanahan, 1986; Lee et al., 1999; Song et al., 2007; Xi et al., 2011).

1.1.3.1 Fermentation Measurement using Carbon dioxide

Due to the stoichiometric relationship between glucose utilization, ethanol production, and yeast growth, the CO_2 evolved is a direct measure of yeast activity in the fermentation broth. Hence, monitoring CO_2 concentration should enable monitoring of the fermentation process in an inexpensive manner (Chen et al., 2008; Dahod, 1993; Daoud and Searle, 1990; El Haloui et al., 1988; Royce and Thornhill, 1991). Carbon dioxide has been widely used as a measure of fermentation progress by several investigators (Golobic and Gjerkes, 1999; Manginot et al., 1997; Montague et al., 1986; Saucedo-Castaneda and Trejo-Hernandez, 1994;Taherzadeh et al., 1999).

Theoretical models have been proposed by El Haloui et al. (1988) to determine the concentration of ethanol and glucose on-line during fermentation based on the volume of CO_2 present in the off-gas stream of the fermenter. This model was found applicable even under VHG environments when induced stresses were not taken into account. The only drawback of this model was the use of off-gas CO_2 measurements. Measurements based on off-gas CO_2 tend to be erroneous due to the dissolution of CO_2 in the fermentation broth. Dahod, (1993) in his investigations concurred that the dissolved CO_2 concentration was always higher than the equilibrium gas phase CO_2 concentration. The variation between dissolved CO_2 and the corresponding equilibrium gas phase concentration increased with increase in air flow rates. This variation and dependence were higher for broths of higher viscosity than for broths of lower viscosity. The observation was extrapolated and concluded that dissolved and off-gas CO_2 never exist in equilibrium in fermentation systems except under near plug flow conditions (Ho and Shanahan, 1986). Works of several authors (Montague et al., 1986; Pattison et al., 2000; Renger et al., 1992) in the area of CO_2 inhibition assumed near equilibrium conditions between off-gas

and dissolved CO_2. However, a few earlier authors (Dixon and Kell, 1989; Ho and Shanahan, 1986; Jones and Greenfield, 1982; Royce and Thornhill, 1991; Royce P. N., 1992; Zosel et al., 2011) recommended against assuming such equilibrium environments except under specific conditions.

Typically the solubility of CO_2 is about 10 times greater than that of oxygen in aqueous media (Kawase et al., 1992; Schumpe and Deckwer, 1979; Schumpe et al., 1982). The protein rich fermentation broths tend to further decrease CO_2 desorption as a result of increased binding of CO_2 to the organic molecules on the cell membrane and in the broth. According to Kruger et al. (1992), Kuriyama et al. (1993) and Kuhbeck et al. (2007) the presence of ethanol during VHG fermentation also enhances CO_2 solubility in the broth. Carbon dioxide is 4.5 times more soluble in aqueous solutions containing ethanol (Isenschmid et al., 1995). The exact threshold of ethanol concentration was not mentioned though. This has been argued in terms of decrease in pH with increase in ethanol concentration as well. As described later in Section 1.1.3.2.1, lower pH favors the presence of CO_2 as dissolved CO_2. Although dissolution of CO_2 in the fermenter broth was accounted for in the models of El Haloui et al. (1988) by the use of constants, most off-gas measurements do not account for this discrepancy. Hence, monitoring fermentations through measurement of dissolved CO_2 concentration is much more relevant and reliable than those based on the measurement of off-gas CO_2.

1.1.3.2 Carbon dioxide Inhibition in Ethanol Fermentation

However despite its ability to represent fermentation progress, CO_2 has been known to have an inhibitory effect on microorganisms typically used in fermentations. Various studies have been conducted on the effects of different parameters on fermentation processes using *S. Cervisiae* like, pH (Dombek and Ingram, 1987), temperature (Saerens et al., 2008), pitching rate

(Verbelen et al., 2009), oxygen requirement (Bonnefond et al., 2002; Verbelen et al., 2009;) and addition of certain flavor active solids (Kuhbeck et al., 2007). Although these apparently visible inhibitions have so far been taken into consideration in industrial VHG ethanol fermentation, the effect of CO_2 produced during yeast metabolism has largely been neglected due to the fact that this effect is not as conspicuous as other forms of inhibition (El-Sabbagh et al., 2006; Jones and Greenfield, 1982; Kuriyama et al., 1993; Kruger et al., 1992; McIntyre and McNeil, 1997; McIntyre and McNeil, 1998; Mostafa and Gu, 2003; Shimoda et al., 2001). Current literature only takes into account inhibitory pressures experienced due to high glucose feeds and high final ethanol concentrations but not inhibitions exerted by CO_2 into consideration (Brown et al., 1981; D'Amore and Stewart, 1987; Devantier et al., 2005; Feng et al., 2012; Liu et al., 2011a, 2011b;).

Primary work in the area of CO_2 inhibition was pioneered by Jones and Greenfield (1982). Works performed in the last 3 decades have been built upon this work as a basis. Jones and Greenfield (1982) were of the opinion that CO_2 not only played the role of an inhibitor in fermentations using *S. cerevisiae*, but also a role in improving yeast survival under conditions of stress in the fermentation broth. They put forward a theory that CO_2 is involved in two different roles in the metabolism of *S. cerevisiae*; one that of a product of decarboxylation reactions (conversion of Pyruvate to Acetaldehyde) or that of a substrate in carboxylation reactions (production of Succinic acid from Ac-CoA in the TCA cycle). They opined that presence of excessive CO_2 in the fermenter would result in growth inhibition while excessive stripping of CO_2 would also stymie yeast metabolism during fermentation. Before reviewing various effects that CO_2 has on microorganism growth and survival there is a need to look at different inhibition mechanisms of CO_2. These theories vary in two aspects. While one set of theories have been

proposed based on the influence of bicarbonate (HCO_3^-) ions, the other set of theories focus on the effect of CO_2 itself in its dissolved form otherwise known as dissolved CO_2 or CO_2 (aq.).

1.1.3.2.1 Carbon dioxide behavior in aqueous systems

All theories pertaining to inhibition of microbial activity by CO_2 have been proposed on the basis of the behavior of CO_2 in aqueous environments. This description is necessary in order to justify the use of CO_2 measurements as measures of microbial activity (Dixon and Kell, 1989; Royce, 1992; Yagi and Yoshida, 1977). CO_2 in aqueous environments primarily can exist as three different species viz., CO_2 (aq.) or dissolved CO_2, HCO_3^- ions and carbonate ions (CO_3^{2-}).The pH of the aqueous system governs the equilibrium between the three species as described by Equation (1.2-1.5). The existence of CO_2 as either dissolved CO_2, HCO_3^- or CO_3^{2-} ions hence depends on the fermentation media in the present case, irrespective of the organism used for fermentation (Daoud and Searle, 1990; Frick and Junker, 1999; Golobic and Gjerkes, 1999; Zosel et al., 2011). The general behavior of the three species was described through Figure 1 of Zosel et al. (2011). According to Zosel et al. (2011) and Frick and Junker (1999), an increase in dissolved CO_2 is usually witnessed with a decrease in pH. Under pH of 4-6 that are prevalent in ethanol fermentation systems, CO_2 exists primarily as dissolved CO_2 with very minor concentrations of HCO_3^- ions. The concentration of CO_3^{2-} ions under this pH range is close to zero and between a pH of 6 and 7, is less than 0.3% (Dixon and Kell, 1989; Frahm, et al., 2002; Zosel et al., 2011).

$$CO_2(aqueous) \rightleftharpoons H_2CO_3 \tag{1.2}$$

$$CO_2\ (gas\ phase) \rightleftharpoons CO_2\ (aqueous) \tag{1.3}$$

$$CO_2 + H_2O \rightleftharpoons H^+ + HCO_3^- \quad K_1 = 5.35\times10^{-7} \text{ mol/L} \tag{1.4}$$

$$HCO_3^- \rightleftharpoons H^+ + CO_3^{2-} \qquad K_2 = 6.12\times10^{-11} \text{ mol/L} \tag{1.5}$$

Due to the instantaneous nature of conversion of dissolved CO_2 to carbonic acid (H_2CO_3) the reactions illustrated by Equations (1.2) and (1.3) are combined and generally written as Equation (1.4). Several investigators (Jones and Greenfield, 1982; Royce and Thornhill, 1991) postulated that CO_2 produced through the oxidation of glucose is released into the aqueous phase as dissolved CO_2 prior to being desorbed into the fermenter headspace. Based on this premise other studies (McIntyre and McNeil, 1997, 1998; Royce and Thornhill, 1991; Royce P. N., 1992) held the view that the effect of dissolved CO_2 will be much more pronounced and observable than that of off-gas CO_2 in the fermenter headspace. Certain physiochemical aspects were also discussed in this regard.

1.1.3.2.2 Mechanism of carbon dioxide inhibition

Carbon dioxide inhibition of microorganism growth can be classified into two distinct categories; inhibition due to HCO_3^- ions and inhibition due to dissolved CO_2. Despite the fact that two different species are involved, the underlying mechanism of inhibition remains the same. Effects exerted by bicarbonate ions or dissolved CO_2 molecules are at the extracellular as well as intracellular level. While extracellular effects depend on the species, intracellular effects do not.

Extracellular effects are localized to the cell membrane hence are generally termed as membrane effects irrespective of the species causing it. These membrane effects result in a cell membrane with altered properties. The change in membrane characteristics due to HCO_3^- ions

has been chiefly attributed to the change in dielectric properties of the membrane. The cell membrane is predominantly made up of sterols, lipids and unsaturated fatty acids (UFA) that contribute towards maintenance of cell integrity and rigidity. The effect of HCO_3^- ions has been posited to be on the charged phospholipid head groups on the surface of the membrane. However, details pertaining to the mechanism of this effect are absent. On the other hand dissolved CO_2 is absorbed into the cell membrane. The absorbed CO_2 molecules react with the sterols and UFA and change the order of the membrane which also modifies membrane fluidity. Altered membrane properties affect transport characteristics across the membrane (Dixon and Kell 1989).

In *S. cerevisiae, E.coli, Aspergillus niger* and other microbes the uptake of glucose during glycolysis from the media is through an active transport mechanism (Galazzo and Bailey, 1990). This transport is regulated by the intracellular Glucose-6-Phosphate concentration through a feedback mechanism that controls the glucose uptake rate as well. The disruption of membrane characteristics results in increased energy requirement for glucose uptake by these microorganisms during metabolism. The increased energy demands of the cell for cell maintenance are met by shift in metabolic flux from the production of NADH and NAD^+ to production of ATP and ADP. This essentially results in diversion of energy to cell maintenance. The trickle-down effect of this phenomenon is an observed decrease in microbial metabolism during fermentation in terms of growth as well as metabolite production. Thus, change in membrane characteristics affects intercellular nutrient transport resulting in metabolic inhibition (Dixon and Kell, 1989; Verduyn et al., 1990).

At the intracellular level both HCO_3^- ions as well as dissolved CO_2 have the same effect on cell metabolism. These effects are pinned upon the delicate intracellular pH balance. Intracellular pH for microorganisms like *S. cerevisiae* is generally neutral at 7 (Devantier et al., 2005; Dixon and Kell, 1989; Dombrek and Ingram, 1987; Galazzo and Bailey, 1990; McIntyre and McNeil, 1997; Pampulha and Loureiro-Dias, 1989; Shimoda et al., 2001). The heavy influx of either species transported into the cells through the cell membrane affects the intracellular pH balance. Authors have extensively studied the intracellular effect of external pH on yeast metabolism (Dombrek and Ingram, 1987; Pampulha and Loureiro-Dias, 1989). Pampulha and Loureiro-Dias (1989) concluded that the regulation of internal pH of the cell is affected by change in external pH of the fermentation media resulting in an intracellular condition non-conducive for glycolysis. Galazzo and Bailey (1990) described the effect of unbalanced pH in terms of enzyme activity during glycolysis. The conversion of Pyruvate to Ethanol is dependent on the activity of pyruvate kinase, an enzyme whose allosteric constant decreases with increase in intracellular pH. Allosteric constants usually represent the equilibrium constant between two different forms of an allosteric protein/enzyme. The decrease in allosteric constant of pyruvate kinase reduces the binding affinity of Phosphoenolpyruvate (PEP). PEP is an important intermediate in the conversion of Pyruvate to Acetaldehyde. These changes in the cell biochemistry due to disturbances in the balance between intracellular and extracellular pH results in reduced ethanol production. In addition, more ATP is produced by the cell to offset pH imbalances. Energy in cells in the form of ATP serves two purposes; cell growth/reproduction and cell maintenance. ATP produced to offset the pH imbalance results in diversion of flux towards cell maintenance rather than cell growth/reproduction (Daoud and Searle, 1990; Galazzo and Bailey, 1990).

The influx of HCO_3^- ions tends to make the intracellular as well as extracellular environment more alkaline (Verduyn et al., 1990). This upsets the above explained pH balance. Consequently cessation of cell activity is witnessed resulting in cell death. The effect of dissolved CO_2 has also been proposed to be similar in nature to HCO_3^- ion based inhibition. Proponents of this theory (Dixon and Kell, 1989; El-Sabbagh et al., 2006; Jones and Greenfield, 1982; Royce, 1992; Shen et al., 2004; Shimoda et al., 2001) have suggested that dissolved CO_2 absorbed into the cell results in intracellular bicarbonate imbalance. In this context Jones and Greenfield (1982) and Dixon and Kell (1989) have advocated that intracellular and extracellular pH regulate the ratio of dissolved CO_2 to HCO_3^- ions both within and outside the cells. Increase in pH as a result of dissolved CO_2 absorption into the cells results in an increase of HCO_3^- ion concentration within the cells.

Thus, theories proposed seem to agree on the fact that the CO_2, whether in its native dissolved form or as HCO_3^- ion, projects its effect on microorganisms on both intracellular as well as extracellular fronts starting with its absorption into the cell membrane. In contrast, literature also points out the importance of the presence of CO_2 in the fermentation system as dissolved CO_2 to aid in the growth and survival of yeast cells by playing a role in the construction of the cell membrane and facilitating transport through the membrane (in carboxylation reactions) (Dixon and Kell, 1989; Jones and Greenfield, 1982).

1.1.3.2.3 Effects of carbon dioxide inhibition on microorganisms

A few authors who have studied CO_2 inhibition in *S.cerevisiae* and other microorganisms (Dixon and Kell, 1989; McIntyre and McNeil, 1997, 1998; Shang et al., 2003; Lacoursiere et al., 1986) have determined CO_2 based inhibition to have varied effects on different microorganisms.

These microbes come from a variety of genus and species like *Aspergillus niger*, *Escherichia coli*, *Penicillium chrysogenum* and *Ralstonia eutropha*. Inhibition due to dissolved CO_2 can be classified into two different categories based on the source of CO_2. The effects of CO_2 are evaluated by either supplying CO_2 from an external source into the fermenter otherwise known as exogenous CO_2 or by measuring CO_2 generated by the microorganism as a metabolic by-product, otherwise known as autogenous CO_2.

Studies conducted by Dixon and Kell (1989) on the effects of pressurized CO_2 on microbial growth have revealed that a CO_2 partial pressure (p_{CO_2}) higher than 6 atm has a negative effect on yeast growth. Other authors have also laid out similar claims with regards to the relationship between CO_2 partial pressure and CO_2 based inhibition of growth in microorganisms. Shimoda et al. (2001) studied inhibitory effects of CO_2 as well as temperature on *S. cerevisiae* and represented these effects in terms of decimal reduction time value or D-value. The D-values were representative of the death kinetics of the cells. From these values they were able to deduce that the D-values exponentially decreased with increasing CO_2 partial pressures. In addition, they were also able to validate previous claims alluding CO_2 inhibition to change in membrane fluidity by linking a similar phenomenon that was caused due to thermal stresses. Renger et al. (1992) studied the impact of p_{CO_2} on fermentations using *S. cerevisiae* to produce higher alcohols in brewery fermentations. They determined that increased CO_2 partial pressures reduced production of esters and fusel alcohols and attributed this reduction in production to growth inhibition caused by CO_2. Jones and Greenfield (1982) earlier cited that p_{CO_2} had to be in the range of at least 0.3-0.5 atm to have an inhibitory effect on the growth of *S. cerevisiae*. Shen et al. (2004) measured off-gas autogenous CO_2 in immobilized cell fermenters. He concluded that CO_2 in the fermentation apart from inhibiting growth also altered the

production of esters and higher alcohols, commonly known as flavor active volatiles, during the preparation of alcoholic beverages using *S. cerevisiae*. His investigations also revealed the relationship between CO_2 concentration and production of flavor active volatiles by showing that additional CO_2 sparged into the fermenter further reduced production of flavor active volatiles in the range of 15-18%. These findings were in agreement with a previous study in this area conducted by Renger et al. (1992). Shen et al. (2004) also proposed the use of cells in immobilized form to reduce CO_2 inhibition by not only protecting the cells from exposure to dissolved CO_2 but also by reducing the concentration of CO_2 in the fermentation broth through gas stripping. He also alluded to the stripping of certain volatiles that might inhibit yeast growth under higher concentrations due to gas sparging.

On the other hand Pattison et al. (2000) classified CO_2 inhibition in the culture of mammalian cells at two levels; acute and severe or prolonged. It was termed acute when the observed inhibition was short lived but not strong enough to be irreversible and severe or prolonged when the effect of inhibition was irreversible and carried over beyond the period of exposure to CO_2. The effects were investigated over a wide variety of partial pressures ranging from 50 to 250 mm Hg. Their investigations also revealed that the observed inhibition was lower and reversible when exposed to gradually increasing p_{CO_2} . A sudden increase in partial pressures from 50 to 250 mm Hg in contrast resulted in maximum and irreversible damage to the mammalian cell culture.

Shang et al. (2003) evaluated the inhibitory effect of CO_2 on growth in an aerobic fed-batch culture of *R. eutropha* by measuring off-gas CO_2. They proposed that operating lab scale fermenters under very low gas flow rates (0.42vvm) would simulate conditions similar to large scale fermenters where accumulation of CO_2 is significant to be measured in the off-gas. It was

concluded that although CO_2 pulse in the early exponential phase reduced cell growth rate to one-third of the standard value, the lag phase was the most sensitive to CO_2 inhibition. But, while evaluating inhibition caused by autogenous CO_2, this is not of concern as the quantity of CO_2 produced in the lag phase is relatively insignificant to that produced in the exponential phase.

McIntyre and McNeil (1997, 1998) concluded from their study of *A. niger* and a few filamentous fungi that dissolved CO_2 effected a change in cell morphology along with growth inhibition. A similar change in cell morphology was also observed in *Z. mobilis* and Streptococcus mutants by Dixon and Kell (1989) due to dissolved CO_2. Galazzo and Bailey (1990) postulated that the effects of CO_2 inhibition on yeast and ethanol production are essentially separate and decoupled. They attributed this to feedback effects of products generated post glycolysis. The conversion of Pyruvate to Acetaldehyde is governed by pyruvate dehydrogenase. This conversion releases CO_2 as a by-product. An increase in the concentration of CO_2 is known to affect pyruvate dehydrogenase activity consequently affecting acetaldehyde production and alcohol dehydrogenase activity. According to Galazzo and Bailey (1990) this sort of inhibition has a higher magnitude of effect on the conversion of pyruvate to Ac-CoA than on the conversion of pyruvate to acetaldehyde. This was extrapolated to conclude that CO_2 inhibition only affects yeast growth and not ethanol production during fermentation.

In contrast to these studies, Kuriyama et al. (1993) suggested that higher CO_2 concentrations actually increase ethanol productivity per cell. To support the claim, they suggested that higher CO_2 concentrations decreased cell viability due to inhibition and this resulted in higher ethanol produced per cell. The reduction in the number of cells also agrees with the findings of Isenschmid et al. (1995). They observed that the presence of CO_2 either in

the off-gas or aqueous phase reduced the number of larger cells. They argued that decrease in cells larger than $5.6x10^{-11}$ mL in volume could be a result of the solvent effect exerted by CO_2 and could result in reduced fermentation rates. They also proposed a mechanism wherein stress alters activity of certain key enzymes in glycolysis. They attributed this alteration under high CO_2 partial pressure to the shift in equilibrium during glycolysis. Since CO_2 is a by-product of the pyruvate-dehydrogenase system, higher CO_2 concentration tends to shift equilibrium to the pyruvate side thereby resulting in increased pyruvate production. This increase in pyruvate translates to increased acetaldehyde production followed by ethanol. This effect is similar to those proposed by Galazzo and Bailey (1990). Thus, support in literature exists for both theories; the one where inhibitions and stress reduce growth as well as metabolite production and the other where inhibitions limit growth but enhance metabolite production, effectively decoupling growth and ethanol production.

1.1.4 Role of Oxygen in Ethanol Fermentation

Oxygen (O_2) has been deemed as an important constituent in aerobic fermentation processes. In certain cases of aerobic fermentation the depletion of O_2 in the fermentation system has been cited as reason for decreased biomass as well as product yield (Belo et al., 2003; Ligthelm et al., 1988). The process of ethanol production through fermentation by *S. cerevisiae* is essentially an anaerobic process while the generation of biomass during this process is O_2 dependent. Metabolic flux in Figure 1.1 is directed elsewhere from pyruvate instead of the production of acetaldehyde during biomass production (Zeng and Deckwer, 1994). Energy in the form of ATP is required for cell growth. In this regard Daoud and Searle (1990) proposed two separate equations, Equations (1.6) and (1.7), for anaerobic and aerobic fermentation of glucose by *S. cerevisiae* respectively. According to these equations, aerobic oxidation of glucose releases

more energy in the form of ATP in comparison to anaerobic oxidation. The energy released in the process is used for cell growth and maintenance.

$$C_6H_{12}O_6 \rightarrow 2C_2H_5OH + 2CO_2 + 2ATP \quad (1.6)$$

$$C_6H_{12}O_6 + 6O_2 \rightarrow 6CO_2 + 6H_2O + 28ATP \quad (1.7)$$

Investigators (Fornairon-Bonnefond et al., 2002; Verduyn et al., 1990) were of the opinion that addition of O_2 to the fermentation broth during sluggish fermentation reduces fermentation time because of the effect of O_2 on cell viability. In light of this fact it is worth mentioning that cell viability is an important parameter to look for in ethanol fermentation (Brown et al., 1981). Cell viability is highly dependent on the structural integrity and fluidity of the cell membrane. Verbelen et al. (2009) stressed on the importance of the role of sterols and UFA in maintaining membrane fluidity. The improvement in cell viability was attributed to the increased structural integrity caused by the increased production of ergosterol and other sterols that makes up the cell membrane in the presence of O_2. The work of Verduyn et al. (1990) bolster this fact by pointing towrads the inability of *S. cerevisiae* to grow anaerobically in the absence of added sterols and UFA which are synthesized only in the presence of oxygen. Verbelen et al. (2009) were also able to correlate the effect of oxygenation to cell density used in high cell density (HCD) fermentations and conclude that optimized oxygenation during high-gravity fermentation is necessary to achieve acceptable improvement in fermentation efficiency and yeast cell viability.

On the other hand researchers have also pointed towards the existence of toxicity due to excess oxygen in the system (Belo et al., 2003; Fornairon-Bonnefond et al., 2002;). Fornairon-Bonnefond et al. (2002) hypothesized that excess O_2 would result in increased membrane fluidity

due to oxidation of sterols and UFA that make up the cell membrane thereby increasing cell susceptibility to inhibition by compounds like ethanol. This fact was pointed out by Belo et al. (2003) and termed as hyperoxia. Hyperoxia was witnessed when *S. cerevisiae* was cultivated under hyperbaric conditions of O_2 partial pressure greater than 0.32 MPa. It was postulated that hyperoxia damaged cells due to peroxidation of the cell membrane resulting in loss of metabolite production. Membrane effects similar to those observed under CO_2 inhibition were also reported. In this respect it is worth mentioning that oxidative stress as a consequence of over oxidation can be identified through measurement of intracellular glutathione concentration. Intracellular glutathione is produced as opposed to glycerol due to oxidative stress brought about by hyperoxia (Devantier et al., 2005).

1.1.5 Carbon dioxide Removal in Submerged Fermentations

Several authors (D'Amore and Stewart, 1987; Kuhbeck et al., 2007; Reddy and Reddy, 2005; Shen et al., 2004;) have shown that the addition of particulate materials improves fermentation. While D'Amore and Stewart (1987) and Reddy and Reddy (2005) have argued it to be due to the osmoprotectant nature of these particulates owing to their nutritional contribution to cell maintanance, others like Kuhbeck et al. (2007) and Shen et al. (2004) have advocated the positive effect in terms of physical phenomena occuring in the presence of the added particulates. It has been postulated that addition of particulates provides higher nucleaton sites for dissolved CO_2 to form bubbles and desorp from the aqueous media. Kuhbecket al. (2007) postulated that addition of particulate matter induces a bubbling effect that results not only in the decrease of dissolved CO_2 concentration due to CO_2 desorption but also increases concentration of cells in suspension. The increase of cells in suspension improves the surface area of contact between the cells and the fermentation broth consequently improving cell metabolic rates and

metabolite production due to improved mass transfer rates. It was also advocated that the additional nutrient effect offered by trub particulates could be a reason for improvement in fermentation rate under HCD conditions. This gains significance because of the fact that VHG fermentation broths are more viscous than traditional fermentation broths that generally contain less than 12% (w/v) sugar. In terms of mass transfer required for desorption of CO_2 from the aqueous to the gas phase, higher viscocity reduces the mass transfer coefficient.

Increasing fermenter gas flow rates in aerobic fermentations has been suggested as one of the methods of reducing dissolved CO_2 cocentration (Frick and Junker, 1999; Shang et al., 2003). Although Frick and Junker (1999) suggest that increase in air flow rates would improve CO_2 stripping from the fermentation broth as a result of increase in mass transfer gradient, this suggestion becomes moot in lab scale anaerobic processes due to low volume, low aeration rates and small scale of the process. The importance of the scale of the process has been stressed by various authors (Dahod, 1993; Frick and Junker, 1999; Ho and Shanahan, 1986; Mostafa and Gu, 2003;). Shang et al. (2003) have also proposed pumping inert gas into the fermenter to reduce CO_2 concentration within the fermenter to prevent inhibition. Since, maintaining a significant and specific O_2 partial pressure is not a requirement for VHG fermentation using *S. cerevisiae*, either of these methods should not pose a considerable challenge. But, decrease in O_2 concentration due to increase in inert gas partial pressure could result in lowering yeast growth and hence fermentation rate.

1.1.6 Redox Potential based Control of Very-High-Gravity Fermentation

The combination of oxidation and reduction reactions mentioned earlier in Section 1.1.2, otherwise known as redox reactions results in the medium being electron rich or electron deficient. This addition or subtraction of charge results in a net potential difference in the

fermentation media (Lin et al., 2010). This potential, otherwise known as redox potential or oxidation-reduction potential (ORP) is used as a measure of fermentation progress.

Redox potential profiles for VHG ethanol fermentation under different glucose concentrations were reported by Lin et al. (2010). Lin et al. (2010) reported that the different regions depicted for the ORP profile correspond to different levels of yeast activity (Fig. 1 of Lin et al., 2010). The decreasing region or Region I corresponded to lag and exponential phases where reducing power outweighs the oxidizing power indicating increase in yeast activity. Metabolic activity is at its highest in the middle of the exponential phase. Increased activity is usually accompanied by net NADH production and hence increased presence of electrons in the system. This is observed as a steeply decreasing ORP. The flatness of Region II was attributed to the balance between oxidzing and reducing powers in the system owing to the air supplied to the fermentation broth as a consequence of ORP control. This balance is due to the oxidizing nature of oxygen in air that acts as an electron acceptor. Towards the end, equilibrium shifts towards a highly oxidizing environment as a result of ethanol toxification, substrate exhaustion and the resulting reduction in metabolic activity. An increase in ORP is usually a sign of reducing concentration of electrons in the system. Hence, the increasing ORP values in Regions III and IV represent the late stationary and death phases. This is the case when yeast activity decreases accompanied by the consumption of NADH.

Redox potential has been used in several instances as a measure of fermentation progress in VHG ethanol fermentations. Feng et al. (2012) is a classic example of such work. Redox potential here was used to determine the point at which fresh feed was to be delivered for a fed-batch ethanol fermentation process. But, the inability to completely consume glucose in the case of 250g/L feed glucose concentration resulted in the failure of this process being used for

glucose concentrations higher than 200g/L. One of the interesting conclusions obtained through this study was the ability of yeast to adapt to ethanol concentrations higher than 85g/L resulting in cell viabilities over 90% even towards the end of a given cycle when substrate concentrations were close to zero.

Liu et al. (2011a, 2011b) utilized ORP as a control measure to improve fermentation efficiencies in VHG environments. They hypothesized ORP could be controlled by sparging air into the fermentation broth. The basis behind their hypothesis was that ORP being a measure of the number of electrons/protons in the system, the oxygen supplied into the fermenter would act as an electron acceptor and maintain the balance of electrons between source and sink. A higher ORP indicated an abundant supply of electron acceptors while a lower ORP indicated a dearth in electron acceptors to compensate for the electrons released into the system by yeast.

Controlled fermentations were carried out in batch and continuous modes to assess their efficacies. It was concluded that maintaining ORP at specific levels (-50, -100 and -150mV) had different effects on the ethanol productivity of the process. While it was easy to maintain control for a longer period at -50mV, the duration of control reduced with decrease in the ORP values. The results also pointed to increased ethanol production at -150mV level when compared to -50mV for four different feed glucose concentrations (150, 200, 250 and 300g/L). Although, these results were promising, the major flaw with the control methodology utilizing ORP was the nature of the measurement made. Redox potential being a measure of electron activity is relative in nature. A relative measure changes with each process run depending on the initial conditions of the process. Thus, this stresses for a need for a novel control technique based on absolute measurements like dissolved CO_2 concentration.

1.2 Knowledge Gaps

A priori observations and fermentation process designs have taken into account only the inhibitory effects of external parameters like the presence of O_2 (aerobic/anaerobic), pH and temperature on the efficacy of the process. Although, inhibitions due to ethanol and glucose concentrations were considered, they did not account for the inhibitory effect of metabolic CO_2 that is present as dissolved CO_2. Moreover, only relations modeled on off-gas measurements exist to relate CO_2 evolution to the growth and activity of microorganisms. These relations do not take into account either inhibitions caused by high concentrations of ethanol and glucose in the fermentation system or the absence of equilibrium between off-gas and dissolved CO_2 in lab scale fermenters. Although authors have tried to establish various relations between off-gas and dissolved CO_2, the applicability of these relations to anaerobic fermentations has been severely restricted and in some cases impossible.

With earlier literature showing the use of CO_2 evolution rate in the off-gas stream to determine microbial activity, the ability of dissolved CO_2 to do the same has not been shown. However, works focused on a novel device for measuring dissolved CO_2 have been published (Kocmur et al., 1999; Shoda and Ishikawa, 1981; Sipior et al., 1996). The relations established so far between CO_2 evolution, glucose consumption and ethanol production no longer seem to be applicable for VHG environments. Moreover the focus of these investigations being CO_2 in the off-gas streams, their utility is rendered moot due to the absence of any measurement during the initial hours (0-12h) of fermentation (Daoud and Searle, 1990; Golobic and Gjerkes, 1999) owing to supersaturation of the fermentation broth with CO_2. Despite this drawback authors have persisted in their measurement of off-gas CO_2 to evaluate microbial growth, metabolite production and fermentation progress.

In addition to these drawbacks there is an utter lack of alternative control methodologies for VHG fermentations for bio-ethanol production. The use of ORP, a relativistic measure, although unconventional might result in non-optimized and reduced ethanol production. Determining the relationship between glucose concentration, cell growth and CO_2 evolution could help in designing new processes and process control schemes for complete utilization of glucose in VHG fermentations. Moreover the new control methodology could help in alleviating dissolved CO_2 based inhibitions in VHG fermentations and improve fermentation performance.

1.3 Objectives

Based on the knowledge gaps identified above the objectives established for the current investigation are listed below. The current investigation proposes to

i. Observe dissolved CO_2 and metabolite concentration profiles for batch fermentations using *S. cerevisiae* under different glucose concentrations.
ii. Assess and develop a semi-empirical relationship between dissolved CO_2 concentration, CO_2 evolution and other physiochemical and biological fermentation parameters like glucose consumption and ethanol production to yeast growth.
iii. Develop a novel and alternative control strategy based on dissolved CO_2 measurement.
iv. Explore the ability of the developed control strategy to improve ethanol production and fermentation performance under VHG conditions.

1.4 Approach

To observe the dissolved CO_2 concentration profiles during VHG fermentation, a commercial dissolved CO_2 sensor was used in batch fermentations under various glucose concentrations. Distinctions between high gravity and very-high-gravity fermentations were

created by using four different glucose concentrations; two concentrations each for high (150 and 200 g/L and very-high-gravity (250 and 300 g/L) conditions.

Development of the semi-empirical relationship was achieved through the application of basic mass balance principles. The physical significance of the terms in the equation was reiterated through various physiochemical and biochemical processes occurring in the fermentation system and a comprehensive analysis of the characteristics of the dissolved CO_2 concentration profiles obtained through direct measurement during fermentation.

Control of dissolved CO_2 was achieved through a series of experiments designed with different CO_2 set points (SP) and different control strategies. Two primary control strategies were explored during the course of this investigation; one involving the use of calcium hydroxide, an inorganic particulate compound and the other using air sparged through the fermentation broth. Due to the inability of calcium hydroxide to sustain cell viabilities at acceptable levels, only dissolved CO_2 control with air was explored further through utilization of two different aeration rates.

The quantity of air supplied along with the final ethanol concentration, glucose conversion efficiency and ethanol productivity were used to evaluate the effectiveness of this novel control strategy and elucidate the advantages and disadvantages of using such control in batch fermentations to efficiently produce high concentrations of ethanol.

CHAPTER 2
EXPERIMENTAL MATERIALS AND METHODS

2.1 Strain and Growth Media

Ethanol Red^{TM} strain of Saccharomyces cerevisiae obtained as dry yeast from Lesaffre Yeast Corp. (Milwaukee, MI, USA) was used during the course of this investigation. Prior to utilizing them batch fermentations, the dry yeast was rehydrated with 50 mL sterilized water, and cultured in YPD agar (10 g/L yeast extract, 10 g/L peptone, 20 g/L dextrose, and 20 g/L agar). Two sub-culture steps were performed to purify yeast strains and were stored in YPD agar coated petri dishes at 4 °C for later use.

The fermentation media was divided into three portions; part A: the required glucose concentration in 600 mL of reverse osmosis (RO) water; part B: 1% (w/v) of yeast extract, 0.2% (v/v) of $MgSO_4$ and 1% (v/v) of Urea in 100 mL of RO water; part C: 0.1% (w/v) of L-(+)-Sodium Glutamate Monohydrate, 0.5% (v/v) of KH_2PO_4, 0.1% (v/v) of $(NH_4)_2SO_4$ and 0.1% (v/v) each of H_3BO_3, Na_2MoO_4, $MnSO_4 \cdot H_2O$, $CuSO_4$, KI, $FeCl_3 \cdot 6H_2O$, $CaCl_2 \cdot 2H_2O$ and $ZnSO_4 \cdot 7H_2O$ in 100 mL of RO water. The concentration of each stock solution used in the media is given in Table 2.1. These portions were steam sterilized at 121 °C for 15 min as such and mixed aseptically in the fermenter/bioreactor after they cooled down to room temperature prior to fermentation. The fermentation media was made-up to the working volume by adding sterilized RO water to the mixture. Yeast extract was obtained from HiMedia Laboratories (Mumbai, India). All other chemicals were of reagent grade or higher purity.

Table 2.1 Concentration of media constituents used as their stock solutions.

Media Constituent	Concentration (M)
Ammonium sulphate, NH_4SO_4	1
Calcium chloride dihydrate, $CaCl_2.2H_2O$	0.082
Copper sulphate, $CuSO_4$	0.0100
Ferric chloride, $FeCl_3.6H_2O$	0.1000
Hydrogen borate, H_3BO_3	0.0240
Magnesium sulphate heptahydrate, $MgSO_4.7H_2O$	1
Manganese sulphate, $MnSO_4.H_2O$	0.0020
Potassium iodide, KI	0.0018
Potassium phosphate (monobasic), KH_2PO_4	0.7350
Sodium molybdenate, Na_2MoO_4	0.0015
Urea	1.6000
Zinc sulphate heptahydrate, $ZnSO_4.7H_2O$	1

2.1.1 Yeast Pre-culture

Prior to inoculation in the fermenter, yeast grown on agar was pre-cultured till the mid-exponential phase in shake-flasks with a working volume of 100 mL for 18 hours at 32.3 °C in an incubator-shaker at 120 rpm. The media for shake-flask cultures was separated into two parts; part A: the required glucose concentration (0.15, 0.20, 0.25 or 0.30% (w/v)) in 90 mL of RO water; part B: 1% (w/v) of yeast extract, 0.2% (v/v) of $MgSO_4$ and 0.5% (v/v) of Urea in 10 mL of RO water. All media constituents used from stock solutions follow the concentrations given in Table 2.1. The media was steam sterilized in an autoclave at 121 °C for 15 min and allowed to

cool down to room temperature prior to mixing. Yeast inoculation from agar plates was done aseptically after mixing.

2.2 Batch Fermentation

2.2.1 Experimental Set up

Production and concentrations of ethanol and CO_2 by *S. cerevisiae* from glucose substrates under VHG conditions was investigated using a batch fermentation process. The fermentation apparatus used in the work were jar fermenters (Model: Omni Culture, New York, NY, USA) with a capacity of 2 L and a 1 L working volume (Figure 2.1). The fermenter was covered with a detachable stainless steel (SS) lid screwed to the top of the jar to maintain sterility during the process. The cover was equipped with ports accessible for measuring temperature, agitation speed, dissolved CO_2 concentration and redox potential. Agitation was achieved through a six-bladed impeller mounted to the agitator shaft that was fixed to the SS cover.

2.2.2 Measurement of Dissolved Carbon dioxide and Redox Potential

Measurement of dissolved CO_2 was done using a commercial autoclavable dissolved CO_2 sensor (InPro®5000, Mettler-Toledo, Bedford, MA, USA). The measurement was done using an M400 controller (Mettler-Toledo, Bedford, MA, USA) and acquired using LabView (Version 8.5, National Instrument, Austin, TX, USA). The calibration of the sensor was performed using 1-point and 2-point procedures provided by the manufacturer using pH buffers of 7.0 and 9.21 at 25 °C. It is to be noted that the measurement of dissolved CO_2 by the InPro®5000 is based on the Severinghaus potentiometric principle (Janata, 2009; Kocmur et al., 1999), which has been previously used to develop and build custom dissolved CO_2 sensors (Ho and Shanahan, 1986; Shoda and Ishikawa, 1981; Zosel et al., 2011;) .

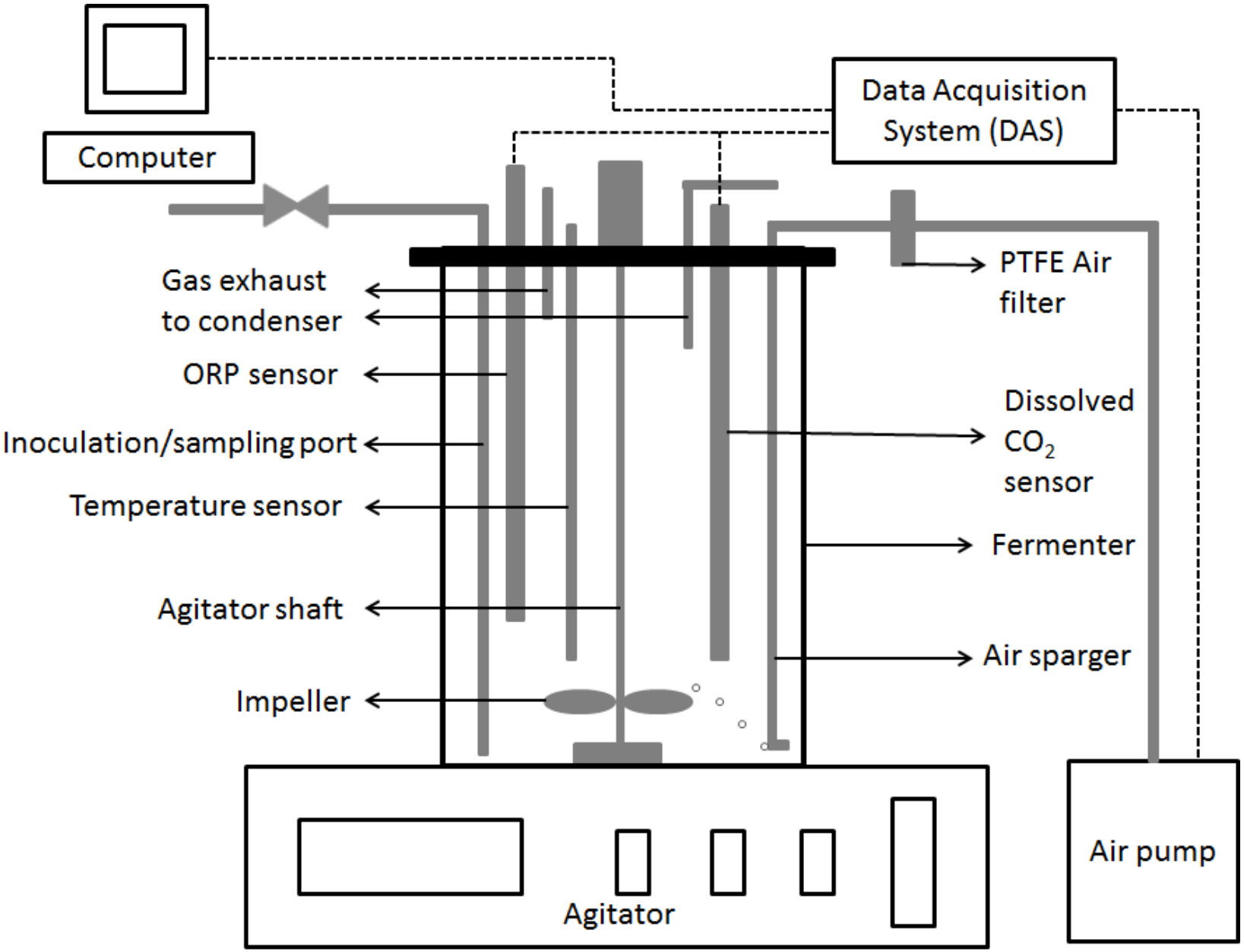

Figure 2.1 Line diagram of the experimental set-up used to perform batch ethanol fermentation

Autoclavable ORP electrodes from Cole-Parmer Inc. (12 mm x 250 mm, Vernon Hills, IL, USA) were used to measure ORP values during batch fermentations. All measurements made through different sensors were acquired using a custom built data acquisition system (DAS) and LabView.

2.2.3 Control of Dissolved Carbon dioxide Concentration

Dissolved CO_2 concentrations during fermentations were controlled using two different techniques. Control was achieved by either using a mixture of calcium hydroxide ($Ca(OH)_2$) and fermentation media or air. Dissolved CO_2 control set points were set based on the maximum solubility of CO_2 in aqueous fermentation media. The maximum solubility of CO_2 in fermentation media is in the range of 1.5-1.8 g/L (Spinnler et al., 1987). The solubility of CO_2 is influenced by the presence of organic and inorganic salts in the fermentation media (Royce and Thornhill, 1991; Royce P. N., 1992). Based on this premise three different dissolved CO_2 control set points were chosen for glucose feeds of ca. 250 g/L while two different set points were chosen for glucose feeds of ca. 300 g/L. Control of dissolved CO_2 was achieved using a PID control algorithm implemented through a LabView VI (Version 8.5, National Instrument, Austin, TX, USA).

2.2.3.1 Carbon dioxide Control using Calcium hydroxide

Calcium hydroxide is a well-known absorbent for CO_2 and is being investigated as a primary sink for CO_2 in sequestration studies (Rendek et al., 2006). The ability of $Ca(OH)_2$ to store CO_2 is enhanced by its ability to store it in solid form as calcium carbonate ($CaCO_3$). The conversion of $Ca(OH)_2$ to $CaCO_3$ follows Equation 2.1

$$Ca(OH)_2 + CO_2 \rightarrow CaCO_3 + H_2O \qquad (2.1)$$

Calcium carbonate is an inert solid as far as ethanol fermentation is concerned. Calcium carbonate does not ionize and hence has negligible to no effect on yeast growth and survival and hence ethanol production. Moreover, the removal of the $CaCO_3$ formed as a result of CO_2 absorption can be achieved through simple decantation of the spent fermentation broth. This is possible since $CaCO_3$ is insoluble in aqueous media.

The ability of calcium hydroxide to absorb CO_2 is based on the dissociation of calcium hydroxide to calcium (Ca^{2+}) and hydroxide (OH^-) ions in aqueous solution (Equation 2.2). The dissociation of $Ca(OH)_2$ is highly favored as indicated by the very high value of its dissociation constant (pKa = 13). The mechanism for the absorption of CO_2 is illustrated in Equations (2.3). The bicarbonate ion is derived through equilibrium reactions described earlier in Equations (1.4-1.5). Although fermentation pH does not support high concentrations of CO_2 in the form of HCO_3^- ions, the increase in pH brought about by the addition of calcium hydroxide would shift the equilibrium towards the conversion of CO_2 (aq.) to HCO_3^- as per Equations (1.4-1.5). In order to counteract the effect of dilution brought about by addition of an aqueous solution to the fermentation media, the $Ca(OH)_2$ suspension was mixed with fresh glucose feed with final feed glucose and $Ca(OH)_2$ concentrations of 250 g/L and 20 g/L respectively.

$$Ca(OH)_2 \rightarrow Ca^{2+} + 2OH^- \tag{2.2}$$

$$Ca^{2+} + HCO_3^- \rightarrow CaCO_3 + H^+ \tag{2.3}$$

For the purpose of controlling dissolved CO_2 concentration in the broth the fermenter was made accessible to three peristallic pump heads (Model 7013-20 and Model 7014-20, Cole-Parmer Canada Inc., QC, Canada). The smaller head was connected to the nutrient and control

solution reservoir, while the bigger head was used to discharge spent fermentation broth from the fermenter. The working volume was kept constant by maintaining the harvesting tube at a fixed position. Level maintenance was achieved through simultaneous addition of nutrient and control solution and removal of spent broth to and from the fermenter respectively through the PID controller.

2.2.3.2 Carbon dioxide Control using Air

Based on the acquired dissolved CO_2 concentration signal, the PID controller was used to actuate an air pump. Air from the pump was passed through a polytetrafluoroethylene (PTFE) membrane filter (PN 4251, Pall Corporation, Ann Arbor, MI, USA) prior to being bubbled through the broth by a sparger. As mentioned earlier in Section 1.1.4, air was selected based on is ability to not only remove dissolved CO_2 but also supply O_2 to the broth.

2.2.4 Fermentation Conditions

The fermentation of glucose to ethanol was carried out aseptically in the steam sterilized fermenter at a working volume of 1 L. The variation in initial glucose concentrations among experiments in the absence as well as presence of control was expressed in terms of standard deviation values between the different initial glucose concentrations. It is to be noted that experiments were performed in triplicate for batches without control and in duplicate for batches under dissolved CO_2 control. The media in the fermenter was inoculated with yeast from the pre-culture flask at 5 % of the working volume, and the pitching rate was adjusted to ca. 10^7 viable yeast cells per mL for all experiments. The temperature of the broth was maintained at 33 °C by circulating water at 33 °C through the equipped heating/cooling coil of the fermenter. The agitation speed was maintained at 150 rpm for the duration of fermentation. Samples for analytical analysis were withdrawn as 5-mL fermentation broth aliquots every 4-6 hours.

2.2.5 Analytical Analysis

The withdrawn aliquots were analyzed for biomass and cell viability. The biomass was estimated semi-empirically in terms of optical density (OD) measurements made using a colorimeter (Klett^{TM} Colorimeter, Belart, NJ, USA) at 600nm. The OD values were calibrated for different values against cell dry weight (CDW) of yeast in order to obtain biomass concentrations for different OD values. Cell viabilities were estimated using the methylene violet staining technique (Smart et al., 1999). In this technique yeast cells were stained with methylene violet stain and observed and counted under a microscope on a hemacytometer (Hausser Scientific, Horsham, PA, USA).

2.2.5.1 Analysis of Carbohydrates and Organic Acids

2 mL of the aliquots were centrifuged at 10,000 rpm for 10 minutes and the concentrations of sugars and organic acids in the culture supernatants were analyzed by HPLC (Series 1100, Agilent Technologies, Mississauga, ON) equipped with a refractive index (RI) detector (HP 1047A, Hewlett Packard, Mississauga, ON). The metabolites were separated using an ion exclusion ION-300 column (Transgenomic, Inc., Omaha, NE, USA) with 8.5 mM H_2SO_4 at 0.4 mL/min as mobile phase. The column temperature was maintained at 65 °C and the RI detector temperature was maintained at 35 °C during the course of analysis. Each sample was injected into the column three times as 10 µL injections each and subject to analysis.

2.3 Determination of Ethanol Toxic Concentrations

Toxic ethanol concentration limits were determined with the help of shake-flask experiments. Shake-flasks with media composition same as that described in Section 2.1.1 were used for this purpose. In addition to the growth medium, ethanol in concentrations varying from 4 % (v/v) through 12 % (v/v) in 2 % increments were added to the shake-flasks. The flasks were

inoculated with yeast and cultured at 32.8 °C at 120 rpm for 24 hours. Measurements of biomass, cell viability and analysis of carbohydrates, organic acids and ethanol were made every two hours during this culture period. Procedures for same have been described earlier in Section 2.2. The biomass and ethanol concentrations were smoothed by a three-parameter logistic growth model as described in Section 2 of Liu et al. (2011a). A plot of biomass production rate (first-order derivative of biomass concentration against time) vs. ethanol concentration was created. The ethanol concentration corresponding to where the biomass production rate approaches to zero was considered to be the ethanol toxic concentration. This toxic ethanol concentration limit was determined to be 85 g/L.

CHAPTER 3
RESULTS AND DISCUSSIONS

The observed dissolved CO_2 concentration profiles in the presence and absence of control for four different glucose concentrations of 150, 200.05±0.21, 250.32±0.12, and 300.24±0.28 g/L are discussed here. While feeds of ~150 and ~200 g glucose/L represent high-gravity fermentations, very-high-gravity fermentations are represented by feeds of ~250 and ~300 g glucose/L. These profiles are representative of the absolute concentration of CO_2 present in the form of dissolved CO_2. Section 3.1 deals with batch fermentations in the absence of any form of control. A theoretical equation based on these observations and relating yeast activity with dissolved CO_2 concentration has also been developed in Section 3.1. The observed dissolved CO_2 profiles have been interpreted in terms of this mathematical relationship. Sections 3.2 discusses results obtained in the presence of a dissolved CO_2 based control methodology in detail and contrasts them with those observed in the absence of control in terms of fermentation rate, performance and efficiency of conversion of glucose to ethanol. A short comparison of the dissolved CO_2 profiles observed under control with the ORP profiles observed in an earlier work (Lin et al., 2010) is also presented in Section 3.3.

3.1 Dissolved Carbon dioxide Concentration and Yeast Growth

To render a theoretical aspect to the measured dissolved CO_2 concentrations and establish a theoretical relationship in terms of physiochemical and biological processes that occur in the fermentation broth, a mass balance equation based on dissolved CO_2 was developed. This mass balance is shown in Equation (3.1). The left hand side (LHS) of Equation (3.1) relates the accumulation of CO_2 as dissolved CO_2 in the fermentation broth as a result of the deficit between

generation and removal of dissolved CO_2 from the fermentation broth owing to the solubility of CO_2 represented on the right hand side (RHS) of Equation (3.1).

$$\left\{\begin{array}{l}\text{Rate of accumulation}\\ \text{of } CO_2 \text{ in aqueous}\\ \text{phase}\end{array}\right\} = \left\{\begin{array}{l}CO_2 \text{ evolution rate}\\ \text{by yeast}\end{array}\right\} - \left\{\begin{array}{l}CO_2 \text{ desorption rate}\\ \text{by physiochemical}\\ \text{process}\end{array}\right\} - \left\{\begin{array}{l}\text{Rate of conversion}\\ \text{of } HCO_3^- \text{ from } CO_2\end{array}\right\} \quad (3.1)$$

The first term on the RHS of Equation (3.1) refers to the rate of generation or production of CO_2, otherwise known as CO_2 evolution rate (*CER(t)*), by yeast as a result of metabolic activity. Metabolic activity being a function of yeast growth can be represented in terms of yeast specific growth rate and instantaneous biomass concentration (Equation 3.2). A constant is used to represent the quantity of CO_2 generated per unit concentration of biomass. Thus, *CER(t)* is related to yeast growth with the assumption that μ is representable of $\hat{\mu}$ and Y_{CO_2} is regarded as constant over the period of fermentation.

$$CER(t) = \mu X Y_{CO_2} \quad (3.2)$$

During VHG batch ethanol fermentation *S. cerevisiae* follows four distinct growth phases viz. lag, exponential, stationary and death phase (Lin et al., 2010; Liu et al., 2011a). While an increase in viable biomass is usually witnessed from the lag to the exponential phase, it remains nearly constant during the stationary phase and decreases abruptly in the death phase. Consequently, *CER(t)* being a function of viable biomass and CO_2 being a metabolic by-product, the value of *CER(t)* increases with the viable cell concentration during the lag and exponential phases and begins decreasing during the stationary phase. As viable cell concentrations drop during the death phase, so does the associated *CER(t)* in Equation (3.2) due to the decline in *X*. This decrease in CO_2 evolution can be attributed to the slowing down of yeast metabolism in the

stationary phase and the absence of it in the death phase. Thus Equation (3.2) relates CO_2 produced during fermentation to yeast activity in the fermenter. In addition, this equation can also be utilized to relate ethanol production to yeast activity during fermentation. Ethanol being a primary metabolite is produced only in the presence of active growth. Hence, a decrease in *CER(t)* not only indicates a reduction in viable cells, but also points to reduction in ethanol production during fermentation.

To mathematically express the conversion of dissolved CO_2 to HCO_3^- ions as a result of pH fluctuations affecting the equilibrium between the different forms of existence of CO_2 in aqueous media, Equations (1.4-1.5) are considered. Based on these equations, the term corresponding to the third term on the RHS of Equation (3.1) was derived in Appendix. The derived term is given in Equation (3.3).

$$\frac{d([HCO_3^-])}{dt} = \frac{k_b[H^+]}{K_1}\left\{\frac{K_1}{[H^+]}[CO_2] - [HCO_3^-]\right\} \tag{3.3}$$

Equation (3.3) considers CO_2 present only in the form of HCO_3^- ion and not as CO_3^{2-} ion due to the pH of the system. Under pH of 4-6 witnessed in the present case, it was reported that less than 0.3% of CO_2 exists as CO_3^{2-}, about 3% exists as HCO_3^- and the rest exists as dissolved CO_2. Carbon dioxide present as dissolved CO_2 over and above the equilibrium concentration, in theory, is desorbed into the fermenter headspace (Frahm, et al., 2002; Fig. 1 of Zosel et al., 2011).

Desorption of CO_2 from the aqueous to the gas phase is a physical process contingent upon the concentration gradient of CO_2 between these two phases. This aspect of CO_2 behavior is represented in the 2nd term on the RHS of Equation (3.1). In mass transfer, the rate of transfer

of mass owing to a concentration gradient is governed by the volumetric mass transfer coefficient, a constant for any given system. In the present experiment, the volumetric transfer coefficient remains constant throughout the fermentation process due to the maintenance of constant agitation rates and the absence of any air flow within the fermenter. Equation (3.4) clarifies this aspect of Equation (3.1).

$$CO_2 \text{ desorption rate} = K_L^{CO_2} a([DCO_2] - \frac{p_{CO_2}}{H^{CO_2}}) \tag{3.4}$$

The rate of desorption is a function of the CO_2 concentration gradient between the gas and liquid phase. The gas phase equilibrium concentration of CO_2 is expressed in terms of partial pressure as governed by Henry's Law in Equation (3.4). Fermentation broths, under lab scale experimental conditions, are always supersaturated with dissolved CO_2 while microorganisms are metabolically active (Frahm, et al., 2002; Ho and Shanahan, 1986; Kuriyama et al., 1993; Song et al., 2007; Zosel et al., 2011). This is due to the very high solubility of CO_2 in aqueous media in comparison to the solubility of O_2 (Typically, in fermentation broths the solubility of CO_2 is ten times that of O_2) (Spinnler et al., 1987). Note that when concentration of the gas dissolved in an aqueous solution is above the equilibrium concentration, the solution is termed to be supersaturated with the gas.

Substituting Equations (3.2-3.4) in Equation (3.1) yields Equation (3.5).

$$\frac{d([DCO_2])}{dt} = CER(t) - K_L^{CO_2} a([DCO_2] - \frac{p_{CO_2}}{H^{CO_2}}) - \frac{k_b}{K_1}[H^+]\left\{\frac{K_1}{[H^+]}[DCO_2] - [HCO_3^-]\right\} \tag{3.5}$$

For simplicity, the following notations were substituted for terms in Equation (3.5). $C = [DCO_2]$; $V_{mt} = K_L^{CO_2} a$; $C_g = \frac{p_{CO_2}}{H^{CO_2}}$ and $\gamma = \frac{k_b}{K_1}[H^+]\left\{\frac{K_1}{[H^+]}[DCO_2] - [HCO_3^-]\right\}$.

$$\frac{dC}{dt} = CER(t) - V_{mt}(C - C_g) - \gamma \tag{3.6}$$

Equation (3.6) was further simplified for the purpose of discussion based on the processes they represent in Equation (3.1). The notations are as follows: $\alpha = CER(t)$ and $\beta = V_{mt}(C - C_g)$.

3.1.1 Dissolved Carbon dioxide Concentration and Evolution

Figure 3.1 and 3.2 show the dissolved CO_2 concentration profiles as observed for 150, 200.05±0.21 and 250.32±0.12, 300.24±0.28 g glucose/L respectively in batch fermentations in the absence of any form of control. The corresponding glucose and ethanol concentration profiles are illustrated in Figure 3.3. In order to describe the combined physical, chemical and biological effects attributable to the changes of dissolved CO_2 concentration in the fermentation broth during the course of VHG ethanol fermentation, the first order derivative was applied to the observed dissolved CO_2 concentration profiles shown in Figure 3.1 and 3.2. The derived profiles as illustrated at the bottom of Figures 3.1 and 3.2 are equivalent to the $\frac{dC}{dt}$ term of Equation (3.6). Two distinct regions are evident in these figures: the first region (Region I), where there is a peak in the accumulation rates, and the second region (Region II), where the accumulation rates remain at or below zero for all glucose feeds. A comparison of the accumulation profiles with their corresponding dissolved CO_2 profiles (Figures 3.1-3.2) shows that transition from the first to the second region is not abrupt but rather spread over a 2-3 hour period of fermentation otherwise termed here as the transition period.

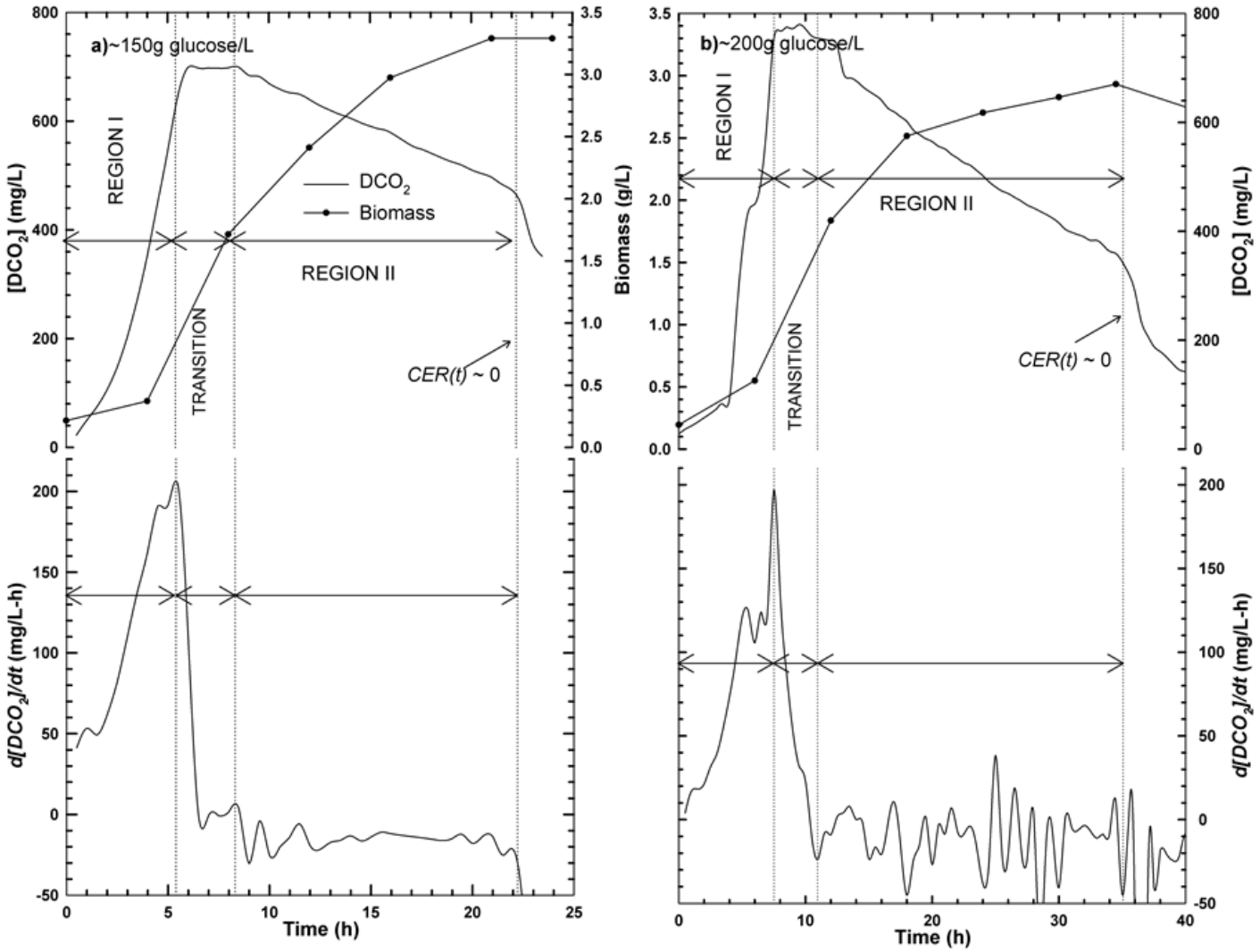

Figure 3.1 Representative profiles of biomass and dissolved CO_2 concentration and dissolved CO_2 accumulation observed during batch ethanol fermentation in the absence of control for a) 150 and b) 200.05±0.21 g glucose/L initial concentration from triplicate experiments. Distinct regions observed during batch ethanol fermentation in the absence of any form of control are demarcated by dotted lines in Figures 3.1 as well as Figure 3.2. The CO_2 accumulation rate ($\frac{d([DCO_2])}{dt}$) is the first-order derivative of the CO_2 concentration shown. '*CER (t)*~0' denotes zero glucose concentration and the resulting abrupt decline in yeast metabolism. Experiments were performed in triplicate.

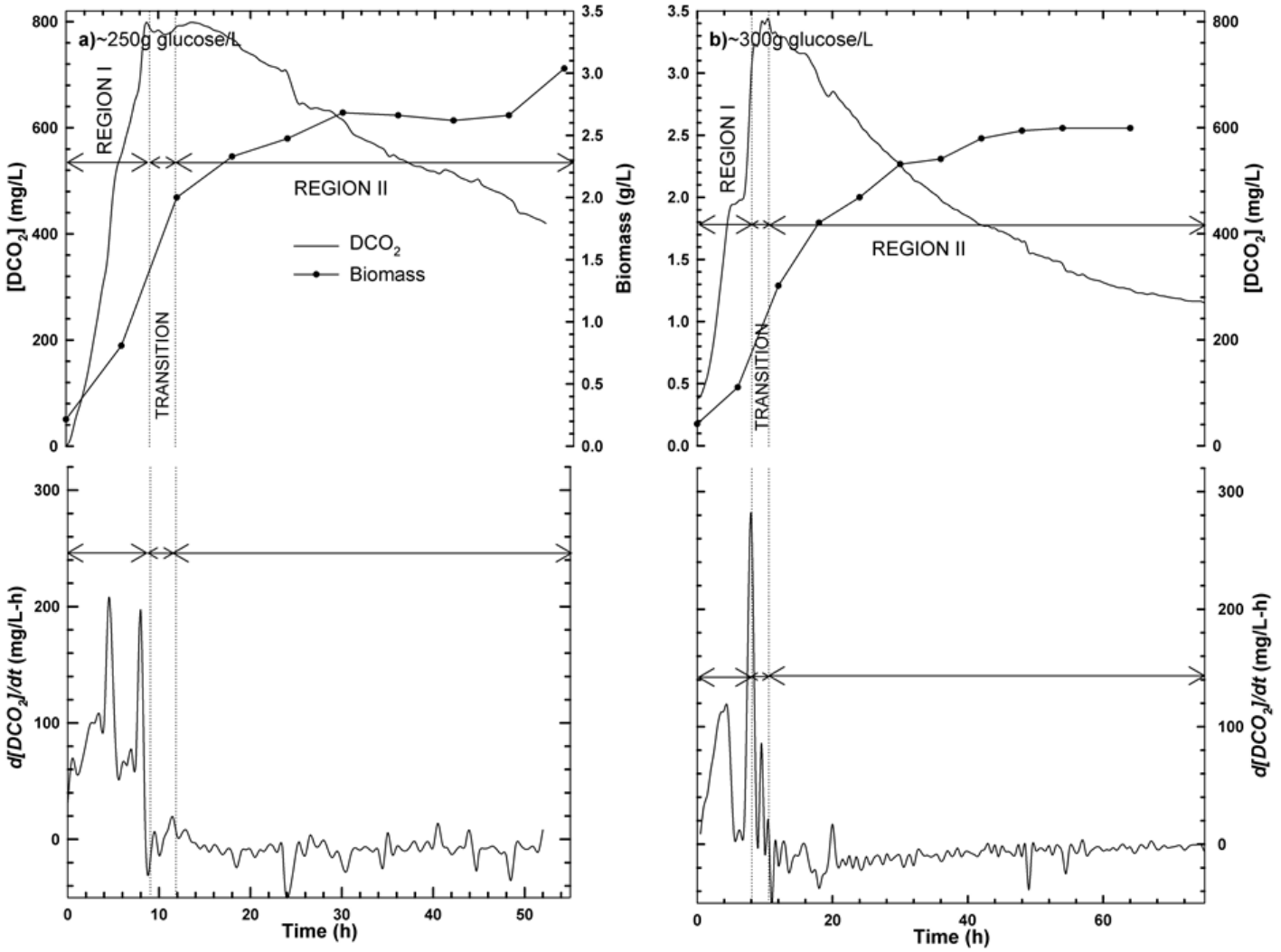

Figure 3.2 Representative profiles of biomass and dissolved CO_2 concentration and dissolved CO_2 accumulation observed during batch ethanol fermentation in the absence of control for a) 250.32±0.12 and b) 300.24±0.28 g glucose/L initial concentration from triplicate experiments. Note the absence of the characteristic drop in dissolved CO_2 concentration as seen in Figure 3.1.

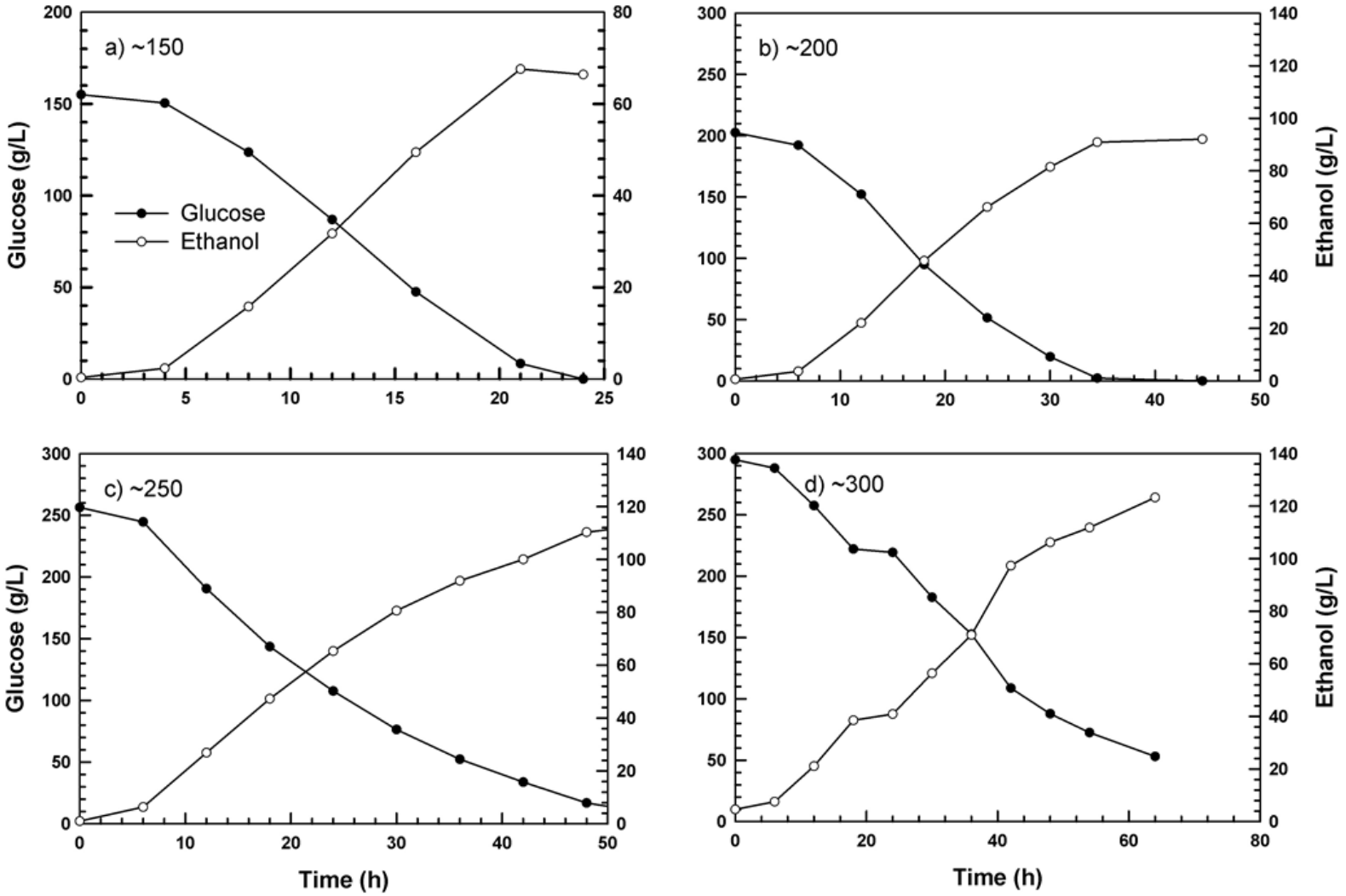

Figure 3.3 Representative concentration profiles of glucose and ethanol for a) 150, b) 200.05±0.21, c) 250.32±0.12 and d) 300.24±0.28 g glucose/L initial concentration in batch ethanol fermentation from triplicate experiments without control. Initial concentration greater than 200 g glucose/L results in residual glucose even after ~50 h of fermentation .

These regions can be interpreted in terms of Equation (3.6). During the lag and exponential phases of yeast growth where cell metabolism and hence CO_2 evolution are at their peaks, *CER(t)* is much higher resulting in $\alpha > (\beta + \gamma)$ in Equation (3.6) and a net $\frac{dC}{dt}$ (It is to be noted that *CER(t)* cannot be negative). This is seen in Region I of Figures 3.1-3.2. In Region I, *CER(t)* is much higher than the CO_2 desorption rate, resulting in a net CO_2 accumulation and a corresponding increase in dissolved CO_2 concentration. Although, the exponential phase lasts as long as 20h, (refer to biomass concentrations in Figure 3.1-3.2) the dissolved CO_2 concentration profiles do not directly correspond to the increase in biomass. This may be due to the fact that the biomass profiles are representative of the total cell concentration rather than the viable cell concentration making it indifferent to detect actual metabolic activity. It is also possible that desorption of CO_2 from the fermentation broth and other physiochemical processes affect measurement of dissolved CO_2 concentration. This would also explain the inability of the dissolved CO_2 concentration profiles to distinguish between the different stages of yeast growth. The peak in the profiles in Figures 3.1 and 3.2 also explains two facts that were stated earlier; (1) the fermentation broth is supersaturated with CO_2 as (2) the desorption of CO_2 does not increase exponentially with increasing dissolved CO_2 concentration.

A negative accumulation of dissolved CO_2, witnessed in Region II of Figures 3.1-3.2, is a physical outcome of CO_2 evolution rate being less than the CO_2 desorption rate resulting in a decreasing dissolved CO_2 concentration (Region II of Figure 3.1-3.2). Correspondingly in Equation (3.6) this would be represented as $\alpha < (\beta + \gamma)$ resulting in a negative $\frac{dC}{dt}$, with γ being considered negligible relative to either α or β. Note that γ value is one to two orders of magnitude

smaller than α and β. The decline in $\frac{dC}{dt}$ in Region II can be ascribed to the decrease in yeast metabolic activity.

Regions between Region I and Region II in Figures 3.1 and 3.2 are marked as transition regions. From the dissolved CO_2 profiles for four glucose concentrations it can be observed that the duration of this region decreases significantly from ~150 g/L to ~300 g/L, with ~150g/L having the longest transition period. It is postulated that the change in duration of the transition period from lower to higher glucose concentration is affected by the presence of high glucose concentrations, i.e. lower glucose concentrations have a longer transition period due to lower osmosis. Note that the residual glucose concentration at the end of the transition periods for 150, 200.05±0.21, 250.32±0.12, and 300.24±0.28 g glucose/L were ~130, ~165, ~210 and ~270 g glucose/L respectively; higher the initial glucose concentration, higher the residual glucose concentration. Inhibitory effects of ethanol on yeast activity were ruled out as the concentration of ethanol at the end of these transition regions were lower than the inhibitory concentration of 40g/L (18, 20, 30, and 28 g ethanol/L for ~150, ~200, ~250, and ~300 g glucose/L respectively; Figure 3.4). It is also possible that the osmotic effect due to higher glucose concentrations extends far beyond the lag phase into the exponential phase.

As illustrated in the dissolved CO_2 profiles, the dissolved CO_2 concentration remains nearly constant in the transition regions resulting in $\frac{dC}{dt}$ being zero for this period (Figure 3.1 and 3.2). Speaking in terms of the dissolved CO_2 mass balance described by Equation (3.6), this would mean $\alpha = \beta$ (assuming a negligible γ similar to previous cases under current operating conditions). In terms of physical quantities this would mean that the rate of removal of dissolved CO_2 from the fermentation broth by desorption is equal to rate of evolution of CO_2 from

microorganisms. This could be either due to the decrease in *CER(t)* (α) as a consequence of decrease in yeast activity or due to the increase in the CO_2 desorption rate (β).

3.1.2 Effect of Ethanol Toxicity and Osmosis on Carbon dioxide Evolution

Higher initial glucose concentrations tend to increase the osmotic stress, ultimately resulting in a longer lag phase (Liu et al., 2011a). Also the buildup of ethanol concentration may arrest yeast propagation, due to the toxic effect of the ethanol produced (Brown et al., 1981; Lin et al., 2010; Liu et al., 2011a;). Note that the ethanol toxic concentration for the yeast used in this study was determined to be ~85 g/L. Rationalization of the differences among the CO_2 accumulation rates and *CER(t)* observed between Region I and II of Figures 3.1 and 3.2 can be done based on the glucose concentration in the media and the toxic effect of ethanol produced by yeast.

The ethanol concentrations in the fermenter measured at the end of Region I of Figure 3.1 and 3.2 for ~150, ~200, ~250 and ~300 g glucose/L were 18, 20, 30, and 28 g ethanol/L, respectively. Notice that these ethanol concentrations are lower than the ethanol toxic level, 85 g/L. Hence, it is postulated that the delay of yeast growth is mainly attributed to the high initial glucose concentration rather than ethanol toxicity. This can be noticed in Figure 3.4 illustrating the cell viabilities and corresponding ethanol concentrations for four glucose concentrations. In Figure 3.4 the cell viabilities decrease with increasing ethanol concentrations as well as progress of fermentation. The drop in viabilities is more drastic with increasing glucose concentrations. Accordingly, due to increase in substrate concentration, yeast growth is enhanced albeit with a delay in the lag phase resulting in an increase of *CER(t)* in Equation (3.6). The absence of exponential increase in CO_2 desorption rate with increase in CO_2 evolution is

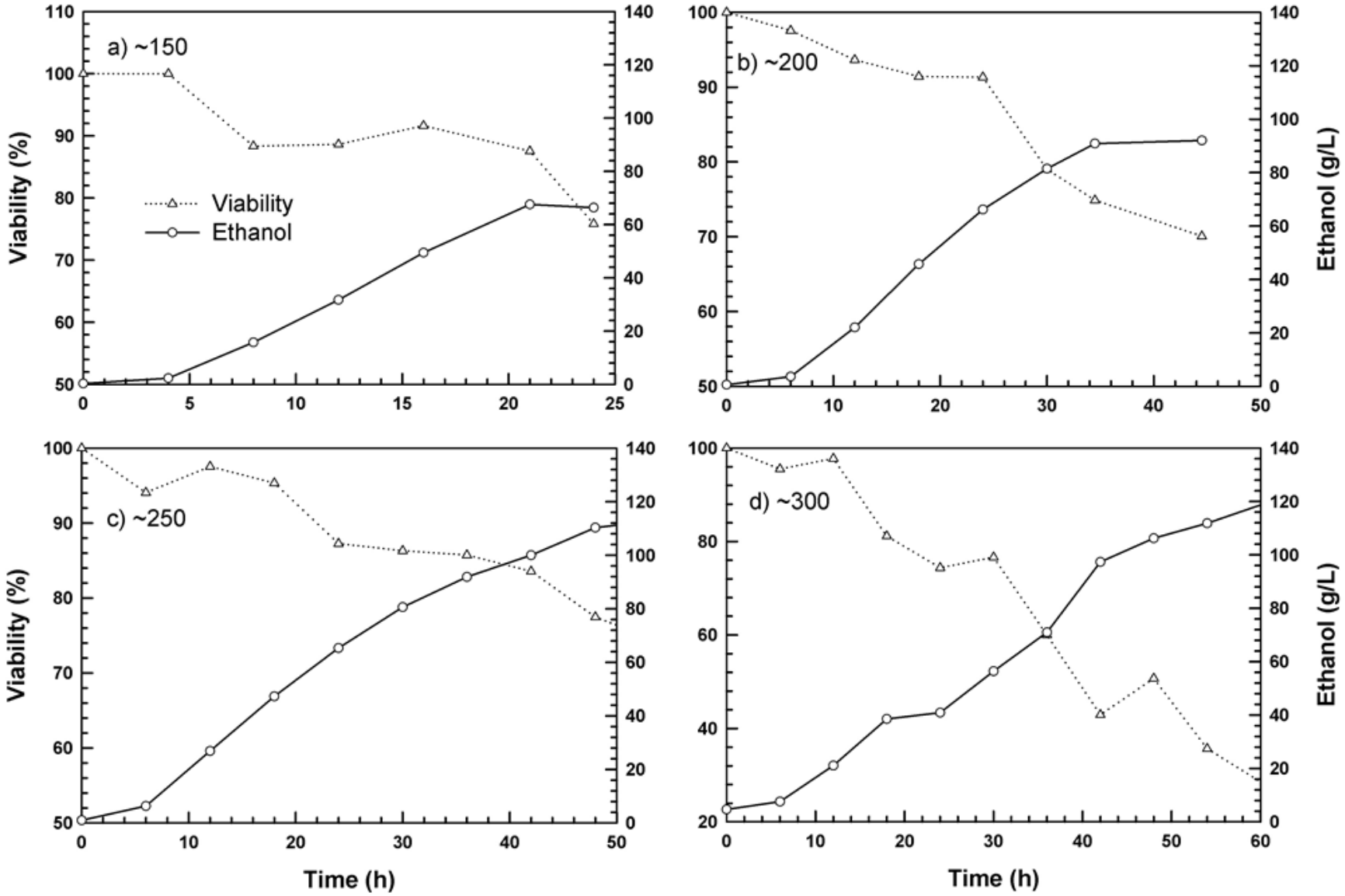

Figure 3.4 Representative plots of ethanol concentration and cell viability profiles corresponding to profiles in Figures 3.1-3.3. The drop in cell viability in high glucose concentration broths is precipitated further by higher ethanol concentrations.

reflected in the corresponding increase in dissolved CO_2 concentration and $\frac{dC}{dt}$ as shown in Figures 3.1 and 3.2. It was also inferred that due to the inability of the dissolved CO_2 profiles to differentiate among the distinct growth stages, especially the lag and exponential phases, it was not possible to observe the osmotic effect of higher glucose concentration on the lag phase from the existing dissolved CO_2 profiles.

In Region II of Figures 3.1 and 3.2, the glucose concentrations after 10-12h of fermentation are much lower than initial values, indicating a moderate reduction in osmotic stress for all four glucose feeds. At initial concentrations of ~150 and ~200 g glucose/L, final ethanol concentrations seen at the end of fermentation when, glucose is completely utilized, are 68 and 72 g/L respectively (Figure 3.3). Hence, yeast metabolism and the production of CO_2 were hampered by glucose depletion rather than ethanol toxicity (Figure 3.3 and 3.4). At initial concentrations of ~250 and ~300 g glucose/L, although sufficient glucose (75 and 150 g/L) is present even following the peak in CO_2 concentrations (32 and 34h respectively, where typically stationary phase begins; Lin et al., 2010; Liu et al., 2011a), the corresponding ethanol concentration exceeds the toxic level of 85 g/L (Figure 3.3 and 3.4). As fermentation continues, the adverse effect of ethanol toxicity worsens. The decrease in dissolved CO_2 concentration and evolution rates inferred from Region II of Figures 3.1 and 3.2 can be attributed to the death of yeast cells that cease to survive in ethanol concentrations exceeding the toxic level (Figure 2 in Lin et al. (2010) and Figure 3.4). Cessation of yeast growth and survival directly impacts the value of *CER(t)* and CO_2 accumulation. This is witnessed from Figure 3.2 where once past the transition region the dissolved CO_2 concentration starts decreasing and $\frac{dC}{dt}$ become increasingly negative.

From Equation (3.6) and Region II of Figure 3.1 and 3.2 it was further concluded that once accumulation of CO_2 in the aqueous phase ceased, there was no change in the rate of decrease of dissolved CO_2 concentration and the value of $\frac{dC}{dt}$ remained fairly constant till *CER(t)* approached zero (denoted by *CER(t)*~0 for the case of ~150 and ~200 g glucose/L and illustrated in Figure 3.1). But for the case of ~250 and ~300 g glucose/L there was no abrupt decline in the dissolved CO_2 concentration leading us to the observation that the point of *CER(t)*~0 was not evident from Figure 3.2. This observation led to the conclusion that the CO_2 desorption rate remained almost constant irrespective of the changing *CER(t)* provided, the assumption of a slowly decreasing *CER(t)* is valid. Thus from Equation (3.6) it can be inferred that the rate of CO_2 desorption remains fairly constant during the entire fermentation process. This strengthens the fact that equilibrium between off-gas CO_2 and dissolved CO_2 does not exist under our current experimental conditions. Furthermore, the decreasing gradient between dissolved and off-gas CO_2 concentrations will result in a reduced driving force for CO_2 desorption from the fermentation broth. Hence, it is postulated that the rate of desorption of CO_2 will decrease with decrease in dissolved CO_2 concentration in the fermentation broth.

3.2 Dissolved Carbon dioxide Control in Very-High-Gravity Fermentation

Subsequently, control of dissolved CO_2 concentration was incorporated into the VHG fermentation process. Earlier Liu et al. (2011a) had concluded that incorporating an ORP based control strategy did not provide any benefit to fermentations processes operated under initial concentrations less than 200 g glucose/L. In addition, glucose was completely consumed in fermentations with initial substrate concentration less that 200 g glucose/L within a reasonable period of time (Figure 3.1) Aiming to improve ethanol fermentation for feeds greater than 200 g glucose/L, dissolved CO_2 was controlled at three different levels of 500, 750 and 1000 mg/L for

the case of ~250 g glucose/L and at two levels of 750 and 1000 mg/L for ~300 g glucose/L. The dissolved CO_2 concentration profiles for each individual case have been presented in this section along with the corresponding biomass, glucose and ethanol concentration profiles.

Control was achieved either using $Ca(OH)_2$ or air. Control with $Ca(OH)_2$ although was capable of absorbing dissolved CO_2 and maintaining dissolved CO_2 levels as dictated by the set points despite its very low solubility, addition of $Ca(OH)_2$ to the fermentation broth reduced the ethanol concentration in the broth. Reduction of ethanol concentration defeated the very purpose of VHG ethanol fermentation which is to produce high concentrations of ethanol. Addition of $Ca(OH)_2$ also increased the pH of the fermentation broth beyond 6. This resulted in an environment non-conducive for yeast growth. Yeast ceases to function at or close to neutral pH. Hence, this caused cell viabilities to drop below 50 % after ~6 h of fermentation when control was initiated. A drop in cell viabilities would reduce yeast growth as well as ethanol production rates. As control using $Ca(OH)_2$ did not yield the desired results, following discussions pertaining to control are based on control achieved using air in their entirety

3.2.1 Characteristics of Dissolved Carbon dioxide Profiles in the Presence of Control

In their basic form the dissolved CO_2 profiles for initial concentrations of ~250 g glucose/L, can be split into 4 distinct regions irrespective of the level of control and aeration rate used. Figures 3.5 and 3.6 illustrate differentiation of the dissolved CO_2 profile into four distinct regions for the case of ~250 and ~300 g glucose/L respectively with dissolved CO_2 controlled at 750 mg/L. These four regions have been hypothesized to represent the different levels of yeast activity and growth phases during fermentation. Initially yeast metabolism is known to be slow during the lag and early exponential phases of growth resulting in slower production of CO_2. The osmotic effects induced by high initial glucose concentrations are known to compound this effect

resulting in an increased duration for the lag phase. The low biomass concentrations in Region I stand witness to this fact (Figure 3.5 and 3.6). Longer lag phase is seen in the form of increase in fermentation duration for ~300 g glucose/L in comparison to ~250 g glucose/L (Table 3.1). Hence, Region I in Figures 3.5 and 3.6 was hypothesized to characterize the lag phase and the very early part of the exponential phase.

The lag phase paves way for the exponential phase towards the end of Region I. Region II of Figures 3.5 and 3.6 characterize yeast growth during the mid and late exponential phases. The increase in metabolic activity in this phase results in increased CO_2 production and accumulation. In addition to the usual increase in metabolic rates witnessed in the mid-exponential phase, the supply of oxygen during transition from Region I to Region II, as a consequence of control is known to further enhance yeast vitality and consequently ethanol production (In reference to Equation (3.6), *CER(t)* is at its highest in this region). The sparged air in addition to supplying oxygen also aids in the stripping of dissolved CO_2 from the fermentation broth. Despite increased desorption, dissolved CO_2 profiles depict an increase in the dissolved CO_2 concentration over and above the set point values in Region II of Figures 3.5 and 3.6. This increase in concentration that can be construed as a net dissolved CO_2 accumulation, has been postulated to represent the additional increase in *CER(t)* owing to oxygen supply as well as CO_2 removal..

Table 3.1 Comparison of fermentation duration[a] in hours for fermentation under different dissolved CO_2 control set points and aeration rates used for control under ~250 and ~300 g glucose/L initial concentration for batch ethanol fermentation

Initial Concentration		~250 g glucose/L			~300 g glucose/L	
DCO_2 set point (mg/L)		500	750	1000	750	1000
Aeration Rate (mL/min)	820	26.35±0.21	27.70±0.85	26.65±0.64	41.65±1.63	32.5±0.0
	1300	26.50±0.71	27.50±0.56	27.45±1.91	36.80±1.13	36.30±0.71

Note: For uncontrolled batches under initial concentrations ~250 and ~300 g glucose/L presented in Section 3.1 glucose was not completely exhausted. Hence, the fermentation duration could not be accurately calculated and has been mentioned to be greater than 50 h.

[a]Fermentation duration was calculated on the basis of glucose concentration in the fermentation broth. A zero glucose concentration as pointed out by the dissolved CO_2 profile was considered as the end of fermentation.

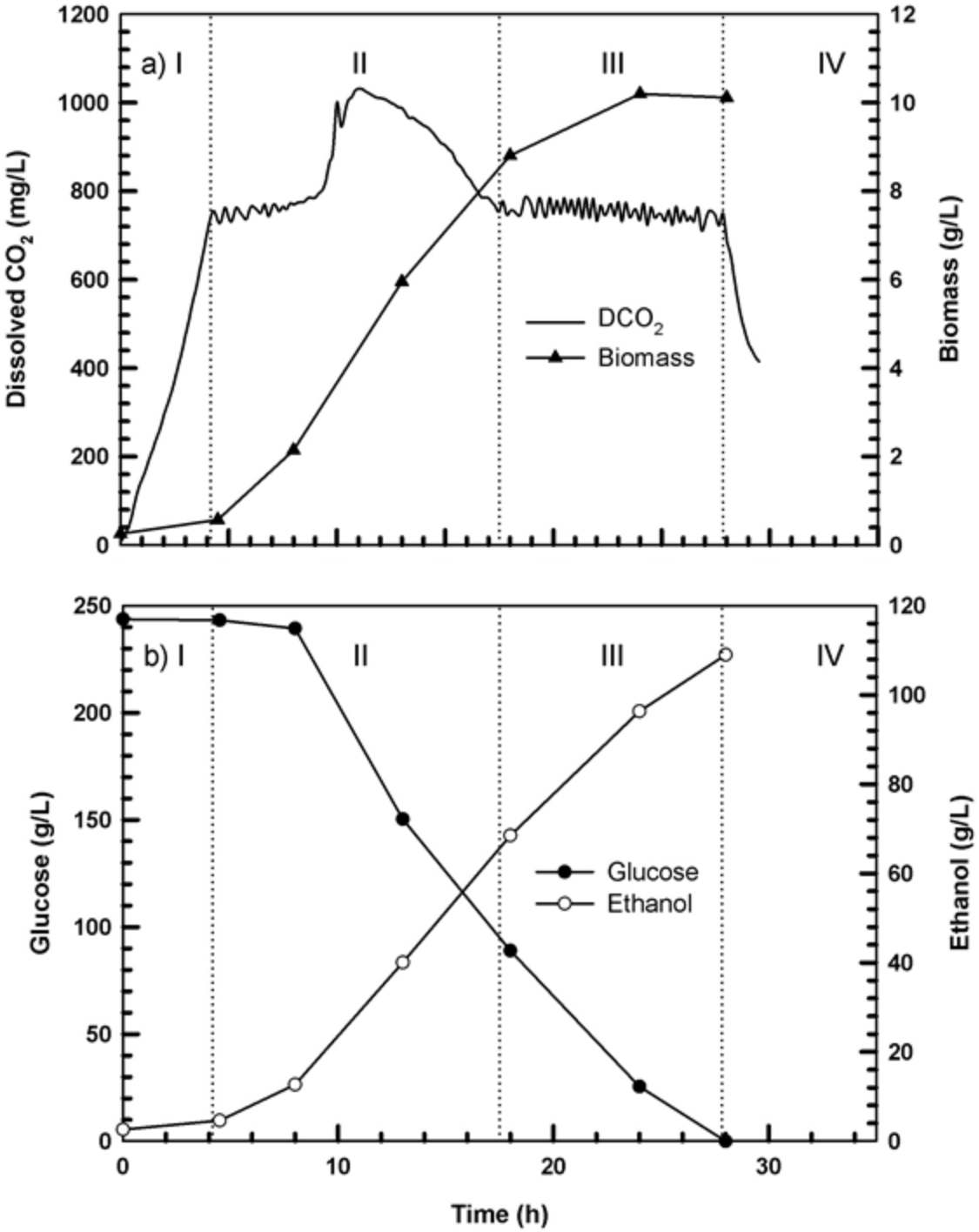

Figure 3.5 Concentration profiles of a) dissolved CO_2 and biomass and b) glucose and ethanol representing the 4 regions of the dissolved CO_2 concentration profile observed in the presence of control for initial concentration of 259.72±7.96 g glucose/L. Dissolved CO_2 was controlled at 750 mg/L using an aeration rate of 1300 mL/min.

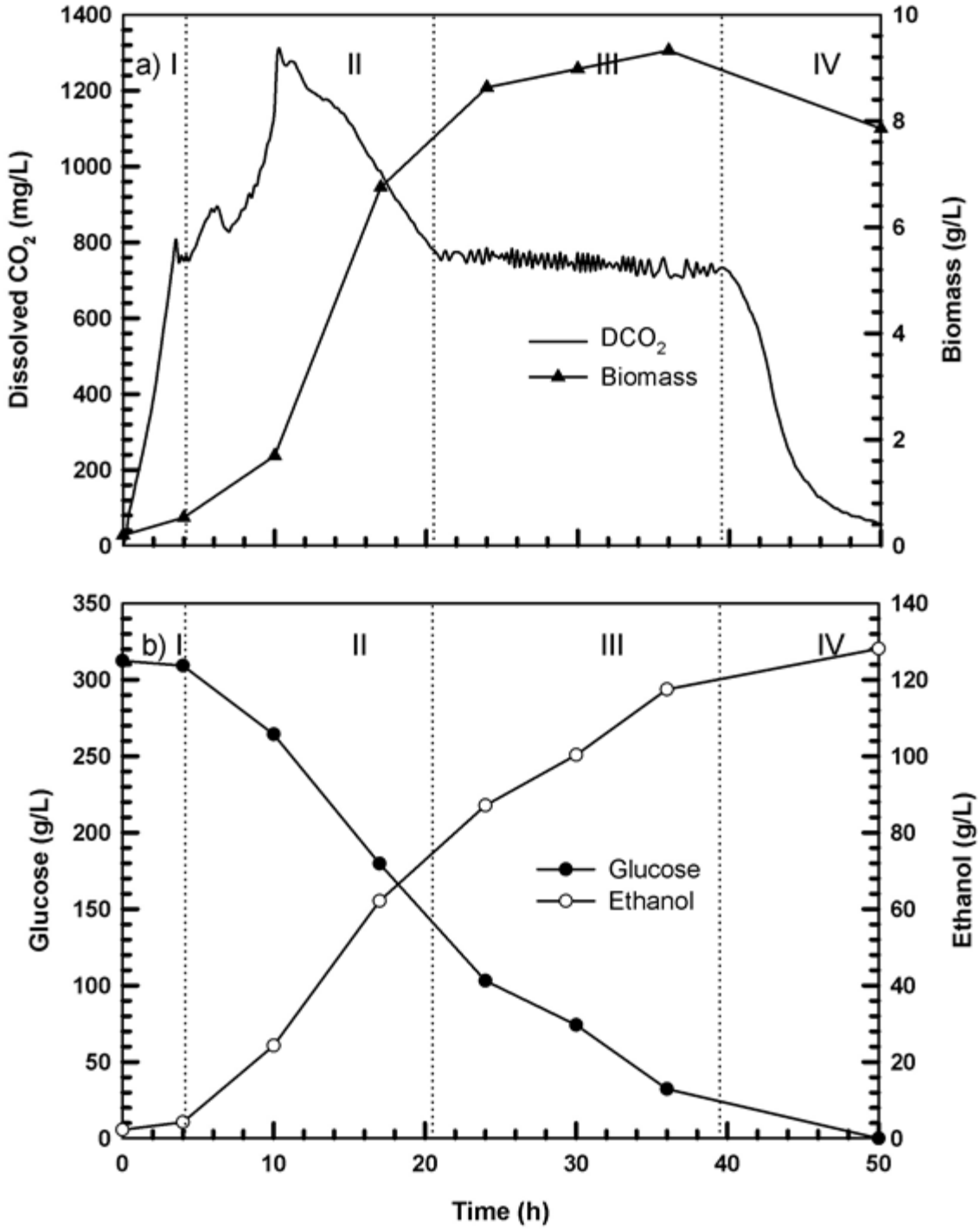

Figure 3.6 Concentration profiles of a) dissolved CO_2 and biomass and b) glucose and ethanol representing the 4 regions of the dissolved CO_2 concentration profile observed in the presence of control for initial concentration of 303.92±10.66 g glucose/L. Dissolved CO_2 was controlled at 750 mg/L using an aeration rate of 820 mL/min.

Further corroboration to this end can be obtained from the higher rate of change of biomass seen in Region II when compared to other regions. While the mid exponential phase is the pinnacle of yeast activity, the late exponential phase signifies the transition to stationary phase growth and the associated reduction in metabolic activity. The complete transition from exponential to stationary phase is postulated to be represented in Region III of Figure 3.5 and 3.6 where the absence of a net dissolved CO_2 accumulation is observed as an unchanging flat plateau in the dissolved CO_2 concentration profiles. In reference to Equation (3.6), the net accumulation of dissolved CO_2 in the fermentation broth, $\frac{dC}{dt}$ is almost zero in Region III.

While the absence of net CO_2 accumulation in Region III could be argued to be a result of increased stripping of CO_2 from the broth, in the present case it is rather a consequence of a decrease in CO_2 production due to drop in yeast metabolic activity. Thus in Equation (3.6), *CER(t)* reduces with no significant change to the rate of CO_2 desorption (β) in comparison to Region II. The decrease in yeast metabolism was inferred from the biomass profiles pertinent to Region III in Figures 3.5 and 3.6. The smaller change in biomass points to growth slowing down post-exponential phase and entering the stationary phase. Despite the reduction in metabolism, yeast still thrives in the fermentation broth with slight drop in viabilities (Figure 3.11) not only due to presence of substrate but also the supply of oxygen through air sparging (Figure 3.11 has been elaborated in Section 3.2.3.3). This ensures yeast survival as well ethanol production even in the stationary phase represented by Region III.

In Region IV of Figures 3.5 and 3.6 the balance between CO_2 production and stripping is offset. This departure from the balance that was present in Region III was attributed to complete substrate exhaustion (Figure 3.5b, 3.6b). Substrate exhaustion results in complete cessation of

yeast metabolism resulting in *CER(t)* in Equation (3.6) becoming zero. This resembles the condition similar to that which was illustrated in Section 3.1.1 where *CER(t)* is less than the rate of CO_2 desorption resulting in a net decline in dissolved CO_2 ($\frac{dC}{dt}$<0). The net decline is observed as the abrupt drop in the dissolved CO_2 concentration depicted in Region IV of Figures 3.5 and 3.6.

The features of the dissolved CO_2 profiles observed in the presence of a dissolved CO_2 based control strategy for VHG fermentation were characteristic for every batch for both initial concentrations of ~250 and ~300 g glucose/L. Except for certain specific cases (for 300 g glucose/L dissolved CO_2 controlled at 1000 mg/L under aeration rates of 820 and 1300 mL/min as well as dissolved CO_2 controlled at 750 mg/L under 1300 mL/min aeration) dissolved CO_2 profiles depicted a marked increase in dissolved CO_2 concentrations over and above the set point values in Region II for 250 as well as 300 g glucose/L.

3.2.2 Comparison of Profiles in the Presence and Absence of Control

While the dissolved CO_2 profiles observed in the absence of control displayed only three distinct regions viz., Regions I, II and a transition region (Figure 3.1 and 3.2), four distinct regions were exhibited when dissolved CO_2 was controlled viz., Regions I, II, III and IV (Figure 3.5 and 3.6).

The primary distinction between the profiles was the absence of a transition region between Regions I and II in the presence of control. Earlier the transition region observed in batch fermentations in the absence of control in Figures 3.1 and 3.2 was attributed to the possible extension of the osmotic effect, exerted by high initial glucose concentrations, beyond the lag phase and into the exponential growth phase of yeast. It was also postulated that the reduction in

the period of the transition region with increase in glucose concentrations from 150 to 300 g/L was due to this osmotic effect.

In the case of profiles observed in the presence of control, the absence of such a transition region could be explained in terms of yeast metabolism observed under conditions of dissolved CO_2 control. In the absence of control no oxygen was supplied to the broth between lag and exponential phases. This essentially would mean a lower level of metabolic activity in batches without control relative to batches with control. The reduced level of metabolic activity could be interpreted as a lower *CER(t)* value in Equation (3.6). It was earlier argued that either a decrease in the value of *CER(t)* or an increase in the value of β, as a result of increased CO_2 desorption would result in a condition where net accumulation of dissolved CO_2 does not occur. This was seen during the transition region in Figures 3.1 and 3.2. In contrast, the supply of oxygen as a consequence of control results in increased yeast metabolism towards the end of Region I and beginning of Region II. The consequential increase in *CER(t)* as a result of increased metabolism thereby eliminates any chance of zero accumulation. This effect is observed despite the increase in CO_2 desorption (β) brought about by air sparging. Hence, it is posited that no transition region is observed between Regions I and II when dissolved CO_2 is controlled through air sparging. Further differences between fermentation characteristics in the presence and absence of control could be made with the biomass concentrations and fermentation duration (Table 3.1). Biomass concentrations for fermentations without control are lower than that of fermentations where dissolved CO_2 was controlled (Figure 3.14). The higher biomass for controlled fermentations could be attributed to air sparging. Further elaboration in this regard has been given in Section 3.2.3.2.4. Higher biomass results in faster glucose consumption resulting in shorter duration for complete substrate utilization in controlled fermentations (Table 3.1).

While distinctions between dissolved CO_2 profiles in the presence and absence of control were focused on the transition region, it is observed that Region I in the dissolved CO_2 profiles in both cases have a similar trend. The similarity can be credited to the fact that Region I (for both cases) represents the lag phase growth of yeast during fermentation. In the lag phase or Region I, control of dissolved CO_2 does not play a role in altering fermentation characteristics in terms of yeast metabolism as is the case for the subsequent regions of the profile.

Similarities can also be pointed out based on the fact that dissolved CO_2 profiles are capable of representing complete glucose consumption during fermentation. While a non-zero residual glucose was observed for batches with initial ca. ~250 and ~300 g glucose/L in the absence of control (Figure 3.3), a zero residual glucose was observed for similar initial glucose concentrations in the presence of control (Figure 3.5 and 3.6). The point of zero residual glucose was portrayed by an abrupt drop in dissolved CO_2 concentration as observed in Region IV of the dissolved CO_2 profiles similar to the drops observed for batches of ~150 and ~200 g glucose/L (Figure 3.1). This observation concluded that irrespective of the presence of a control strategy, the dissolved CO_2 profiles were able to accurately represent complete glucose exhaustion in VHG fermentation environments.

3.2.3 Effect of Dissolved Carbon dioxide Set Point on Very-High-Gravity Fermentation

Controlling dissolved CO_2 at different levels yielded distinct values for the various fermentation parameters like glucose consumption, ethanol production and conversion efficiency. As reported earlier higher initial glucose concentrations (>200 g/L) resulted in incomplete and sluggish fermentations with unspent residual glucose present at the end of batches without a control strategy. Similar observations have also been reported by Feng et al. (2012) and Liu et al. (2011a) even under the presence of control. Incorporation of dissolved CO_2

control not only facilitated complete substrate consumption for initial glucose of ~250 as well as ~300 g/L but also reduced fermentation times and improved ethanol productivities. Contrasts among these observations could be drawn on the basis of the level of dissolved CO_2 control, the initial glucose concentrations and the aeration rate used to achieve control.

Incorporating the present control strategy in VHG fermentation processes achieves two objectives: 1) Removal of dissolved CO_2 from the fermentation broth and 2) Oxygenation of the broth through aeration. Thus, for control to improve fermentation both the aforementioned factors have to be manipulated at optimum levels. To choose the optimum set point, dissolved CO_2 was controlled at three distinct levels of 500, 750 and 1000 mg/L that represented 30, 45 and 60% of the maximum CO_2 solubility in fermentation media respectively. While this was the case for ~250 g/L initial glucose, only two set points of 750 and 1000 mg/L were used for ~300 g glucose/L. Dissolved CO_2 profiles observed when dissolved CO_2 was controlled for the case of ~250 and ~300 g glucose/L using different aeration rates are shown in Figures 3.7, 3.9, 3.10, 3.14 and 3.15. Figures 3.8, 3.11 and 3.16 illustrate the corresponding glucose and ethanol concentration and cell viability profiles.

3.2.3.1 Dissolved Carbon dioxide Controlled at 500 mg/L

3.2.3.1.1 Effect of carbon dioxide removal

Jones and Greenfield (1982) mentioned that CO_2 inhibited yeast growth through several physiological changes in yeast. Thus, choosing an appropriate set point to control dissolved CO_2 is of prime importance. Figures 3.7, 3.9, 3.10, 3.14, 3.15 display profiles for dissolved CO_2 controlled at 500, 750 and 1000 mg/L under different initial glucose concentrations and aeration

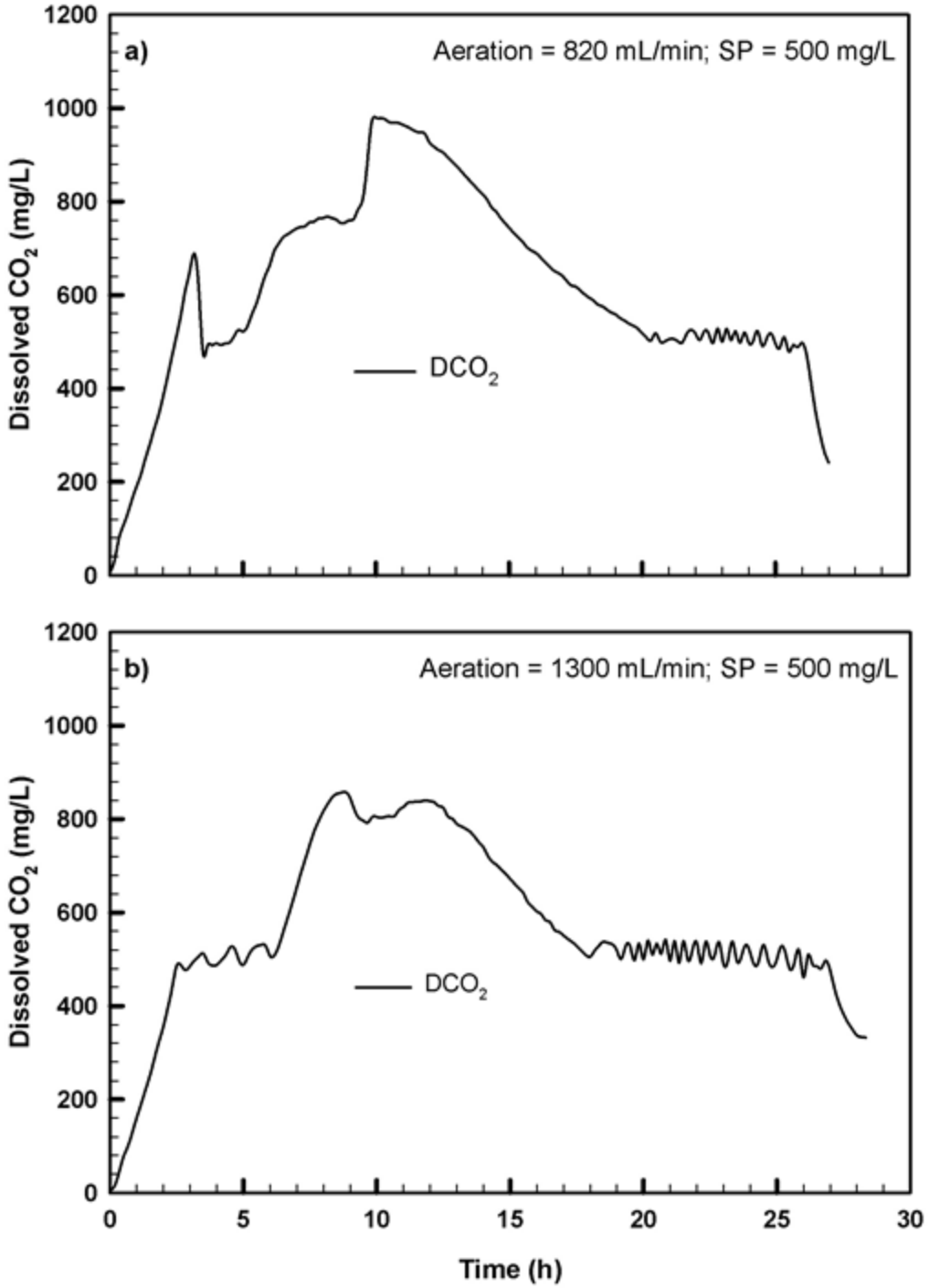

Figure 3.7 Representative profiles of dissolved CO_2 concentration controlled at 500 mg/L under aeration rates of a) 820 and b) 1300 mL/min for initial concentration of 263.76±5.55 g glucose/L. Observed values were obtained from duplicate experiments.

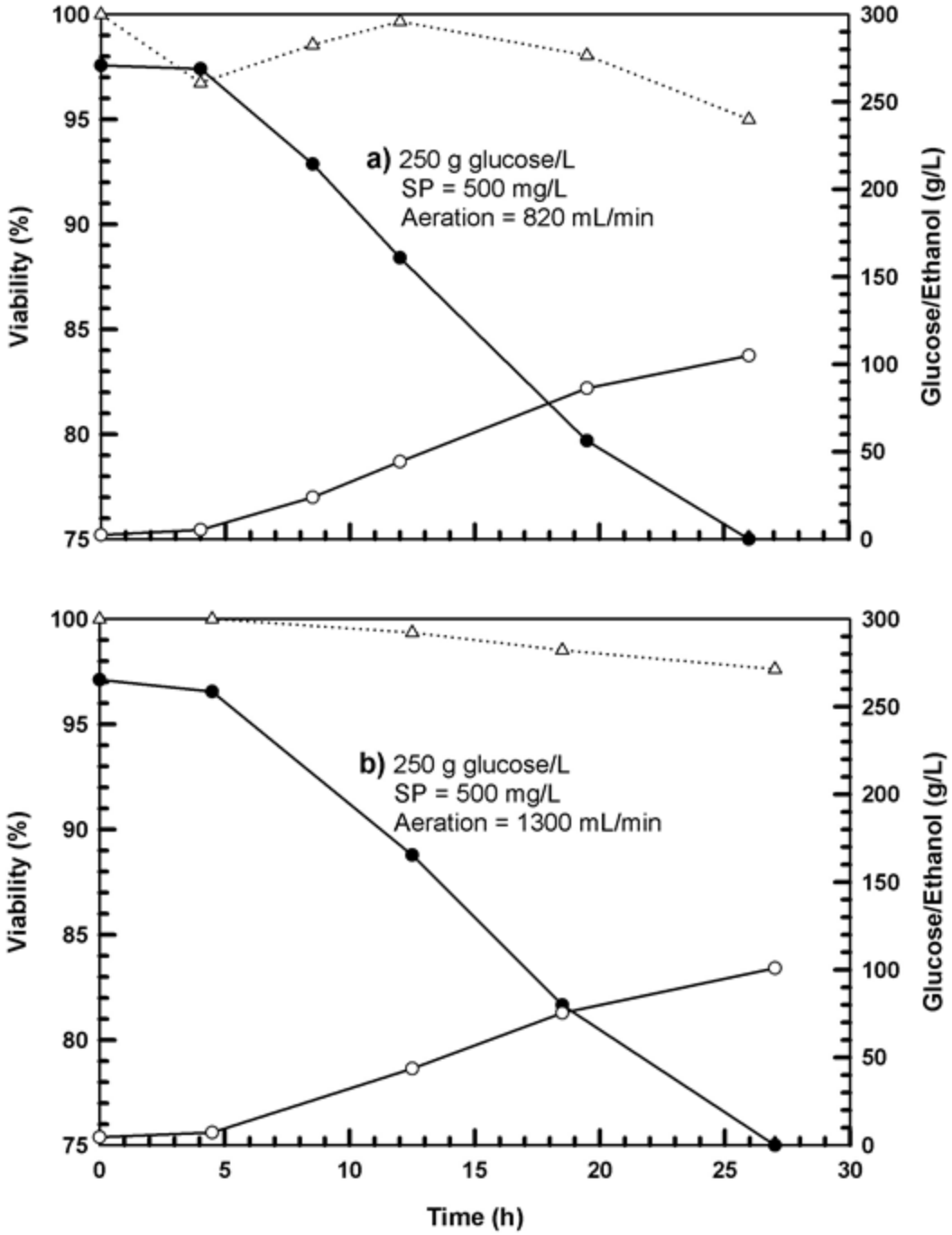

Figure 3.8 Profiles of glucose and ethanol concentration and cell viability representing duplicate experiments with dissolved CO_2 controlled at 500 mg/L under aeration rates of a) 820 and b) 1300 mL/min for initial concentration of 263.76±5.55 g glucose/L. A final ethanol concentration of 103.31±2.19 g/L was obtained irrespective of the aeration rates.

rates respectively. Dissolved CO_2 profiles in Figure 3.7 (500 mg/L), 3.9 (750 mg/L) 3.10a (750 mg/L) and 3.14 (1000 mg/L) were obtained under 263.76±5.55, 259.85±9.02 308.49±12.87 and 255.55±8.65 g glucose/L initial condition and have attributes similar to those shown in Figure 3.5 and 3.6 and discussed in detail earlier in Section 3.2.1. In comparison dissolved CO_2 profiles shown in Figures 3.10b and 3.15 obtained for dissolved CO_2 set points under initial conditions of 750 mg/L, 308.49±12.87 g glucose/L and 1000 mg/L, 299.36±6.66 g glucose/L respectively have different characteristics from that shown in Figure 3.6. The difference in characteristics has been elaborated upon later in Section 3.2.3.2.

It was observed from Figure 3.8 that in comparison to controlling dissolved CO_2 at 750 (Figure 3.11) and 1000 mg/L (Figure 3.16), a control set point of 500 mg/L yielded lower final ethanol concentrations. The difference in ethanol concentration could be explained on the basis that controlling dissolved CO_2 at 500 mg/L resulted in excessive stripping of CO_2 from the broth. Excessive stripping might deprive yeast cells of the required quantity of CO_2 leading to a reduction in metabolism that is reflected in the lower ethanol concentration. Jones and Greenfield (1989) noted that CO_2 is a requirement for various carboxylation reactions that are a part of yeast metabolism. Carboxylation reactions play an important role in maintaining the rigidity and fluidity of the cell membrane (Jones and Greenfield, 1989). Excess stripping of CO_2 might lead to lack of CO_2 for maintenance of membrane fluidity that in turn affects inter-cellular transport characteristics of the cells as well as making them susceptible to ethanol inhibition and toxicity. Based on the same premise it could be argued that controlling dissolved CO_2 at 1000 mg/L resulted in insufficient stripping of CO_2 from the broth causing an inhibitory effect. This would result in reduced conversion efficiencies for both 500 and 1000 mg/L set points. In contrast to the above two cases, controlling dissolved CO_2 at 750 mg/L could have resulted in optimum

stripping of CO_2 so as to not only diminish the effect of inhibition but also support cell maintenance at optimum levels for efficient ethanol production. Ethanol concentrations in the fermentation broth exceeding ~90 g/L (Figure 3.8, 3.11 and 3.16) also tend to exacerbate the aforementioned effects. Reduction in glucose consumption rates are also a possibility as a result.

3.2.3.1.2 Effect of oxygen supply

While the hypothesis stated earlier explains the differences among the set points based on dissolved CO_2 concentration, it did not explain the effect that aeration would have on these dissolved CO_2 levels. Two different aeration rates (820 and 1300 mL/min) were studied for the purpose of stripping dissolved CO_2 from the fermentation broth to achieve control. Generally aeration rates were seen to be interrelated to the dissolved CO_2 set points.

Dissolved oxygen concentrations in VHG broths are less in comparison to their low gravity counterparts because of the higher gravity and viscosity (Schumpe and Deckwer, 1979; Schumpe et al., 1982). The need for oxygen during fermentation is further necessitated by the very nature of the process itself. Although ethanol production in yeast is essentially anaerobic, yeast growth and proliferation require oxygen. Furthermore, the production of a primary metabolite like ethanol is dependent on yeast growth. Aeration improves the dissolved O_2 level in the broth leading to increase in cell viability (Fornairon-Bonnefond et al., 2002; Ligthelm et al., 1988; Verduyn et al., 1990).

Yeast viability in the absence of air supply was observed to characteristically reduce with the progress of batch fermentation (Figure 3.4). This was not just due to progressive substrate depletion but also a concomitant increase in ethanol concentrations. Ethanol concentrations over 40 g/L are known to cause inhibitions for yeast growth while concentrations over 85 g/L result in

cell death due to toxicity (Lin et al., 2010; Liu et al., 2011a, 2011b). Hence, it is possible that supply of oxygen could have improved the ethanol tolerance of yeast resulting in higher cell viabilities. Figures 3.8 shows cell viabilities to be over 90% for the entire duration of fermentation when compared to those seen in Figure 3.4 for batches without control. Higher viabilities not only result in higher CO_2 production (as a result of increase in *CER(t)*) but also result in faster consumption of glucose resulting in shorter durations in comparison to batches without control (Table 3.1).

However more oxygen does not necessarily result in a parallel increase in fermentation performance. Higher aeration in cases where dissolved CO_2 was controlled at 500 mg/L could have also resulted in hyperoxia eventually facilitating a reduction in cell metabolism (Belo et al., 2003; Fornairon-Bonnefond et al., 2002) and hence a lower conversion efficiency and final ethanol concentration. An argument could also be made that excess oxygen supplied could have diverted the metabolic flux towards biomass generation rather than ethanol production resulting in reduced efficiencies but not significant reduction in productivities (Zeng and Deckwer, 1994).

Based on the hypothesis that controlling dissolved CO_2 at 500 mg/L not only resulted in excessive stripping of CO_2 from the broth but also excessive oxygenation leading to hyperoxia it was postulated that control of dissolved CO_2 at 500 mg/L would have lower conversion efficiency than when dissolved CO_2 was controlled at 750 mg/L. Hence, it was decided not to control dissolved CO_2 at 500 mg/L for ~300 g glucose/L. Subsequently it would also be proved in Section 3.2.4 that controlling dissolved CO_2 at 500 mg/L for ~250 g glucose/L was indeed inefficient despite the similarity in the duration of fermentation among the different control set points.

3.2.3.2 Dissolved Carbon dioxide Controlled at 750 mg/L

In VHG fermentation initial glucose concentration was seen to play an important role in determining the duration of every batch of fermentation. Seeing how two different initial glucose concentrations were fermented using the same dissolved CO_2 control set point, it was necessary to discuss the effects such a control had on various measurable parameters like the concentration profiles of dissolved CO_2, glucose, ethanol and biomass. The dissolved CO_2 profiles for control at 750 mg/L under different aeration rates and initial glucose concentrations are shown in Figure 3.9 and 3.10. Figure 3.11 illustrates the corresponding glucose, ethanol and biomass concentration and cell viability profiles.

3.2.3.2.1 Effect on dissolved carbon dioxide profiles

Although, characteristics of dissolved CO_2 profiles for ~250 g glucose/L when dissolved CO_2 was controlled at 750 mg/L (Figure 3.9), resembled that shown in Figure 3.5 and discussed in Section 3.2.1, it was observed that dissolved CO_2 profiles differed from Figure 3.6 for the case of ~300 g glucose/L (Figure 3.10b) depending on the set point as well as the aeration rate used to achieve control. It was observed that the difference between Figure 3.10b and Figure 3.6 was restricted to Region II of Figure 3.6 or Figure 3.10a. In Section 3.2.1 it was established that the increase in dissolved CO_2 concentration over the set point value in Region II of Figures 3.5 and 3.6, despite the presence of control could be due to a combination of physiochemical as well as biological processes. While yeast metabolism was the only biological activity in the fermenter, discussions on physiochemical processes were restricted to CO_2 desorption. Based on this postulation it was deduced that the rise in dissolved CO_2 concentration was a result of increased yeast activity and increased CO_2 dissolution.

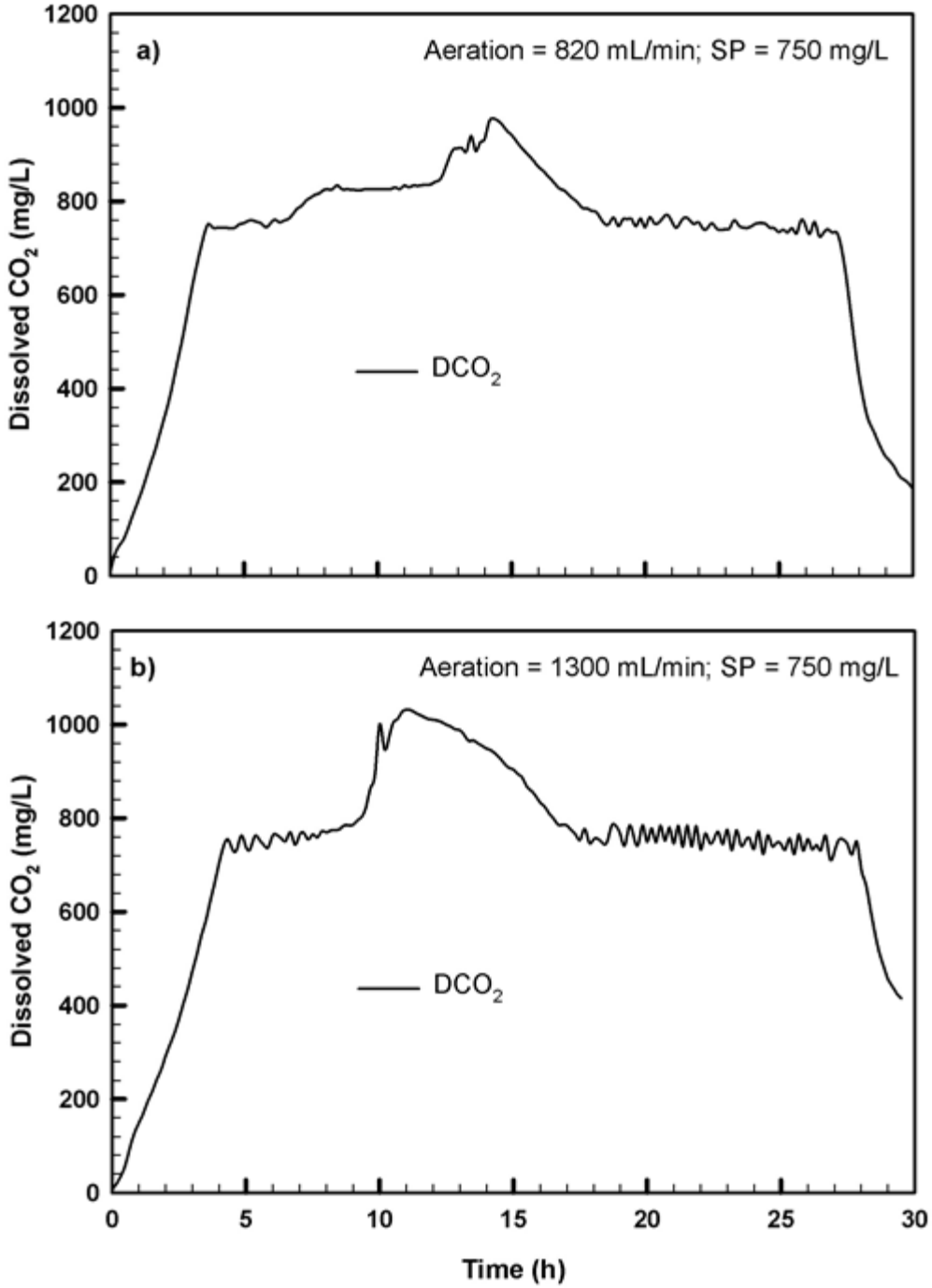

Figure 3.9 Representative profiles of dissolved CO_2 concentration controlled at 750 mg/L under aeration rates of a) 820 and b) 1300 mL/min for initial concentration of 259.85±9.02 g glucose/L. Observed values were obtained from duplicate experiments.

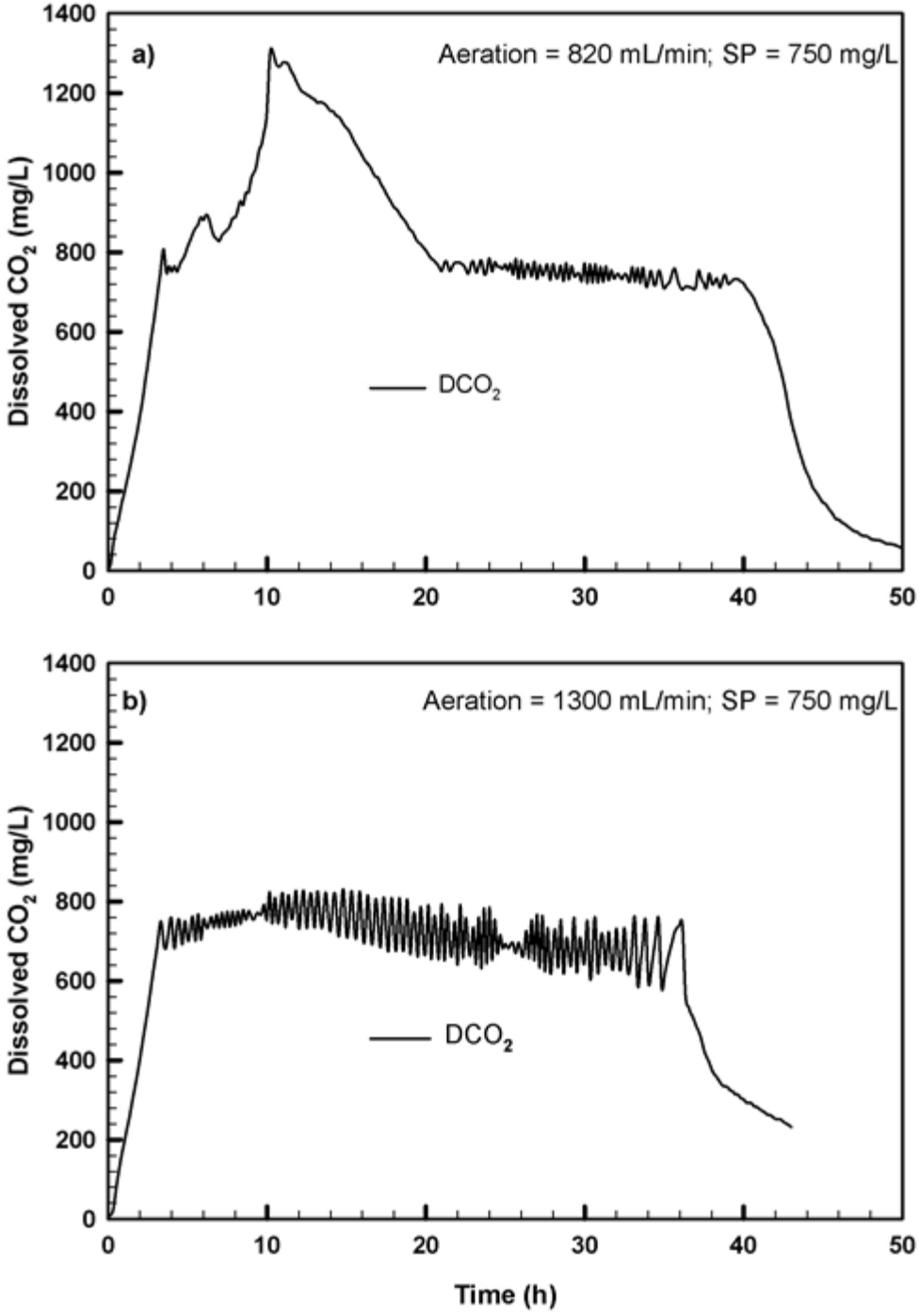

Figure 3.10 Representative profiles of dissolved CO_2 concentration controlled at 750 mg/L under aeration rates of a) 820 and b) 1300 mL/min for initial concentration of 308.49±12.87 g glucose/L. Observed values were obtained from duplicate experiments.

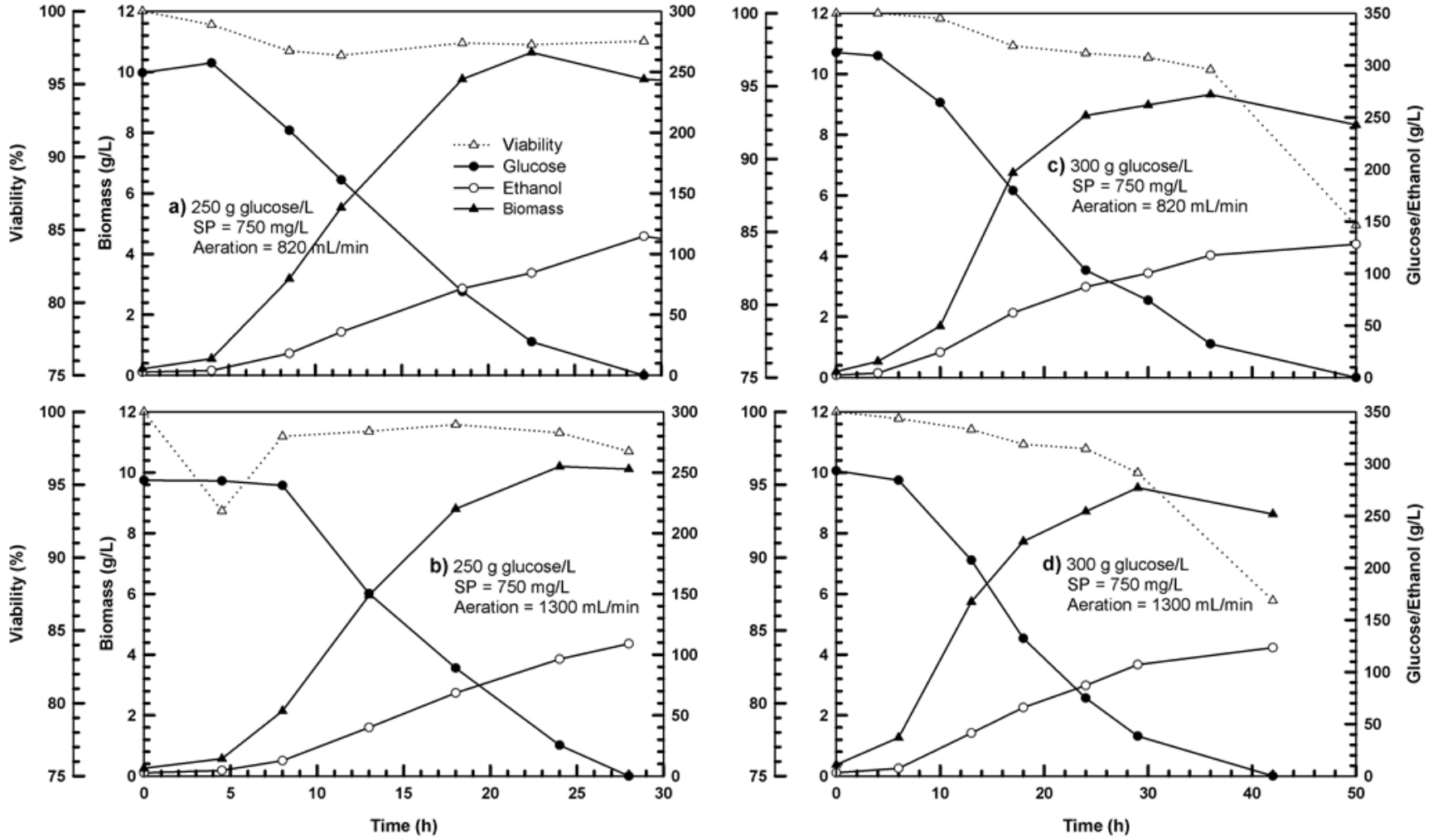

Figure 3.11 Profiles of glucose, ethanol and biomass concentration and cell viability representing duplicate experiments with dissolved CO_2 controlled at 750 mg/L under initial concentrations and aeration rates of a) 259.85±9.02 and 820, b) 259.85±9.02 and 1300, c) 308.49±12.87 and 800 and d) 308.49±12.87 g glucose/L and 1300 mL/min respectively.

Therefore, the loss of resemblance between Figures 3.10a and b in Region II was construed as a lack of increase in yeast activity as well as improved stripping of dissolved CO_2. These effects could arise due to various reasons.

The first and foremost reason could be the higher osmotic pressure in the case of ~300 g glucose/L. In comparison to the ~250 g glucose/L case, initial concentrations of ~300 g glucose/L experience higher osmosis. This could be witnessed in the slow rate of decrease of glucose concentration as well as slow rate of increase in biomass concentration in Figure 3.11c and 3.11d when compared to that seen in Figure 3.11a and 3.11b. Osmosis could also explain the higher duration of fermentation required for ~300 g glucose/L to attain zero residual glucose (Table 3.1). On the other hand, the higher quantity of substrate supplied to the fermenter may in itself be responsible for the longer duration required to completely exhaust glucose to mark the end of fermentation in the case of ~300 g glucose/L.

It could be argued that certain physiochemical effects pertaining to the solubility of CO_2 in the fermentation broth could have also affected the dissolved CO_2 profiles. Chief among them are broth viscosity and pH. Viscosity of the fermentation broth increases with increase in specific gravity of the broth or an increase in the initial glucose concentration. Increased broth viscosity not only lowers the solubility of oxygen but also improves the binding of dissolved CO_2 to the protein molecules present in the broth (Dixon and Kell, 1989; Ho and Shanahan, 1986). Increased binding reduces the rate and quantity of CO_2 desorption from the broth thereby enhancing dissolved CO_2 accumulation and inhibition as well. As for pH, it is known to affect the equilibrium of dissolved CO_2 mentioned in Equation (1.4-1.5). Lower pH favors the presence of CO_2 as dissolved CO_2. Fermentation broth pH is known to drop from 5.5 to 3.9 when left uncontrolled with the progress of fermentation thereby facilitating CO_2 dissolution rather than

desorption. Thus viscosity and pH do not play a significant role towards the effects observed in Region II of the dissolved CO_2 profiles for 300 g glucose/L in Figures 3.10.

The second reason for a lack of resemblance in Region II could be the aeration rate. A lower *CER(t)* as a result of osmosis combined with a higher aeration rate results in removing excess dissolved CO_2 thereby preventing net accumulation in Region II of Figure 3.10b as opposed to that seen in Figures 3.5-3.6 or Figure 3.10a.

3.2.3.2.2 Effect on aeration

It was earlier pointed out in Section 3.2.3.1.2 that the effect brought about by a change in aeration rate is interrelated with that brought about by change in dissolved CO_2 set point for a given glucose concentration. Higher set points would mean lesser CO_2 would have to be removed in comparison to its lower set point equivalent. This would mean that lesser quantity of air is needed to remove the corresponding dissolved CO_2 accumulated in the broth. This can be verified from Figure 3.12 illustrating the quantity of oxygen supplied for each case. Data shown in Figure 3.12 was estimated with the assumption that 21% of air was oxygen by volume under experimental conditions. Considering the fact that the duration of fermentation as well as control did not vary much between the two aeration rates for a given glucose concentration it is no surprise that more oxygen was bubbled through when higher aeration rates were used. It can also be noted from this figure that the quantity of oxygen bubbled through decreases progressively with increase in the dissolved CO_2 set point. Hence, the quantity of oxygen bubbled through for control at 750 mg/L was lower than the case of 500 mg/L when initial glucose was at ~250 g/L. But, the difference in the duration of fermentation is seen to have impacted the quantity of oxygen bubbled through for the case of ~300 g glucose/L with dissolved CO_2 controlled at 750 mg/L (Figure 3.12). .

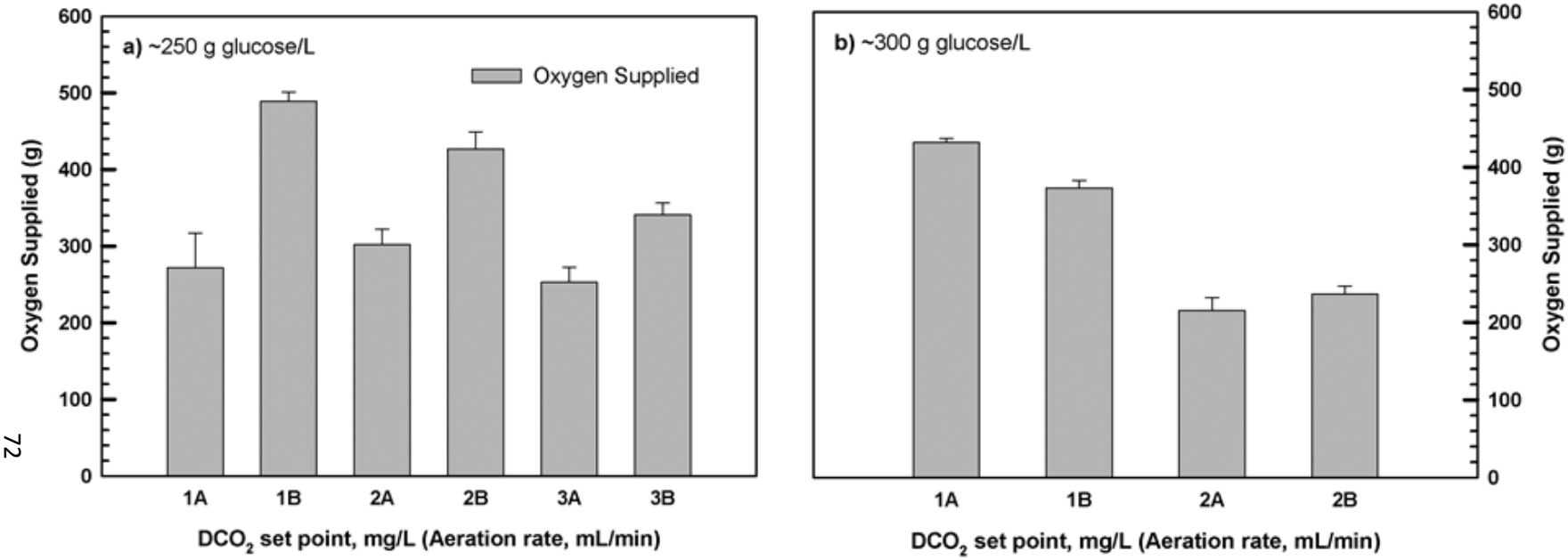

Figure 3.12 Quantity of oxygen bubbled through the fermentation broth representing the quantity of air bubbled through for initial concentrations of a) 259.72±7.96 and b) 303.92±10.66 under different set points and aeration rates. In Figure 3.12a 1, 2 and 3 represent dissolved CO_2 set points 500, 750 and 1000 mg/L respectively. In Figure 3.12b 1 and 2 represent dissolved CO_2 set points 750 and 1000 mg/L; A and B represent aeration rates 820 and 1300 mL/min respectively.

Here the trend in the quantity of oxygen supplied is reversed, i.e. a higher quantity of oxygen is supplied when control is achieved using an aeration rate of 820 mL/min than when an aeration rate of 1300 mL/min is used (Figure 3.12). This difference has solely been attributed to the longer duration of fermentation under aeration rates of 820 mL/min (Table 3.1) in comparison to aeration rates of 1300 mL/min for ~300 g glucose/L. The longer duration also explains the general increase in the quantity of oxygen supplied for the case of ~300 g glucose/L when compared to the case of ~250 g glucose/L for both dissolved CO_2 set points of 750 and 1000 mg/L.

It is highly probable that the higher quantity of oxygen supplied was in part also responsible for the distinction seen in Region II of Figure 3.10b from Figure 3.10a. Higher aeration in conjunction with higher dissolved CO_2 set points result in more efficient stripping of CO_2 from the broth and prevents net accumulation of dissolved CO_2. Reduction in metabolic activity also plays an important role as it results in reduced net *CER(t)*.

3.2.3.2.3 Effect on metabolite consumption and production

Controlling dissolved CO_2 at 750 mg/L yielded the highest final ethanol concentration amongst the three set points for 250 g glucose/L (Figure 3.11). While rate of change of ethanol concentration did not vary much with aeration rates, they varied with initial glucose concentrations. Slower change in ethanol as well as biomass concentration was observed with increase in initial glucose concentration (Figure 3.11). This was reasoned to be due to higher osmosis in higher glucose concentrations during the first 10-12 h of fermentation.

However, during the later stages of fermentation the above said reasoning would not hold when glucose concentrations have reduced and osmosis is negligible (glucose concentrations after 12-15 h are lower than ~150 g/L for 250 g glucose/L and ~200 g/L for 300 g glucose/L). In comparison, the ethanol concentrations at this point are higher than their initial values and over the inhibitory concentration of 40 g/L (Figure 3.11). While this would explain the decrease in growth as well as associated glucose consumption and ethanol production in the case of ~250 g glucose/L, it would also explain the reduced cell viabilities seen in the case of ~300 g glucose/L despite oxygen supply. Although controlling dissolved CO_2 at 750 mg/L improved fermentations for both initial glucose concentrations, fermentation was longer for ~300 g glucose/L (Table 3.1) along with a need for increased air supply (Figure 3.12).

Glucose and ethanol aside, glycerol was one other metabolite whose concentrations followed a particular trend with variation in glucose concentrations (Figure 3.13). There were no appreciable differences in glycerol concentration with changes in aeration rate and dissolved CO_2 set points. Despite the fact that supply of oxygen results in alleviating oxidative stresses associated with reduced dissolved oxygen concentration, glycerol concentrations increase with increasing initial glucose (Figure 3.13). While the increase in substrate alone could not result in an increase in glycerol, it stands to reason that other associated factors may also be responsible. These factors may include but not limited to the higher osmotic pressure as well as ethanol inhibition and toxicity seen with increasing glucose concentrations.

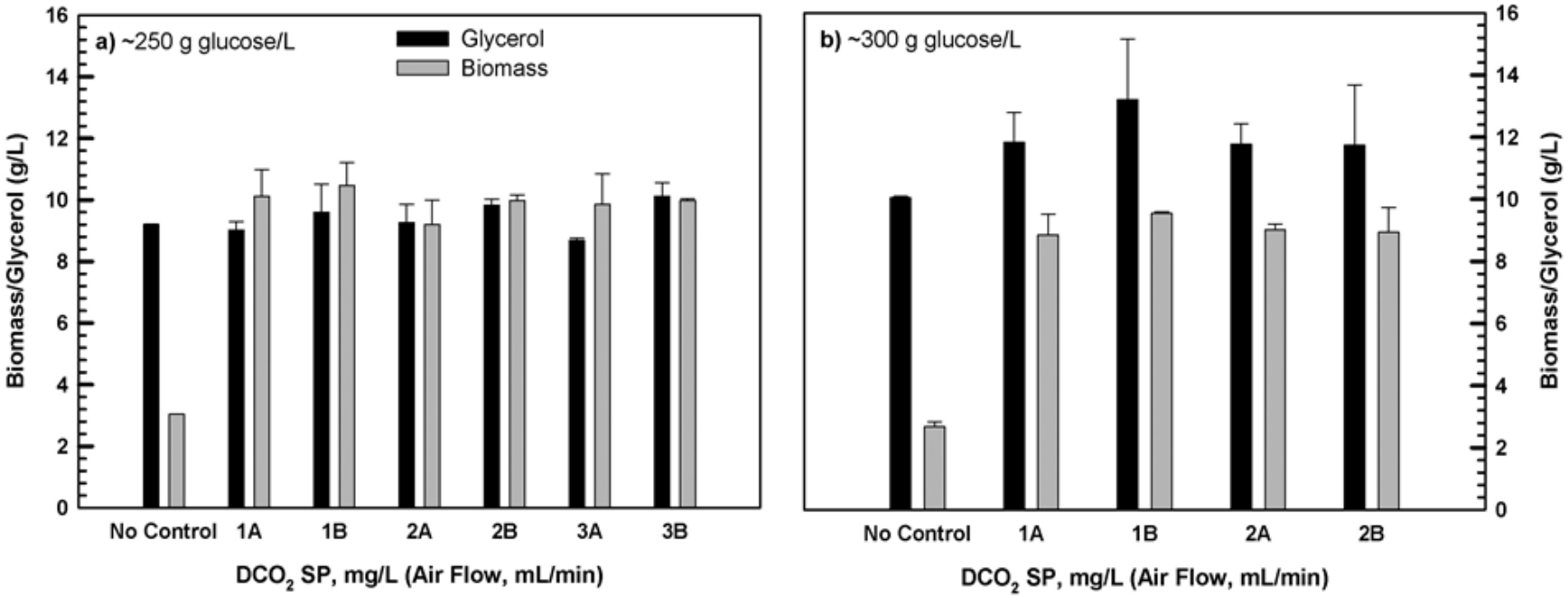

Figure 3.13 Maximum biomass and glycerol concentrations measured during the course of batch ethanol fermentation for different dissolved CO_2 set points and aeration rates for initial concentrations of a) 259.72±7.96 and b) 303.92±10.66 g glucose/L in duplicate experiments for each case listed. 1, 2 and 3 in Figure 3.13a denote dissolved CO_2 set points of 500, 750 and 1000 mg/L respectively; 1 and 2 in Figure 3.13b denote dissolved CO_2 set points of 750 and 1000 mg/L while A and B refer to aeration rates of 820 and 1300 mL/min respectively.

3.2.3.2.4 Effect on yeast growth and viability

Changes in yeast growth and survival characteristics also tend to affect metabolite consumption and production patterns. As pointed out earlier controlling dissolved CO_2 at 750 mg/L could be the optimum level in relation to the quantity of CO_2 stripped as well as oxygen supplied. This could have resulted in not only the increased cell viabilities explained earlier but consequential higher biomass concentrations relative to the VHG fermentation batches without control (Figure 3.13). However, differences in biomass concentration and cell viability profiles were observed between the two glucose concentrations (Figure 3.11).

Yeast growth is affected in the lag phase due to osmosis associated with high glucose concentrations. Osmosis not only leads to slower growth but also to slower ethanol production as noted in the previous section (Figure 3.11). But, this does not explain the reduction in the maximum biomass concentration with increase in glucose concentration (Figures 3.11 and 3.13). This observation has been made despite the higher viabilities seen in the case of ~300 g glucose/L (Figure 3.11c and 3.11d). It is expected that the higher ethanol concentrations are responsible for this effect. Although in comparison to the 250 g glucose/L case, ethanol concentrations are at similar levels (~110 g/L) for 300 g glucose/L at 30 h of fermentation, it is likely that despite the increase in cell viability, cell tolerance to higher ethanol concentrations is reduced with increase in glucose concentration. This would not only explain the reduction in ethanol production with increase in broth ethanol concentration but also the concomitant reduction in cell viabilities with the progress of fermentation for ~300 g glucose/L in comparison to ~250 g glucose/L (Figure 3.11a and 3.11b). The associated reduction in cell metabolism and growth should also explain the lower biomass concentrations observed for the case of ~300 g glucose/L especially during the final stages of fermentation.

3.2.3.3 Dissolved Carbon dioxide Controlled at 1000 mg/L

While controlling dissolved CO_2 at 750 mg/L had a plethora of positive influence on fermentation performance, controlling dissolved CO_2 at 1000 mg/L did not significantly change the interpretation of fermentation performance. These changes although insignificant, were observed due to change in the initial glucose concentration. Figure 3.14 and 3.15 show the dissolved CO_2 profiles under ~250 and ~300 g glucose/L initial concentration for different aeration rates respectively. The corresponding glucose, ethanol and biomass concentration and cell viability profiles are plotted in Figure 3.16.

3.2.3.3.1 Effect on dissolved carbon dioxide profile

As explained earlier and illustrated in Figure 3.5, 3.6 and 3.10 differences in dissolved CO_2 profiles between ~250 and ~300 g glucose/L were restricted to Region II. All arguments pertaining to this effect were presented earlier in Section 3.2.3.2.1 and no deviations from phenomenon observed in Figure 3.10b were observed in Figure 3.15, i.e., Region II in Figure 3.15 was similar to Region II of Figure 3.10b. Thus, distinctions in the dissolved CO_2 profiles are glucose concentration dependent rather than set point or aeration dependent.

3.2.3.3.2 Effect on aeration

Lower oxygen supply and a higher dissolved CO_2 set point could be blamed for increase in CO_2 inhibition in the broth. However, inhibitory effects due to dissolved CO_2 do remain to be seen and studied before such a justification could be made. The observed cell viabilities (>90%) and biomass concentrations in both ~250 and ~300 g glucose/L (Figure 3.16) stand witness to the fact that yeast metabolism is not inhibited at the macroscopic level. Lower oxygen supply for dissolved CO_2 controlled at 1000 mg/L seen in Figure 3.12 could be justified in terms of the shorter fermentation duration seen for these cases in comparison to control at 750 mg/L (Table

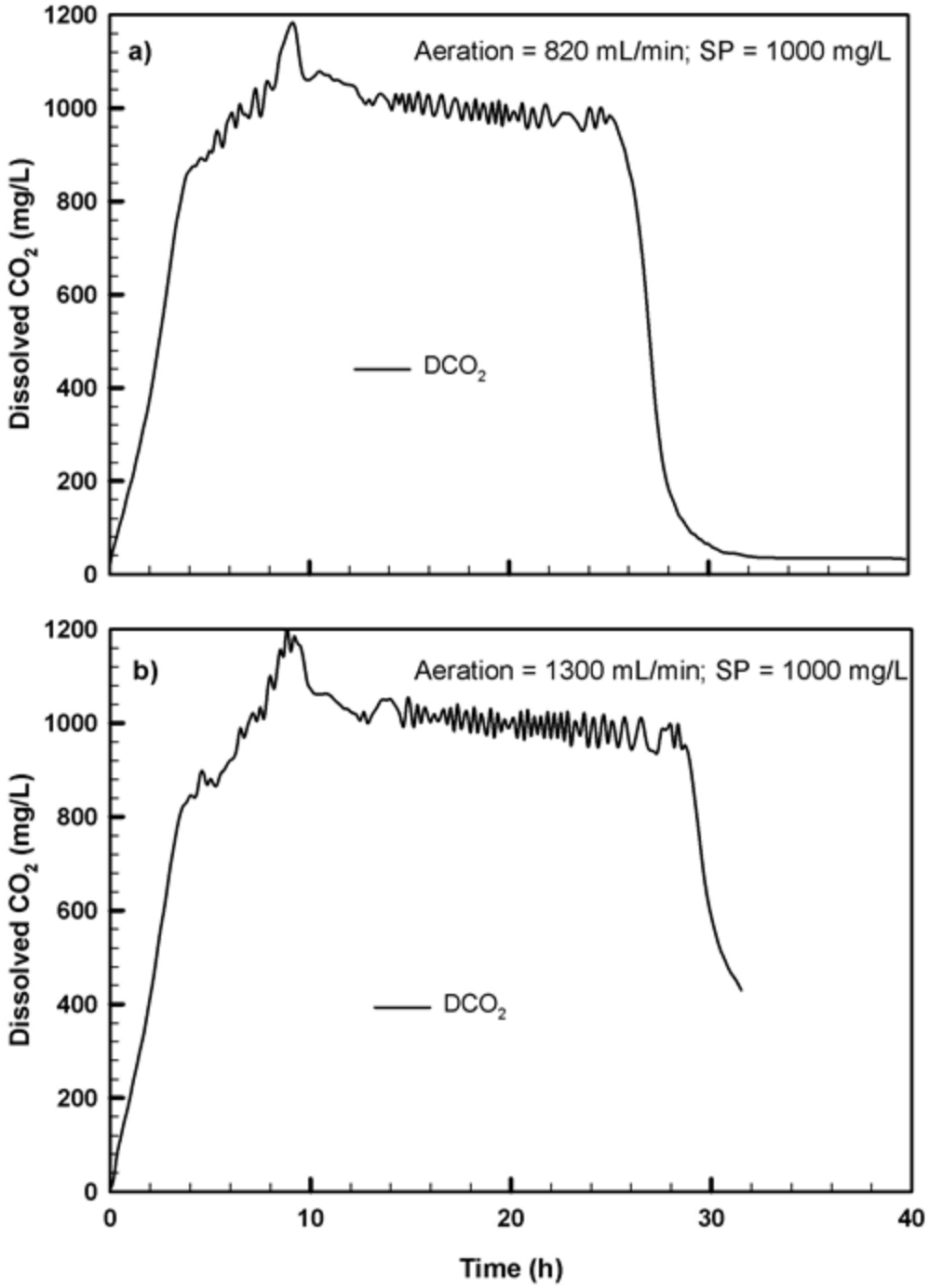

Figure 3.14 Representative profiles of dissolved CO_2 concentration controlled at 1000 mg/L under aeration rates of a) 820 and b) 1300 mL/min for initial concentration of 255.55±8.65 g glucose/L. Observed values were obtained from duplicate experiments.

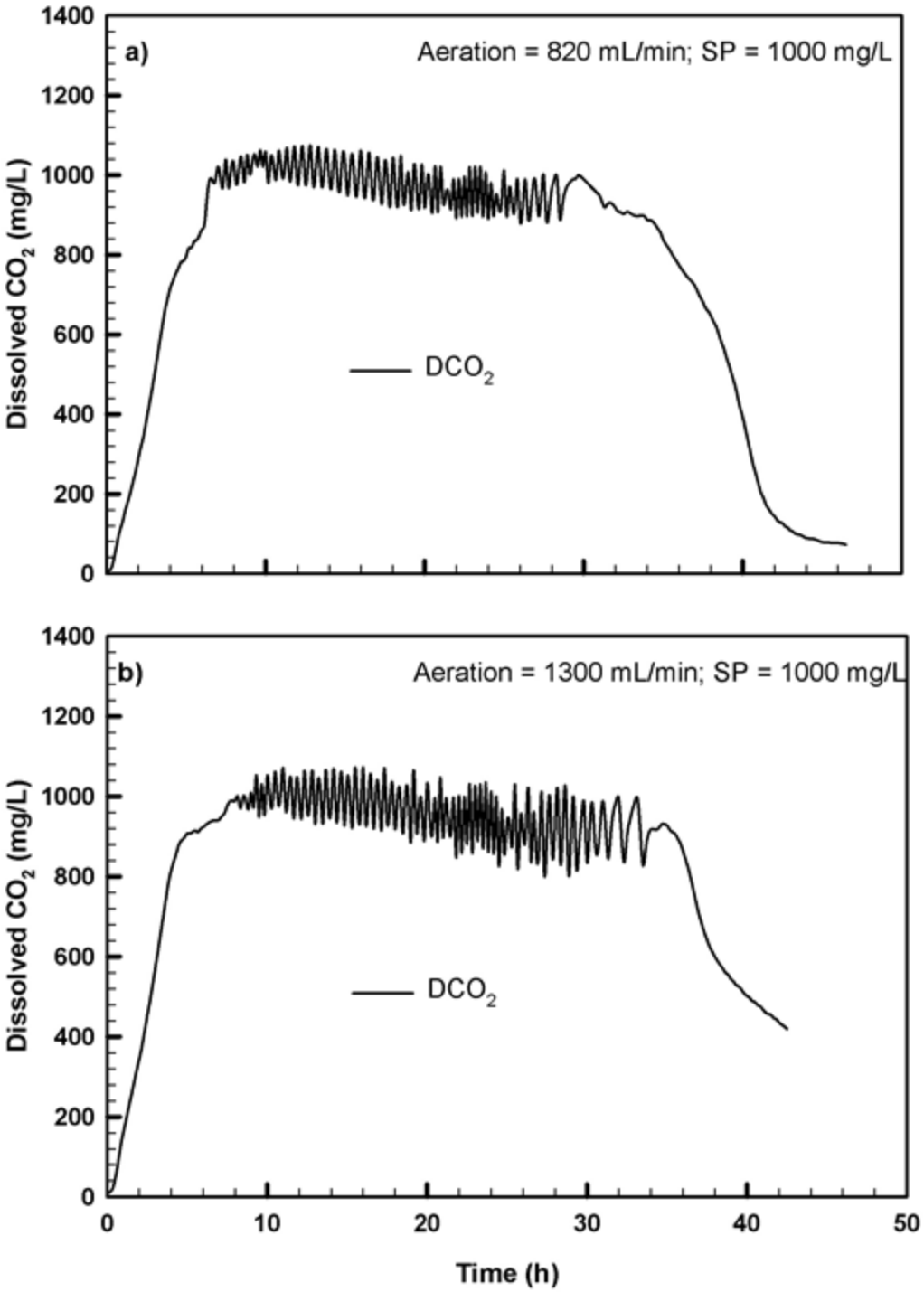

Figure 3.15 Representative profiles of dissolved CO_2 concentration controlled at 1000 mg/L under aeration rates of a) 820 and b) 1300 mL/min for initial concentration of 299.36±6.66 g glucose/L. Observed values were obtained from duplicate experiments. .

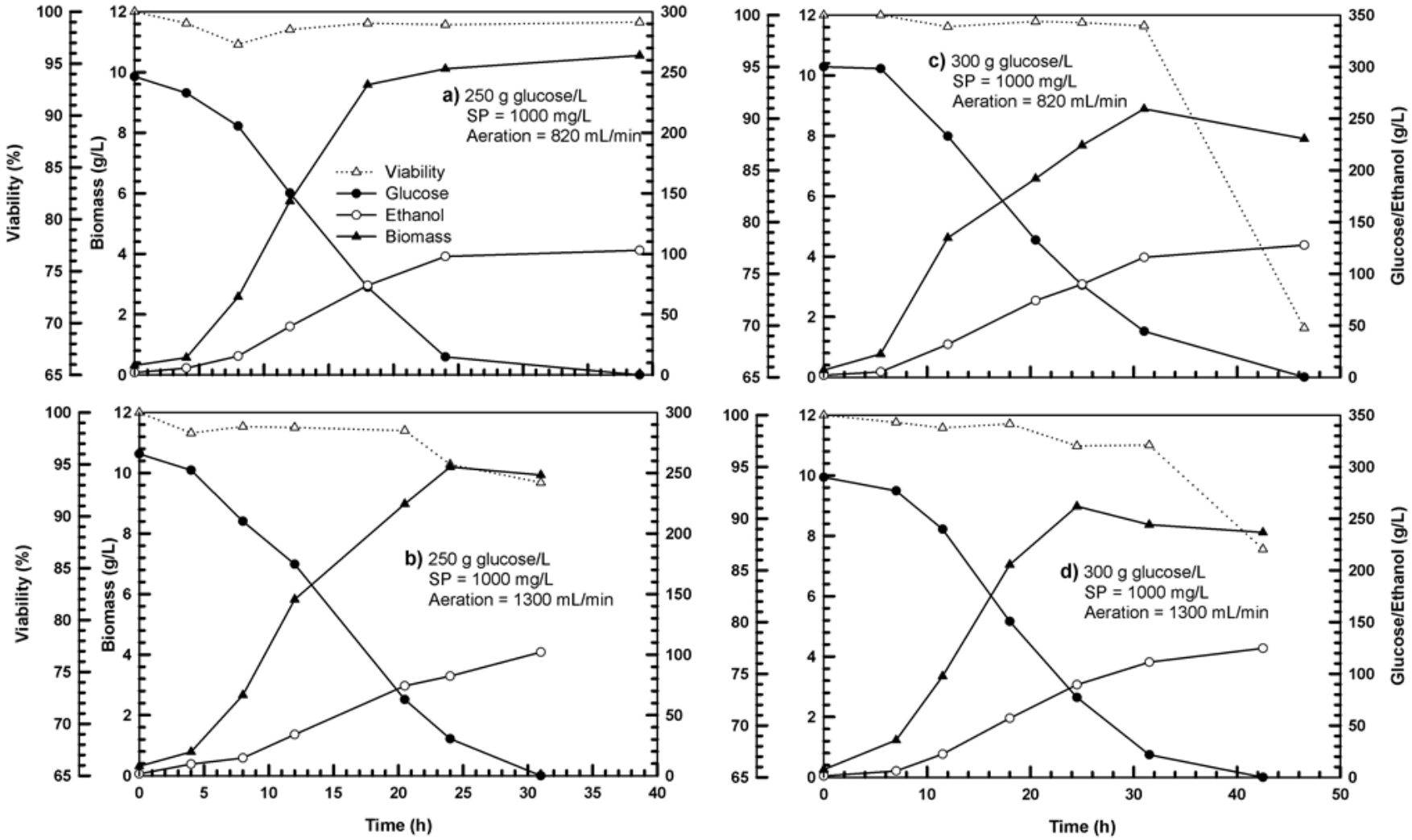

Figure 3.16 Profiles of glucose, ethanol and biomass concentration and cell viability representing duplicate experiments with dissolved CO_2 controlled at 1000 mg/L under initial concentrations and aeration rates of a) 255.55±8.65 and 820, b) 255.55±8.65 and 1300, c) 299.36±6.66 and 800 and d) 299.36±6.66 g glucose/L and 1300 mL/min respectively.

3.1). Lower air supply might also economically justify the use of a higher set point and lower aeration rate for the case of ~300 g glucose/L.

3.2.3.3.3 Effect on metabolite consumption and production

Apart from the effects mentioned in Section 3.2.3.2.3 no significant differences were observed as a result of increase in dissolved CO_2 set point from 750 to 1000 mg/L. Hence, differences in ethanol production were not contingent upon either the dissolved CO_2 set point or aeration rate but only on the initial glucose concentration.

3.2.3.3.4 Effect on yeast growth and viability

While cell viabilities were maintained at very high levels (>90%) for the case of ~250 g glucose/L for the entire process, abrupt drop in viabilities were observed for the case of ~300 g glucose/L towards the end of the process (Figure 3.16). While it is possible that the higher dissolved CO_2 set point is responsible for this effect, it could be argued otherwise given that a similar trend was observed when dissolved CO_2 was controlled at 750 mg/L (Figure 3.11). Hence, it is possible that other factors apart from dissolved CO_2 inhibition may be involved.

One such factor could be deduced from the glycerol concentrations. Glycerol concentrations were uniform irrespective of the dissolved CO_2 set point as well as aeration rate but increased with increase in initial glucose (Figure 3.13). One could argue that the glycerol production pathway in yeast shown in Figure 1.1 could be robust and rigid to stresses and beyond control. In this regard it is of significance to note that glycerol concentrations did not vary significantly from batch counterparts without control for a given glucose concentration (Figure 3.13). Glycerol is produced as one of the several by-products of NAD^+ generation, just like ethanol. Given that ethanol production is strongly affected by changes in fermentation

environment, ethanol production is neither a reliable nor a robust source for NAD^+. Glycerol production on the other hand being reliable as well as robust, contributes to a fixed flux for NAD^+ regeneration. Thus, it is highly possible that the shortfall in NAD^+ to maintain the $NADH/NAD^+$ balance is offset by directing flux to other pathways. From the current experimental data it is impossible to point out these pathways as not all precursor metabolites were measured. At the same time, an equally valid argument would be that the inability of the cell to offset this shortfall results in loss of cell viability. These factors get magnified especially in the presence of high toxic ethanol concentrations during the final stages of fermentation as well as high initial glucose concentrations.

3.2.4 Effect of Dissolved Carbon dioxide Control on Glucose Conversion Efficiency and Ethanol Productivity

Glucose conversion efficiencies and ethanol productivities under various fermentation conditions discussed previously are compared in Figures 3.17 and 3.18. The values of conversion efficiency point to the fact established earlier that controlling dissolved CO_2 at 500 mg/L was the least efficient. This fact was hypothesized earlier in Section 3.2.3.1 from the low ethanol concentration (Figure 3.8) as well as the highest quantity of air supplied (Figure 3.12). The differences arising out of variation in dissolved CO_2 set points was hypothesized to be a result of the compounded effect of CO_2 removal as well as oxygen supply. These could explain the slightly lower conversions witnessed when dissolved CO_2 was controlled at 1000 mg/L in comparison to when dissolved CO_2 was controlled at 750 mg/L for ~250 g glucose/L.

But, the hypothesis does not explain the uniformity in ethanol productivities for ~250 g glucose/L initial concentration irrespective of the aeration rates or the very slight difference in

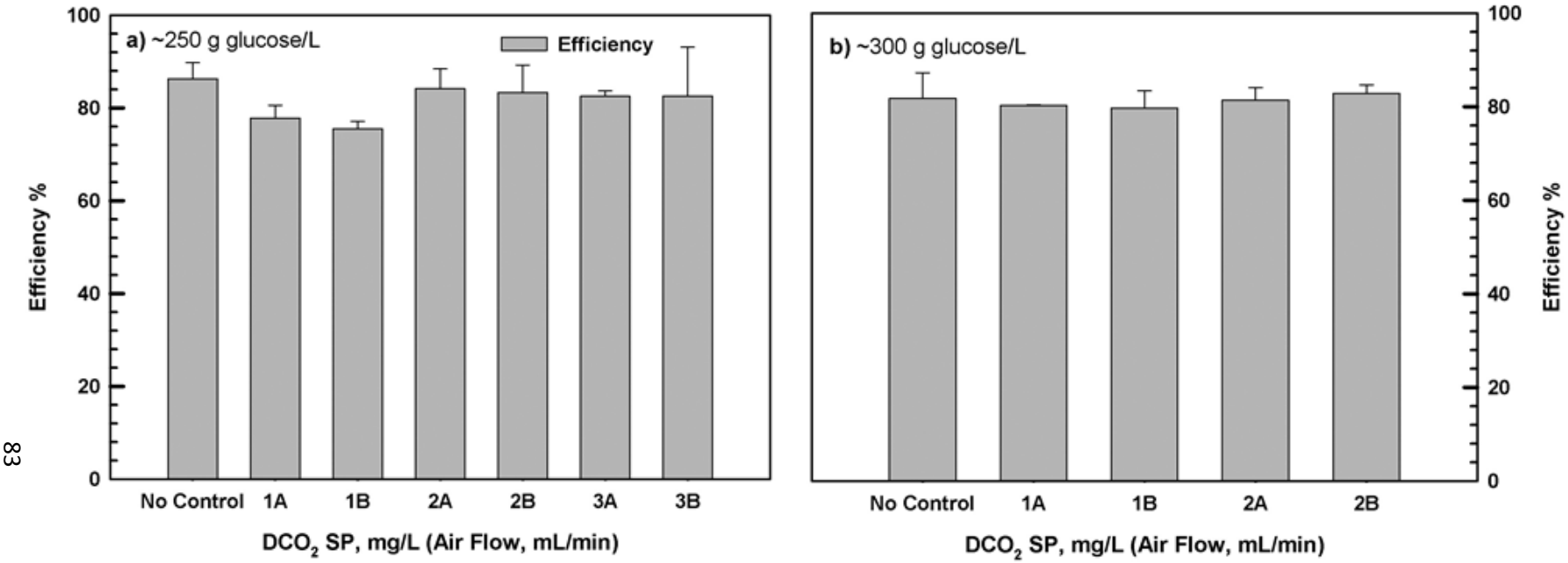

Figure 3.17 Glucose conversion efficiencies obtained in the presence of control for initial concentration of a) 259.72±7.96 and b) 303.92±10.66 g glucose/L from duplicate experiments. 1, 2 and 3 in Figure 3.17a denote dissolved CO_2 set points of 500, 750 and 1000 mg/L respectively; 1 and 2 in Figure 3.17b denote dissolved CO_2 set points of 750 and 1000 mg/L while A and B refer to aeration rates of 820 and 1300 mL/min respectively. Conversion efficiency was calculated as $\frac{[\text{Ethanol Produced}]}{[\text{Glucose Consumed}]\times 0.511}\times 100\ \%$

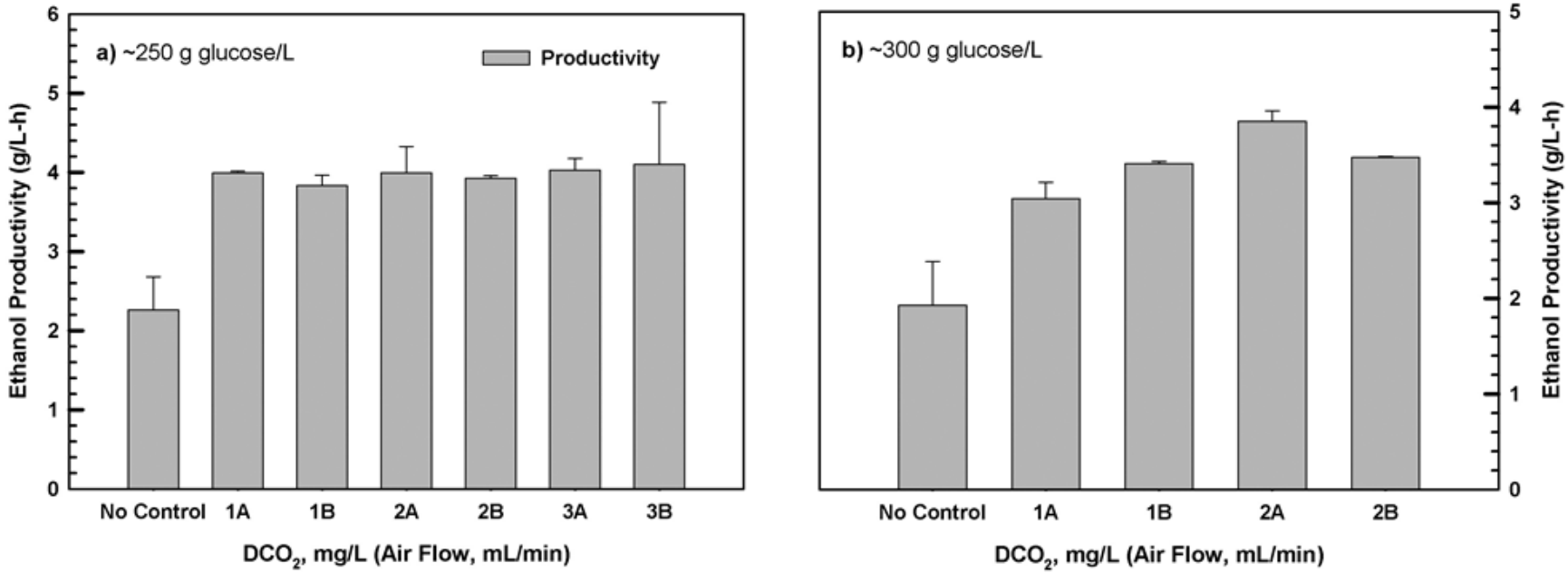

Figure 3.18 Ethanol productivities obtained in the presence of control for initial concentration of a) 259.72±7.96 and b) 303.92±10.66 g glucose/L from duplicate experiments. 1, 2 and 3 in Figure 3.18a denote dissolved CO_2 set points of 500, 750 and 1000 mg/L respectively; 1 and 2 in Figure 3.18b denote dissolved CO_2 set points of 750 and 1000 mg/L while A and B refer to aeration rates of 820 and 1300 mL/min respectively. Ethanol productivity was calculated as $\frac{\text{[Ethanol Produced]}}{\text{Fermentation Duration}}$ g/L-h

conversion efficiencies between 750 and 1000 mg/L for either glucose concentrations (Figure 3.18). It is possible that bubbling of air for dissolved CO_2 control is responsible for this effect.

Air bubbling is also known to have a positive influence on the physiochemical aspects of fermentation. Air bubbling not only strips dissolved CO_2 from the broth but also increases the concentration of cells that are in suspension. Increase in the suspended cell concentration improves mass transfer. The summation of these effects could explain the very small variation in conversion efficiencies among the 750 and 1000 mg/L dissolved CO_2 set points for different aeration rates under a given initial glucose concentration.

Increase in suspended cell concentration could also explain the variations seen in the biomass estimations of processes under control (Figure 3.11 and 3.16). Suspended cell concentration is typically higher when air is being bubbled through the broth. In the absence of any air bubbling, cells tend to precipitate from the fermentation broth. Since the final biomass estimated is usually in the absence of any air bubbling, biomass estimations tend to be significantly lower than a previous measurement. An increase in suspended cell concentration translates into an increase in number of active cells. This combined with the higher viabilities and higher biomass (Figure 3.13) could explain the higher fermentation rates and ethanol productivities as seen in the form of reduced fermentation times and complete glucose utilization even for glucose concentrations as high as 300 g/L. This physiochemical effect could also be responsible for the higher ethanol productivities seen when dissolved CO_2 was controlled at 1000 mg/L rather than at 750 mg/L for ~300 g glucose/L (Figure 3.19).

However, ethanol productivities and conversion efficiencies for ~300 g glucose/L were lower than that of ~250 g glucose/L by 13.77±9.60 % and 2.27±5.27 % respectively irrespective

of the dissolved CO_2 set points and aeration rates. The relatively lower biomass concentrations (Figure 3.13) may be responsible in part for the reduced conversion efficiencies and ethanol productivities seen in the ~300 g glucose/L case. In addition, longer duration of fermentation (Table 3.1) in the case of ~300 g glucose/L could be a factor for decrease in ethanol productivities. Longer durations in conjunction with higher osmosis and increasing ethanol concentrations as the fermentation progresses also tend to induce collective inhibitory pressure in this regard as explained earlier. In addition, physiochemical effects of lower pH and higher broth viscosity exacerbate the inhibitory effects of dissolved CO_2 thereby affecting fermentation performance.

3.3 Comparison with Redox Potential Measurement and Profiles

3.3.1 Similarities between Dissolved carbon dioxide and Redox Potential Measurements

Relationship between dissolved CO_2 and ORP profiles was established through their mutual association to yeast growth in terms of similarities and contrasts between the two measurement profiles. Figure 3.19 compares profiles of dissolved CO_2 and ORP for VHG ethanol fermentations in the presence of dissolved CO_2 and ORP based control methodologies under similar initial glucose of ~300 g/L. Visually, the two bath tub-shaped profiles are seen to be mirror images of each other. Due to the nature of ORP measurement the scrutiny of this discussion is restricted to the two major drawbacks of VHG ethanol fermentation; osmotic effects due to high initial glucose feeds and inhibition and toxicity due to high final ethanol concentrations. While osmotic effects increase the duration of the lag phase, ethanol inhibition and toxicity reduce cell viability resulting in sluggish fermentations and incomplete substrate utilization (Feng et al., 2012; Lin et al., 2010; Liu et al., 2011a). Hence, similarity between the

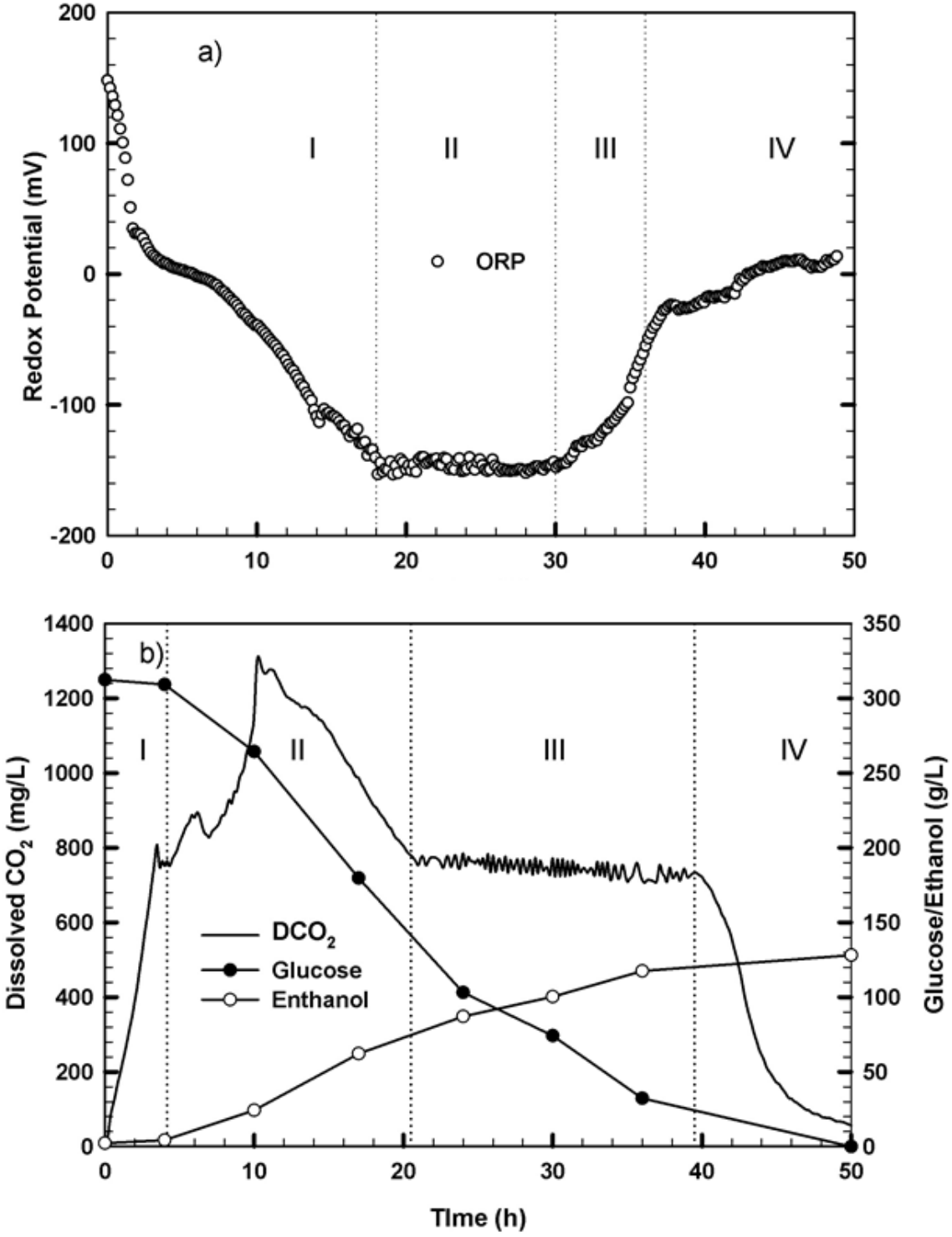

Figure 3.19 A comparison of the a) ORP and b) dissolved CO_2 profiles observed under control of the respective quantities for ~300 g glucose/L initial concentration showing the four distinct regions of each profile. Figure 3.19a was adapted from Lin et al. (2010) and Figure 3.19b is same as Figure 3.6 and Figure 3.10a.

measurement of ORP and dissolved CO_2 are restricted to Regions I and IV of both profiles. The increment in lag phase duration can be observed as a decrease in slope of the ORP and dissolved CO_2 curves in Region I of the respective figures (Figure 3.19). Region IV is a result of decreasing yeast activity in both cases. In reference to Fig. 3.19b (Region IV) where VHG fermentation was conducted under ~300 g glucose/L condition, it can be seen that the concentration of ethanol is well beyond the toxic limit of 85 g/L, and glucose is nearly utilized. In comparison, 12.53±11.06 g glucose/L was unfermented when ORP control was implemented. Hence, it was hypothesized that although differences exist in Region IV in terms of the glucose concentration represented by the two profiles, both measurements represent the common element of cessation/reduction in yeast activity and conseuquential end of fermentation. ORP measurements are capable of representing loss of cell viability as a result of ethanol toxicity but not due to glucose exhaustion. In contrast, loss of cell activity or metabolism as a result of substrate exhaustion was much more accurately represented and conspicuously observed in fermentations with dissolved CO_2 based control irrespective of the feed glucose concentrations.

3.3.2 Contrasts between Dissolved Carbon dioxide and Redox Potential Measurements

Although there are similarities that exist between the two measurements in terms of physical and dynamic properties of the system they represent, these similarities do not extend beyond Regions I and IV. The contrast between the two profiles on the other hand can be drawn in terms of physio-chemical and biological factors that ultimately result in cessation of yeast metabolism and hence fermentation. These contrasts focus on Regions II and III of either profile. In Regions II and III although the profiles capture similar regions of yeast growth, the difference in quantities they measure is the reason for their dissimilar nature. In Region II of the dissolved

CO_2 curve, an increase in yeast activity is witnessed as a result of oxygen supplied to the system (Section 3.2.1); while no change in activity is seen in the case of ORP (referring to Regions II). Even if there were a change in activity, it is not possible to observe the change through measurement of ORP. This is due to the very nature of ORP control that is based on maintaining a redox balance in the system. Control action in case of ORP measurement is initiated in response to imbalance of redox powers. Redox potential measurements are thus relative in nature, constrained upon the initial electron/proton/redox activity in the fermentation broth. A low initial redox potential would result in more air being pumped into the system to maintain the redox balance during ORP control. In the case of dissolved CO_2 based control, dissolved CO_2 set point values are based on the solubility of CO_2 for a given media under given conditions of temperature and pressure. Moreover, initial dissolved CO_2 concentrations remain the same in the absence of any yeast activity prior to inoculation, i.e. an accurate estimate of yeast activity can be made for a given dissolved CO_2 concentration based on the size of the inoculum, which is not possible in case of ORP measurements. Hence, dissolved CO_2 measurements are absolute unlike their ORP counterparts. Evidently control of dissolved CO_2 levels is not based on maintaining a balance between relativistic measures but absolute measures instead.

Region III in the dissolved CO_2 curve is very similar in appearance to Region II of the ORP curve. While the zero slope regions in both the curves cannot be explained in terms of either the glucose or ethanol concentrations, it can be seen that alteration in yeast activity if any, due to the supply of air cannot be deciphered from the ORP curve. This is regarded as one of the major drawbacks of using a relativistic measure to control VHG ethanol fermentations. These similar regions (Region II in Fig. 3.19a and Region III in Fig. 3.19b) also represent regions of perfect control in their respective cases; i.e., a balance between reduction and oxidation is

reached in case of ORP, and a balance between production and consumption of CO_2 is reached in case of dissolved CO_2.

Thus, despite the similarities and contrasts between ORP and dissolved CO_2 measurement, when used in conjunction with each other they shall be capable of representing cessation of yeast metabolism due to both glucose exhaustion as well as ethanol toxicity.

CHAPTER 4
CONCLUSIONS

In the current study, a comprehensive analysis of the characteristics of dissolved CO_2 concentration profiles obtained through direct measurement during fermentation was presented. Dissolved carbon dioxide measurement was established as an important method for measuring the progress of VHG ethanol fermentation because of its ability to exemplify transient changes in dissolved CO_2 concentration. Due to the absence of apparent delays in measurement in contrast to off-gas measurements, it was also found that dissolved CO_2 measurements were true representations of biological activity in the fermenter. The concentration profiles of dissolved CO_2 were also able to represent the extent of glucose consumption in the fermentation broth in the presence as well as absence of control.

Contrary to available literature where most relationships involving CO_2 in fermentation are based on off-gas measurements, dissolved CO_2 was used to develop an equation to study dissolved CO_2 concentrations in terms of physiochemical and biological properties of the VHG fermentation system. The equation developed on the basis of material balance principles was able to relate the measured dissolved CO_2 concentration with actual CO_2 evolution from yeast and hence yeast activity. This equation was able to corroborate the cessation of yeast activity due to substrate exhaustion as represented by the dissolved CO_2 concentration. It was also concluded that the rate of desorption of CO_2 from the fermentation broth after cessation of yeast activity remained constant.

In addition, an alternative control methodology based on the measured dissolved CO_2 was proposed and its effectiveness evaluated in batch VHG fermentation systems. Two

techniques involving $Ca(OH)_2$ and air were evaluated for this purpose. Addition of an inorganic compound like $Ca(OH)_2$ while effectively reduced dissolved CO_2 concentration, also increased the pH of the fermentation broth consequently reducing cell viabilities. In addition it also resulted in diluting the broth ethanol concentration effectively nullifying the effect of VHG fermentation.

Incorporating a dissolved CO_2 based control methodology utilizing air improved otherwise sluggish batch fermentation for glucose concentrations higher than 200 g/L. Completion of fermentation was marked by zero residual glucose in the fermentation broth as represented by the dissolved CO_2 concentration. Control also achieved conversion efficiencies of 81.00±5.18 and 81.07±2.25 % for 259.72±7.96 and 303.92±10.66 g glucose/L respectively and higher ethanol productivities of 3.98±0.28 for 259.72±7.96 and 3.44±0.32 g/L-h g/L-h for 303.92±10.66 g glucose/L when compared to batches without control. Higher ethanol productivities were characterized by reduction in fermentation duration to ~27 h and ~37 h for ~250 and ~300 g glucose/L initial concentration respectively

Among the various dissolved CO_2 set points studied for ~250 g glucose/L, maintaining dissolved CO_2 at 750 mg/L using either aeration rate resulted in the highest conversion efficiency of 83.75±4.11 %. However, no distinction could be drawn among the uniform ethanol productivities for all set points as well as aeration rates. It was concluded that this was a result of optimum oxygen supply as well as CO_2 stripping thereby enhancing performance of VHG fermentation.

In comparison for ~300 g glucose/L, the conversion efficiencies did not vary across set points and aeration rates but, controlling dissolved CO_2 at 1000 mg/L yielded higher ethanol

productivity of 3.66±0.23 g/L-h than control at 750 mg/L that yielded 3.23±0.23 g ethanol/L-h. Further from the corresponding quantities of oxygen supplied it was determined that controlling dissolved CO_2 at 1000 mg/L would make more economic sense than control at 750 mg/L due to the lower quantity of oxygen that was pumped in.

Higher ethanol productivities observed under control were attributed to higher cell viabilities and biomass concentrations. However, the positive effect that air supply had on cell viabilities was mitigated by the magnified and collective effects of increase in glucose concentration and the associated increase in ethanol concentration as well. This was witnessed as abrupt drops in cell viabilities with the progress of fermentation. In conjunction, maximum biomass concentrations also dropped with increase in initial glucose concentration.

The insignificant change in glycerol concentration in contrast to ethanol and biomass concentrations in the presence as well as absence of control under a given glucose concentration was concluded to be a result of the glycerol production pathways being more robust in *S. cerevisiae*.

It was also established that while redox potential may be sensitive to the activity of yeast in the fermenter, dissolved CO_2 measurement is directly correlated to yeast activity in the fermenter and can discern the moment of zero residual glucose much more accurately than the redox potential profiles. In comparison to the ORP controlled counterparts, higher ethanol productivities were achieved. Thus, it was established that ethanol production through VHG fermentation could be improved despite its drawbacks by utilizing an appropriate control strategy.

CHAPTER 5
FUTURE RECOMMENDATIONS

While the current process provides across the board improvements to the existing VHG fermentation process, recommendations and suggestions for further improvement of the process have been suggested in this section. These recommendations are based on the lab-scale observations and their interpretations made in Section 3.2.

One of the primary observations of concern is the lower conversion efficiencies in comparison to batches without control. While the higher productivities might off-set certain costs associated with reduced efficiencies, it is highly imperative that efficiencies be improved before industrial implementation. In this regard a change in approach to the type of process is suggested. It was earlier reported that implementing a repeated-batch process (Her et al., 2004) with ORP measurement improved glucose utilization and conversion for 200 g glucose/L (Feng et al., 2012). It is suggested that a similar process scheme be followed in the presence of dissolved CO_2 control to improve conversion efficiencies. It is hypothesized that implementing such a process and control scheme would improve conversion efficiencies from the current ~84% to at least 90% with concomitant improvement in annual ethanol production. The implementation of repeated-batch processes is facilitated by the dissolved CO_2 profiles that could be utilized to determine the point for fresh feed introduction in such processes. In addition it was suggested that repeated-batch processes increase ethanol tolerance of yeast thereby reducing ethanol inhibition and toxicity. Although the process failed to account for the inhibitory effect of CO_2, the process itself provided considerable improvement in ethanol production under VHG environments through improved conversion efficiencies and ethanol productivities in comparison

to batch and continuous processes. It is hypothesized that when used in conjunction with a dissolved CO_2 control methodology, such a process scheme would also be able to account for inhibitions due to dissolved CO_2.

Although the glycerol production in yeast during fermentation was established as a robust pathway, diversion of carbon substrate from ethanol production is of primary concern. Diversion of metabolic flux away from glycerol production and towards ethanol production might improve conversion efficiencies. It is recommended that such endeavors be undertaken through metabolic flux analysis and subsequent development of improved strains that are capable of converting glucose to ethanol more efficiently.

Regardless of the advantages that air supply offers, operation of industrial scale air compressors might increase operating costs per batch. It is recommended that apart from the conclusion drawn from the study regarding 750 mg/L as the most efficient set point, further optimization of air supply and dissolved CO_2 set point needs to be done to build upon the cost savings achieved under the current process scheme. Also of importance in this regard is the study of the deleterious effects of excess dissolved CO_2 as well as excess dissolved O_2.

Due to the ability of ORP measurements to point out ethanol toxicity in the broth more accurately, it is being suggested that future investigations in this area try utilizing ORP as well as dissolved CO_2 measurement in conjunction with each other to determine points of glucose exhaustion and ethanol toxicity.

REFERENCES

Belo, I., Pinheiro, R., and Mota, M. (2003). Fed-batch cultivation of *Saccharomyces cerevisiae* in a hyperbaris bioreactor. *Biotechnol. Prog. , 19*, 665-671.

Brown, S. W., Oliver, S. G., Harrison, D. E., and Righelato, R. C. (1981). Ethanol Inhibition of yeast growth and fermentation: Differences in the magnitude and complexity of the effect. *Eur. J Appl. Microbiol. Biotechnol. , 11*, 151-155.

Chen, Y., Krol, J., Huang, W., Cino, J. P., Vyas, R., Mirro, R., et al. (2008). DCO_2 measurement used in rapamycin fed-batch fermentation process. *Process Biochem. , 43*, 351-355.

Dahod, S. K. (1993). Dissolved carbon dioxide measurement and its correlation with operating parameters in fermentation processes. *Biotechnol. Progr. , 9*, 655-660.

D'Amore, T., and Stewart, G. G. (1987). Ethanol tolerance of yeast. *Enzyme Microb. Technol. , 9*, 322-330.

Daoud, I. S., and Searle, B. A. (1990). On-line monitoring of brewery fermentation by measurement of CO_2 evolution rate. *J. Inst. Brew. , 96*, 297-302.

Devantier, R., Scheithauer, B., Villas-Boas, S. G., Pederson, S., and Olsson, L. (2005). Metabolite profiling for analysis of yeast stress response during very high gravity ethanol fermentations. *Biotechnol. Bioeng. , 90* (6), 703-714.

Dixon, N. M., and Kell, D. B. (1989). The inhibition by CO_2 on growth and metabolism of micro-organisms. A review. *J. Appl. Bacteriol. , 67*, 109-136.

Dombrek, K. M., and Ingram, L. O. (1987). Ethanol production during batch fermentation with *Saccharomyces Cerevisiae*: Changes in glycolytic enzymes and internal pH . *Appl and Environ Microbiol* , 1286-1291.

El Haloui, N., Picque, D., and Corrieu, G. (1988). Alcoholic fermentation in winemaking: On-line measurement of density and carbon dioxide evolution. *J. Food Eng. , 8*, 17-30.

El-Sabbagh, N., McNeil, B., and Harvey, L. M. (2006). Dissolved carbon dioxide effects on growth, nutrient composition, penicillin synthesis and morphology in batch cultures of *Penicillium chrysogenum*. *Enzyme Microb. Technol. , 39* (1), 185-190.

Feng, S., Srinivasan, S., and Lin, Y.-H. (2012). Redox potential-driven repeated batch ethanol fermentation under very-high-gravity conditions. *Process Biochemistry , 47* (3), 523-527.

Fornairon-Bonnefond, C., Demaretz, V., Rosenfeld, E., and Salmon, J.-M. (2002). Oxygen addition and sterol synthesis in *Saccharomyces cerevisiae* during enological fermentation. *J. Biosci. Bioeng. , 93* (2), 176-182.

Frahm, B., Blank, H.-C., Cornand, P., Oelbner, W., Guth, U., Lane, P., et al. (2002). Determination of dissolved CO_2 concentration and CO_2 production rate of mammalian cell suspension culture based on off-gas measurement. *J. Biotechnol. , 99*, 133-148.

Frick, R., and Junker, B. (1999). Indirect methods for characterization of carbon dioxide levels in fermentation broth. *J. Biosci. Bioeng. , 87* (3), 344-351.

Galazzo, J. L., and Bailey, J. E. (1990). Fermentation pathway kinetics and metabolic flux control in suspended and immobilized *Saccharomyces cerevisiae*. *Enzyme Microb. Technol. , 12*, 162-172.

Golobic, I., and Gjerkes, H. (1999). On-line estimation of specific growth rate in bacitracin fermentation process. *AIChe J. , 45* (12), 2550-2556.

Gros, J. B., Dussap, C. G., and Catte, M. (1999). Estimation of O_2 and CO_2 solubility in microbial culture media. *Biotechnol. Prog. , 15*, 923-927.

Her, S. -L., Duan, K. -J., Sheu, D. -C., and Lin, C. -T. (2004). A repeated batch process for cultivation of *Bifidobacterium longum*. *J. Ind. Microbiol. Biotechnol. , 31,* 427-432.

Ho, C. S., and Shanahan, J. F. (1986). Carbon dioxide transfer in bioreactors. *CRC Crit. Rev. Biotechnol. , 4* (2), 1-68.

Ingledew, W., and Lin, Y.-H. (2011). Biofuels and bioenergy: Ethanol from starch based feedstocks. In M.-Y. Murray, *Comprehensive Biotechnology* (2 ed., Vol. 3, pp. 37-49). Elsevier.

Isenschmid, A., Marison, I. W., and von Stockar, U. (1995). The influence of pressure and temperature of compressed CO_2 on the survival of yeast cells. *J. Biotechnol. , 39*, 229-237.

In J. Janata (2009), *Principles of Chemical Sensors* (Second ed., pp. 171-173). New York: Springer.

Jones, R. P., and Greenfield, P. F. (1982). Effect of carbon dioxide on yeast growth and fermentation. *Enzyme Microb. Technol. , 4*, 210-223.

Kawase, Y., Halard, B., and Moo-Young, M. (1992). Liquid phase mass transfer coeeficients in bioreactors. *Biotechnol. Bioeng. , 39* (11), 1133-1140.

Kocmur, S., Corton, E., Haim, L., Locascio, G., and Galagosky, L. (1999). CO_2-Potentiometric determination and electrode construction, a hands-on approach. *J. Chem. Ed. , 76* (9), 1253-1255.

Kruger, L., Pickerell, A. T., and Axcell, B. (1992). The senstivity of different brewing strains to carbon dioxide inhibition: Fermentation and production of flavour-active volatile compounds. *J. Inst. Brew. , 98*, 133-138.

Kuhbeck, F., Muller, M., Back, W., Kurz, T., and Krottenthaler, M. (2007). Effect of hot trub and particle addition on fermentation performance of *Saccharomyces Cerevisiae*. *Enzyme and Microbial Technology , 41*, 711-720.

Kuriyama, H., Mahakarnchanakul, W., Matsui, S., and Kobayashi, H. (1993). The effect of p_{CO_2} on yeast growth and metabolism under continuous fermentation. *Biotechnol. Lett. , 15* (2), 189-194.

Lacoursiere, A., Thompson, B. G., Kole, M. M., Ward, D., and Gerson, D. F. (1986). Effects of carbon dioxide concentration on anaerobic fermentations of *Escherichia coli*. *Appl. Microbiol. Biotechnol. , 23*, 404-406.

Lee, C. P., Lee, G. W., Kwon, S., Lee, Y. S., and Chang, N. H. (1999). Succinic acid production by *Anaerobiospirillum succiniciproducens*: effects of the H_2/CO_2 supply and glucose concentration. *Enzyme Microbiol. Technol. , 24*, 549-554.

Ligthelm, M. E., Prior, B. A., and du Preez, J. C. (1988). The oxygen requirements of yeasts for the fermentation of D-xylose and D-glucose to ethanol. *Appl. Microbiol. Biotechnol. , 28*, 63-68.

Lin, Y.-H., Chien, W.-S., and Duan, K.-J. (2010). Correlations between reduction-oxidation potential profiles and growth patterns of *Saccharomyces cerevisiae* during very-high-gravity fermentation. *Process Biochem. , 45*, 765-770.

Liu, C.-G., Lin, Y.-H., and Bai, F.-W. (2011a). A kinetic growth model for *Saccharomyces cerevisiae* grown under redox potential-controlled very-high-gravity environment. *Biochemical Engineering Journal , 56*, 63-68.

Liu, C.-G., Lin, Y.-H., and Bai, F.-W. (2011b). Ageing vessel configuration for continuous redox potential-controlled very-high-gravity fermentation. *J. Biosci. Bioeng. , 111* (1), 61-66.

Maiorella, B., Blanch, H. W., and Wilke, C. R. (1983). By-product inhibition effects on ethanolic fermentation by *Saccharomyces cerevisiae*. *Biotechnol. Bioeng. , 25*, 103-121.

Manginot, C., Sablaryolles, J. M., Roustan, J. L., and Barre, P. (1997). Use of constant rate alcoholic fermentation to compare the effectiveness of different nitrogen sources added during the stationary phase. *Enzyme Microbiol. Technol. , 20*, 373-380.

McIntyre, M., and McNeil, B. (1997). Effects of elevated dissolved CO_2 levels on batch and continuous cultures of *Aspergillus Niger* A60. *Appl Environ Microbiol* , 4171-4177.

McIntyre, M., and McNeil, B. (1998). Morphogenetic and biochemical effects of dissolved carbon dioxide on filamentous fungi in submerged cultivation. . *Appl Microbiol Biotechnol* , 291-298.

Montague, G. A., Morris, A. J., Wright, A. R., Aynsley, M., and Ward, A. C. (1986). Online estimation and adaptive control of penicillin fermentation. *IEE Proceedings , 133* (5), 240-246.

Mostafa, S. S., and Gu, X. (2003). Strategies for improved dCO_2 removal from large-scale fed-batch cultures. *Biotechnol. Prog. , 19*, 45-51.

Pampulha, M. E., and Loureiro-Dias, M. C. (1989). Combined effect of acetic acid, pH and ethanol on intracellular pH of fermenting yeast. *Appl. Microbiol. Biotechnol. , 31*, 547-550.

Pattison, R. N., Swamy, J., Mendenhall, B., Hwang, C., and Frohlich, B. T. (2000). Measurement and control of disolved carbon dioxide in mammalian cell culture processes using an in situ fibre optic chemical sensor. *Biotechnol. Prog. , 16*, 769-774.

Piddocke, M. P., Kreisz, S., Heldt-Hansen, H. P., Nielsen, K. F., and Olsson, L. (2009). Physiological characterization of brewer's yeast in high-gravity beer fermentations with glucose or maltose syrups as adjuncts. *Appl. Microbiol. Biotechnol. ,* 453-464.

Reddy, L. V., and Reddy, O. V. (2005). Improvement of ethanol production in very-high-gravity fermentation by horse gram (Dolichos biflorus) flour supplementation. *Letters in Applied Microbiology , 41*, 440-444.

Rendek, E., Ducom, G., and Germain, P. (2006). Carbon dixode sequestration in municipal solid wast incinerator (MSWI) bottom ash. *J. Haz. Mat. , B128*, 73-79.

Renger, R. S., van Hateren, S. H., and Luyben, K. C. (1992). The formation of esters and higher alcohols during brewery fermentation; The effect of carbon dioxide pressure. *J. Inst. Brew. , 98*, 509-513.

Royce, P. N. (1992). Effect of changes in pH and carbon dioxide evolution rate on the measured respiratory quotient of fermentations. *Biotechnol. Bioeng. , 40*, 1129-1138.

Royce, P. N., and Thornhill, N. F. (1991). Estimation of dissolved carbon dioxide concentrations in aerobic fermentations. *AIChE J. , 37* (11), 168-1686.

Saerens, S. M., Verbelen, P. J., Vanbeneden, N., Thevelein, J. M., and Delvaux, F. R. (2008). Monitoring the influence of high-gravity brewing and fermentation temperature on flavour formation by analysis of gene expression levels in brewing yeast. *Appl. Microbiol. Biotechnol. , 80*, 1039-1051.

Saucedo-Castaneda, G., and Trejo-Hernandez, M. R. (1994). On-line automated monitoring and control systems for CO_2 and O_2 in aerobic and anaerobic solid-state fermentations. *Proc. Biochem. , 29*, 13-24.

Schumpe, A., and Deckwer, W.-D. (1979). Estimation of O_2 and CO_2 solubilities in fermentation media. *Biotechnol. Bioeng. , 21*, 1075-1078.

Schumpe, A., Quicker, G., and Deckwer, W.-D. (1982). Gas solubilities in microbial culture media. In *Advances in Biochemical Engineering/Biotechnology* (Vol. 24, pp. 1-38). Berlin/Heidelberg: Springer.

Shang, L., Jiang, M., Ryu, C. H., Chang, H. N., Cho, S. H., and Lee, J. W. (2003). Inhibitory effect of carbon dioxide on the fed-batch culture of Ralstonia eutropha: Evaluation by CO_2 pulse injection and autogenous CO_2 methods. *Biotechnol and Bioengineering* , 312-320.

Shen, H. -Y., De Schrijver, S., Moonjai, N., Verstrepen, K. J., Delvaux, F., and Delvaux, F. R. (2004). Effects of CO_2 on the formation of flavour volatiles during fermentation with immobilized brewer's yeast. *Appl. Microbiol. Biotechnol. , 64*, 636-643.

Shimoda, M., Cocunubo-Castellanos, J., Kago, H., Miyake, M., Osajima, Y., and Hayakawa, I. (2001). The influence of dissolved carbon dioxide concentration on the death kinetics of *Saccharomyces cerevisiae*. *J. Appl. Microbiol. , 91*, 306-311.

Shoda, M., and Ishikawa, Y. (1981). Carbon dioxide sensor for fermentation systems. *Biotechnol. and Bioengng. , 23* (2), 461-466.

Sipior, J., Randers-Eichhorn, L., Lakowicz, J. R., Carter, G. M., and Rao, G. (1996). Phase flurometric optical carbon dioxide gas sensor for fermentation off-gas monitoring. *Biotechnol. Prog. , 12*, 266-271.

Smart, K., Chambers, K., Lambert, I., and Jenkins, C. (1999). Use of methylene violet staining procedures to determine yeast viability and vitality. *J. Am. Soc. Brew. Chem. , 57* (1), 18-23.

Song, H., Lee, J. W., Choi, S., You, J. K., Hong, W. H., and Lee, S. Y. (2007). Effects of dissolved CO_2 levels on the growth of *Mannheimia succiniciproducens* and succininc acid production. *Biotechnol. Bioeng. , 98* (6), 1296-1304.

Spinnler, H. E., Bouillane, C., Desmazeaud, M. J., and Coorieu, G. (1987). Measurement of partial pressure of CO_2 for estimating the concentration of *Streptococcus thermophilis* in coculture with Lactobacillus bulgaricus. *Appl. Microbiol. Biotechnol. , 25*, 464-470.

Taherzadeh, M. J., Gustafsson, L., Niklasson, C., and Liden, G. (1999). Conversion of furfural in aerobic and anaerobic batch fermentation of glucose by *Saccharomyces cerevisiae*. *J. Biosci. Bioeng. , 87* (2), 169-174.

Thomas, K. C., Hynes, S. H., and Ingledew, W. M. (1994). Effects of particulate materials and osmoprotectants on very-high-gravity ethanolic fermentation by *Saccharomyces cerevisiae*. *Appl. and Environmental Microbio. , 60* (5), 1519-1524.

Verbelen, P. J., Saerens, S. M., Van Mulders, S. E., Delvaux, F., and Delvaux, F. R. (2009). The role of oxygen in yeast metabolism during high cell density brewery fermentations. *Appl Microbiol Biotechnol* , 1143-1156.

Verduyn, C., Postma, E., Scheffers, W. A., and van Dijken, J. (1990). Physiology of *Saccharomyces cerevisiae* in anaerobic glucose-limited chemostat cultures. *Journal of General Microbiology , 136*, 395-403.

Xi, Y.-l., Chen, K.-q., Li, J., Fang, X.-j., Zheng, X.-y., Sui, S.-s., et al. (2011). Optimization of culture conditions in CO_2 fixation for succininc acid production using *Actinobacillus succinogenes*. *J. Ind. Microbiol. Biotechnol. , 38*, 1605-1612.

Yagi, H., and Yoshida, F. (1977). Desorption of carbon dioxide from fermentation broths. *Biotechnol. Bioeng. , 19*, 801-819.

Zeng, A.-P., and Deckwer, W.-D. (1994). Pathway analysis of oxygen utilization and tricarboxylic acid cycle activity in *Saccharomyces cerevisiae* growing on glucose. *J. Biotechnol. , 37*, 67-77.

Zosel, J., Oelbner, W., Decker, M., Gerlach, G., and Guth, U. (2011). The measurement of dissolved and gaseous carbon dioxide concentration. *Meas. Sci. Technol. , 22*, 1-46.

APPENDIX

The conversion of dissolved CO_2 (DCO_2) to HCO_3^- ion is governed by the forward and backward reactions depicted by Equations (A.1-A.2).

$$CO_2 + H_2O \xrightarrow{k_b} H^+ + HCO_3^- \quad \text{(A.1)}$$

$$HCO_3^- + H^+ \xrightarrow{k_{-b}} CO_2 + H_2O \quad \text{(A.2)}$$

The rate of conversion of DCO_2 to HCO_3^- in aqueous media is governed by the rate equation illustrated by Equation (A.3). Note that due to the absence of a limiting effect on the equilibrium of these ions, the concentration of water is left out of Equation (A.3).

$$\frac{d([HCO_3^-])}{dt} = k_b[CO_2] - k_{-b}[HCO_3^-][H^+] \quad \text{(A.3)}$$

$$\frac{d([HCO_3^-])}{dt} = \frac{k_b[H^+]}{K_1}\left\{\frac{K_1}{[H^+]}[CO_2] - [HCO_3^-]\right\} \quad \text{(A.4)}$$

where $K_1 = \frac{k_b}{k_{-b}}$ is the equilibrium constant for Equation (A.4). Under the steady state condition, $\frac{d([HCO_3^-])}{dt}$ in Equation (A.4) is equal to zero. Hence, Equation (A.4) reduces to Equation (A.5). The reaction rate constants k_b and k_{-b} can be determined with the aid of the Arrhenius relation for reaction rate constants.

$$[HCO_3^-] = \frac{K_1}{[H^+]}[CO_2] \quad \text{(A.5)}$$

Note that $[CO_2]$ in Equation (A.5) refers to the dissolved CO_2 concentration that is symbolized as $[DCO_2]$ in Equation (3.6).